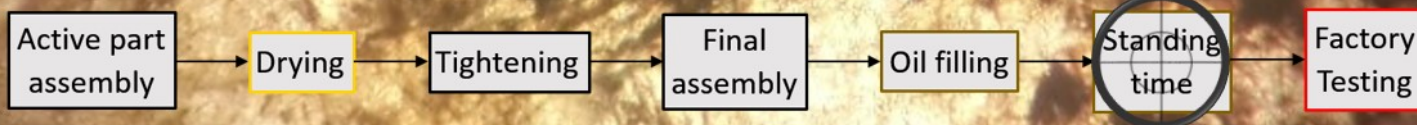




Influence of Moisture in Insulating Paper on Reducing Post-impregnation Standing Time of Oil-filled Power Transformers

Pranav P. Karhade

Master of Science Thesis



Cover page image credits:

Transformer images - Royal SMIT Transformers B.V.

Stopwatch - <http://www.clipartkid.com/images/119/stopwatch-clip-art-mvnIDU-clipart.png>

Cross-hairs - https://openclipart.org/image/2400px/svg_to_png/89035/Crosshairs-3456.png

Influence of Moisture in Insulating Paper on Reducing Post-impregnation Standing Time of Oil-filled Power Transformers

MASTER OF SCIENCE THESIS

For the degree of Master of Science in Electrical Engineering at Delft University of Technology

Pranav P. Karhade

Student number: 4417852

September 23, 2016

Faculty of Electrical Engineering, Mathematics and Computer Science (EEMCS)



The work in this thesis was commissioned by and performed in collaboration with Royal SMIT Transformers B.V., Nijmegen.



Copyright © Electrical Sustainable Energy (ESE)
All rights reserved.



DELFT UNIVERSITY OF TECHNOLOGY
DEPARTMENT OF
ELECTRICAL SUSTAINABLE ENERGY (ESE)

The undersigned hereby certify that they have read and recommend to the Faculty of Electrical Engineering, Mathematics and Computer Science (EEMCS) for acceptance a thesis entitled

INFLUENCE OF MOISTURE IN INSULATING PAPER ON REDUCING
POST-IMPREGNATION STANDING TIME OF OIL-FILLED POWER TRANSFORMERS

by

PRANAV P. KARHADE

in partial fulfillment of the requirements for the degree of
MASTER OF SCIENCE ELECTRICAL ENGINEERING

Dated: September 23, 2016

Thesis Committee:

Prof.dr. P. Palensky

Dr. A. Rodrigo Mor

Ir. M. Deutekom

Dr. L. Chmura

Abstract

Standing time, prior to testing, is a necessary part of the oil-filled transformer manufacturing process and its duration is design dependent. Caution on part of the manufacturer to avoid failure of expensive transformers leads to the overestimation of standing time, consequently impacting annual production. Thus, a need for optimizing (reducing) standing time arises.

The absence of Partial Discharges (PDs), above predetermined limits, during testing indicates sufficient standing time. Moisture in oil-paper insulating system is a source of PDs. Thus, moisture and its migration between oil and paper can determine the duration of standing time. Moisture is absorbed by and extracted from paper during the tightening and vacuum steps of the production process, respectively. The aim of this thesis is to determine if paper actually plays a role in determining the standing time.

Two investigations were conducted using presspaper and crêped presspaper samples having different geometries. One investigation was to characterize the moisture ingress and egress processes related to non-impregnated paper. Moisture ingress was studied by exposing dried paper samples to air (60 °C, 75% Relative Humidity (RH)) in a climate chamber for 24 hours while moisture egress was studied by placing the climate exposed samples in vacuum (10 mbar) at 25 °C for 48 hours. The other investigation was to study the changes in PD behaviour of Oil Impregnated Paper (OIP) with respect to standing time. PD tests were performed on samples conditioned to different levels of moisture content and impregnated with dry, hot (70 °C), PD free oil. The effect of clamping force was also considered.

Both presspaper and crêped presspaper samples attained an average moisture content of 8%, by weight, within 7 hours of exposure, whereas their moisture content reduced to 1% within 24 hours (conventional duration) of placing them in vacuum. No PDs were observed in samples exposed to the chosen climate for 24 hours and placed in vacuum for 4 hours (24cc/4vac) when tested at the normal testing electric field level of 6 kV/mm. Moisture saturated samples exhibited PD activity at 3 kV/mm immediately after impregnation whereas, 24cc/4vac samples had Partial Discharge Inception Fields (PDIFs) in excess of 8 kV/mm. The results indicated that paper did not determine the standing time for transformers.

Table of Contents

Acknowledgements	xi
1 Introduction	1
1-1 Manufacturing an oil-filled power transformer	2
1-1-1 Overview: Parts of an oil-filled transformer	2
1-1-2 Transformer manufacturing process	3
1-2 Standing time optimization and previous research	4
1-3 Problem Statement	5
1-4 Research Questions	6
1-5 Thesis Outline	6
2 Theoretical Backdrop	7
2-1 Paper in oil-filled transformers	7
2-1-1 Types of paper and their location	7
2-1-2 Method of wrapping paper	10
2-2 Moisture in paper	10
2-2-1 Effect of absorbed moisture on paper	11
2-2-2 Factors affecting rate of moisture absorption by dry paper	12
2-3 Transformer testing	13
2-3-1 Overview of equipment testing	13
2-3-2 Typical test plan of an oil-filled transformer	13
2-4 PD due to moisture in oil-paper insulation	15

3	Sample and Oil Preparation	17
3-1	Sample geometries	17
3-1-1	Samples for studying moisture ingress and egress	17
3-1-2	PD test samples	19
3-2	Effect of Clamping	21
3-3	Selection of sample conditioning parameters	24
3-4	Sample conditioning process	25
3-5	Oil preparation	27
4	PD Test Setups and Procedure	29
4-1	Measuring discharges	29
4-2	Test setups	31
4-2-1	Test tank description	33
4-2-2	Setup 1	34
4-2-3	Setup 2	34
4-3	Oil impregnation process	35
4-4	Test Procedure	37
5	Results of the Investigations	41
5-1	Climate exposure and vacuum duration test	41
5-2	PD test results	46
5-2-1	Sample bars without clamping	47
5-2-2	Sample bars with clamping	52
5-2-3	Field simulation study	55
5-2-4	Tests to determine PDIF	58
6	Conclusions and Recommendations	65
6-1	Conclusions	66
6-2	Recommendations for further research	67
A	Clamping Frame	69
B	Datasheets of insulating paper	73
C	Oil parameters measured during PD tests	79
	Bibliography	83
	List of Abbreviations	87

List of Figures

1-1	Age distribution of various substation facilities (1998) [5,6]	1
1-2	3-winding power transformer: Internals and after site erection	3
1-3	Transformer manufacturing process	3
2-1	Thermally upgraded presspaper	8
2-2	Thermally upgraded crêped presspaper	8
2-3	Active part of a transformer from HV side (Courtesy: Royal SMIT)	9
2-4	Front view of a winding (Courtesy: Royal SMIT)	9
2-5	Top view of a section of a winding (Courtesy: Royal SMIT)	9
2-6	Schematic illustrating 50% registration [25]	10
3-1	Substrate for wrapping paper	18
3-2	Dimensions of the substrate	18
3-3	Samples for moisture ingress and egress study	18
3-4	Substrate for PD test samples	19
3-5	Substrate wrapped with Crêped presspaper	19
3-6	Representative electrode placement on a sample bar during PD testing	20
3-7	Top view of the clamping frame	22
3-8	Underside of the top block of a clamping frame	22
3-9	Schematic representation of the clamping frame with sample bar	22
3-10	Load cell arrangement	23
3-11	Level check performed while setting clamping force	23
3-12	Simplified schematic representation of the convection air currents	24
3-13	Drying samples in the oven	25
3-14	Conditioning samples in the climate chamber	26

3-15 Oil preparation skid	27
4-1 Apparent charge measurement [35]	29
4-2 Example of a PRPD pattern - internal discharge	30
4-3 Schematic circuit for straight detection	30
4-4 Block representation of straight detection circuit used in the experiments	31
4-5 Measuring impedance used in the experiments	32
4-6 Test tank - external view	33
4-7 Test tank - internal view	33
4-8 Oil filling and draining port (centre) and stud for connection of test object to earth (left)	34
4-9 Test tank to vacuum pump connection with tank air outlet valve marked	34
4-10 Connector and electrode used for samples without clamping	34
4-11 Test transformer, test object and coupling capacitor connection - setup 1	35
4-12 Test transformer, test object and coupling capacitor connection - setup 2	35
4-13 Oil filling in progress	36
4-14 Air bubbles in oil during degassing interval	36
4-15 Activities to be performed while testing each location	38
4-16 Time sequence for the application of test voltage for PD test	39
5-1 Paper samples placed in climate chamber	42
5-2 Paper samples placed in the vacuum oven (10 mbar (abs.), 25 °C)	42
5-3 Changes in avg. moisture content of paper during climate exposure	43
5-4 Changes in avg. moisture content of paper during vacuum cycle	44
5-5 Samples placed in ambient conditions after vacuum cycle	45
5-6 Changes in avg. moisture content of paper during post vacuum ambient exposure	45
5-7 Electric field plot of part of a transformer winding	46
5-8 Testing of sample 1.3 in progress	47
5-9 Burst of discharges observed during testing of sample 1.1 at 13.8 kV	48
5-10 Burst of discharges observed during testing of sample 1.2 at 18 kV	48
5-11 Monitoring of oil parameters during testing of sample bar 1	49
5-12 Monitoring of oil parameters during testing of sample bar 2	50
5-13 Monitoring of oil parameters during testing of sample bar 6	51
5-14 Testing of sample 7.2 in progress	52
5-15 Discharges observed during testing of sample 7.4	53
5-16 Distortion seen in the synchronizing voltage signal	54
5-17 Object model used in the simulation	55
5-18 Field stress pattern (normal component) - 0.1 mm oil film, 1 mm paper layer, 12 kV applied voltage	56
5-19 Field stress pattern (normal component) - zoomed in	57

5-20	Field stress pattern - x component	57
5-21	PDIF variation with standing time for presspaper with differing moisture content	58
5-22	PRPD pattern obtained at breakdown of sample 9.1	59
5-23	Punctures in sample bar 9 caused by the breakdown events	59
5-24	PRPD pattern obtained while testing sample 9.2 (at 6.8 kV)	60
5-25	PRPD pattern obtained while testing sample 11.2 (at 31.2 kV)	60
5-26	Carbonization caused by heavy discharges on sample bar 11	60
5-27	Depression caused by clamping force in crêped presspaper	61
5-28	Measurement spots marked on the sample bar	61
5-29	Measuring depth of the depression using a dial gauge	61
5-30	Field stress pattern - 3.3 mm paper layer, 1.8 mm depression, 20 kV applied voltage	63
5-31	PDIF variation with standing time for crêped presspaper with differing moisture content	63
C-1	Monitoring of oil parameters during testing of sample bar 7	79
C-2	Monitoring of oil parameters during testing of sample bar 8	80
C-3	Monitoring of oil parameters during testing of sample bar 9	80
C-4	Monitoring of oil parameters during testing of sample bar 10	81
C-5	Monitoring of oil parameters during testing of sample bar 11	81
C-6	Monitoring of oil parameters during testing of sample bar 3	82
C-7	Monitoring of oil parameters during testing of sample bar 4	82

List of Tables

3-1	Specifications of the samples for moisture ingress and egress study	19
3-2	Particulars of the sample bars prepared during the research	20
3-3	Conditioning parameters and durations applied to each sample bar	26
4-1	Differences in component ratings between the two test setups	32
4-2	PD test program - Testing schedule for each impregnated sample bar	37
4-3	PD test program - Specifications of sample conditioning parameters	37
4-4	Test voltage calculation and duration of voltage application	38
5-1	Average weight of each sample type before and after drying at 80 °C, 1 atm.	41
5-2	Avg. moisture content (% w/w) of each sample type after climate exposure	42
5-3	Avg. moisture content (% w/w) of each sample type after vacuum cycle	43
5-4	Weights of sample bars 1 and 2 pre and post climate exposure	47
5-5	Test voltages used for sample bars 1 and 2	48
5-6	Revised testing field stresses for different types and configurations of paper	50
5-7	Test voltages used for sample bar 6	51
5-8	Weight of sample bar 6 pre and post climate exposure	51
5-9	Test voltages used for sample bar 7	53
5-10	Conditioning duration, oil humidity and RH of air - sample bars with clamping	64

Acknowledgements

I firmly believe that an individual's accomplishments are always a result of the support and efforts of a group of people. Thus, I would like to take this opportunity to express my sincerest gratitude to all those who have been a part of my time at TU Delft.

My decision to pursue a thesis within the High Voltage domain stemmed from the exceptional teaching efforts of Dr.ir. Peter Morshuis, Dr. Armando Rodrigo Mor and Dr. Lukasz Chmura.

I would like to thank Dr. Chmura for introducing me to this topic. His mentoring during this research, and the extra project, has been invaluable to me. His inputs on scientific writing, in general, and on the manuscript were instrumental in enhancing the final output.

I would like to convey my deepest gratitude to Dr. Rodrigo Mor for agreeing to supervise this project and being available for discussions despite being overburdened with teaching and administrative duties. His timely and valuable insights at crucial junctures enabled me to find the right solutions. The thesis is certainly better on account of the suggestions provided by him after having reviewed the manuscript.

I would like to thank Ir. Maarten Deutekom for all his mentoring, assistance and supervision during the execution of this project. The support and encouragement he provided by listening to ideas, promptly answering queries and reviewing and commenting on the draft and the presentations spurred me to deliver a better final product.

I would like to sincerely thank the fantastic team at Royal SMIT Transformers B.V. for giving me the opportunity to work on this project and enthusiastically following the progress. I would like to thank them for providing the necessary information, explaining the manufacturing process during the factory visits and for arranging interesting demonstrations. It was a privilege to learn from and interact with Ir. Kees Spoorenberg. A special mention is reserved for those who demonstrated the insulating paper wrapping process which was an essential component of my research work.

This research task could not have been accomplished without the support of the ever-helpful High Voltage Laboratory team. It was truly a pleasure to work with and learn from them over the past year. Sharing knowledge, experiences and discussing world issues over tea is something I will always cherish. I would like to thank Ing. Paul van Nes for sharing his vast experience, always being receptive to ideas and questions and giving me the freedom to learn by doing. The test setups used in this research were a direct result of the work put in by Mr. Remko Koornneef and Mr. Wim Termorshuizen. They were always ready with a solution

for any practical query that I had. The numbers 221, 191 and 142 are firmly etched in my memory! I would like to thank both of them, wholeheartedly, for all their support.

I also wish to appreciate Dr. Huifei Jin for all her guidance, advice and support. The report has been enriched because of her critical and constructive feedback and I would like to thank her for taking time out of her busy schedule to review the manuscript. I would also like to thank Ms. Jiayang Wu and Mr. Alessandro Iannarelli for sharing their experience and ideas.

Mr. Siddharth Kumar, who worked on another aspect of the project, deserves a special mention. It was truly a pleasure working and learning together and I wish to thank him for sharing his knowledge and perspective which would sometimes get me out of proverbial "hot water".

Spending two years in a foreign country is nigh on impossible without the company of friends and I have been blessed to have unearthed some rare gems. I thoroughly enjoyed the time spent with my Electrical Sustainable Energy colleagues and my gang of close friends who were my family away from home. A special mention goes to Mr. Amit Pathak for being my sounding board and critiquing my work.

I would not be here without the ever present support of my family. Their unwavering confidence and faith in my abilities were just the boost that I needed at times to overcome difficult situations.

Delft, University of Technology
September 23, 2016

Pranav P. Karhade

I wish to dedicate this thesis to my late mother, Prajakta Karhade. She taught me to be the best I can be and to always perform to the best of my abilities. Although I will always miss her, I know that she watches over me and pushes me to strive for improvement.

Chapter 1

Introduction

Power transformers, as defined in the International Electrotechnical Vocabulary, were first developed in the late 1800s for the purpose of connecting power generators to lighting systems and the use of oil, copper, cardboard and steel in transformers came soon thereafter. The same materials are still in use today although the exact form and composition is not the same. Over 100 years of developing and improving both material and manufacturing technology have brought oil-filled transformers to their present state [1–4]. The development is set to continue, at least in part, due to the following reasons.

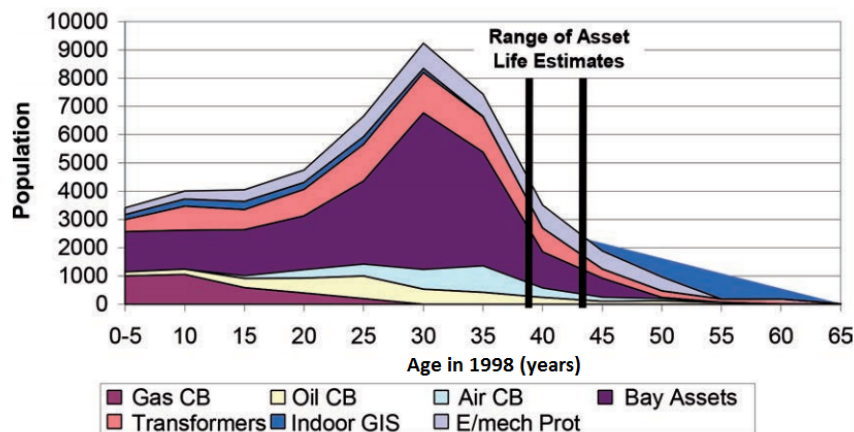


Figure 1-1: Age distribution of various substation facilities (1998) [5,6]

Manufacturers of power network assets generally quote a figure of about 25 to 40 years as life expectancy [7]. In the case of large power transformers, the figure is most often 40 years. Figure 1-1 shows the age distribution of substation facilities, as of 1998, recorded in a study by CIGRE WG 37.27. It can be clearly observed that a large percentage of transformers have been in operation for more than 40 years if extrapolated to today. This ageing infrastructure needs to be replenished with equipment that is at least equally reliable.

Moreover, the infrastructure also needs augmentation to cater to the increasing global power demand. New transformers are therefore required.

The alternatives to oil-filled are dry-type and gas-filled transformers. These three, together, constitute the types of transformers when classified on the basis of insulating material [8]. The cooling medium used in dry-type transformers is air which has inferior heat conveying properties relative to oil. Thus, they are bigger than oil-filled transformers of same rating as a larger volume of air needs to be circulated to take away the heat. Dry-type transformers are thus unsuitable for high power applications [9]. Gas-filled transformers use Sulphur hexafluoride (SF₆) as insulating and cooling medium. Environmental regulations such as EU 517/2014, which talks about reducing greenhouse (fluorinated) gases, threaten to impact the use of these transformers in the near future, despite being suited for high voltage, high power applications and being relatively safer than oil-filled transformers [10–12]. Thus, oil-filled transformers will still be needed as far as high voltage, high power applications are concerned.

Oil-filled transformers are here to stay for some time yet. Manufacturers will therefore strive to improve their business by supplying economically produced, reliable products and garnering a larger clientèle which entails increasing production. Optimizing the production process is thus beneficial to match the demanded throughput and knowledge of the production process is crucial to achieve optimization. The work done in this research constitutes a part of such an optimization initiative.

1-1 Manufacturing an oil-filled power transformer

In order to identify the part of a process that needs to be optimized, the entire process must be accurately known. It is useful to know the parts (Section 1-1-1) that make up an oil-filled power transformer before attempting to understand the way in which the pieces are put together (Section 1-1-2).

1-1-1 Overview: Parts of an oil-filled transformer

These transformers generally consist of the following parts (marked in Figure 1-2) [13]:

- Active part
 - Magnetic core
 - Windings (paper insulated)
 - Support insulation viz. barriers, cleats, shielding rings (paper, pressboard, wood)
- Tank
- Bushings
- Insulating medium - Oil
- Tap changers

The active part of a 3-winding power transformer is shown in Figure 1-2a and Figure 1-2b shows the same transformer after it has been erected at site. Additional accessories such as external cooling equipment, measurement and protective devices are also required depending on the purchase specifications.

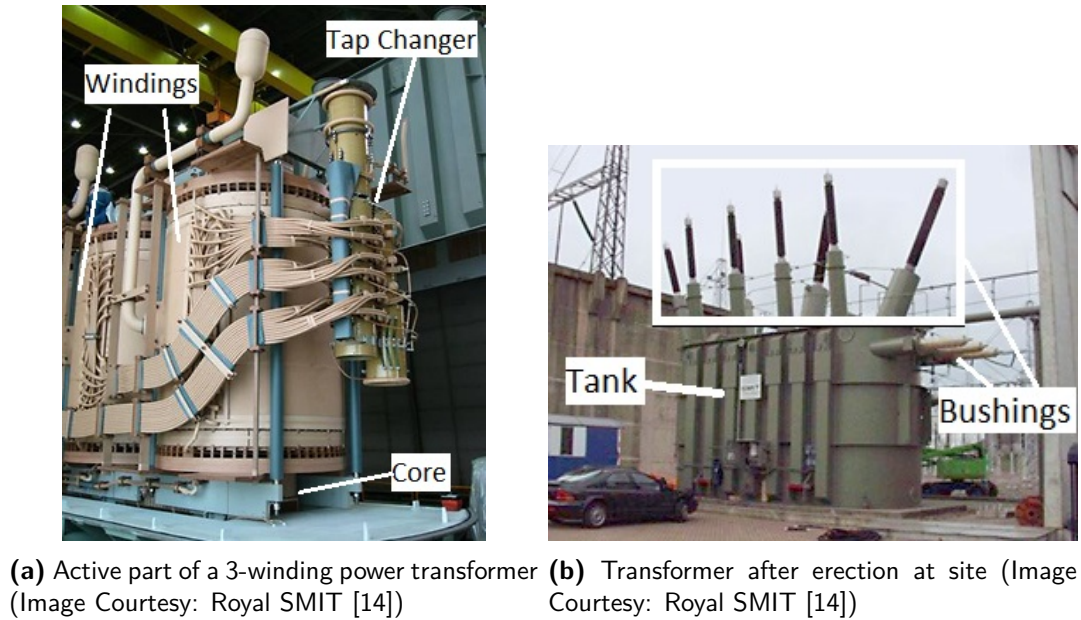


Figure 1-2: 3-winding power transformer: Internals and after site erection

Transformer Manufacturing Process

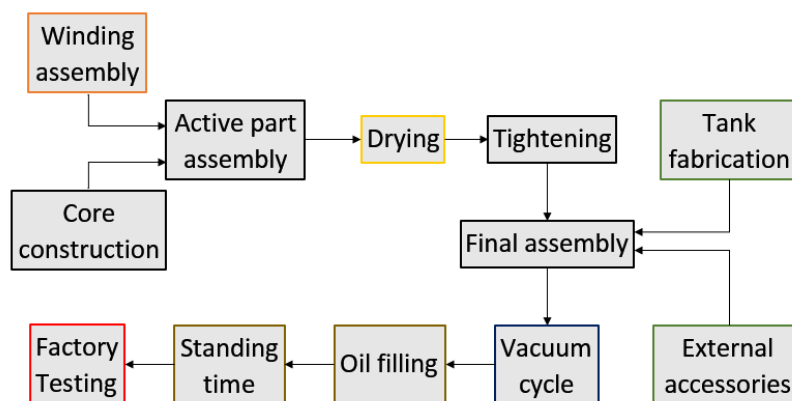


Figure 1-3: Transformer manufacturing process

1-1-2 Transformer manufacturing process

A flowchart describing the manufacturing process is shown in Figure 1-3. The process begins with core construction and winding assembly. Tank fabrication is scheduled in such a way that the tank is ready for the final assembly stage.

Active part assembly begins after the core and windings are prepared. The windings are mounted onto the limbs of the core and the active part is completed by adding the supporting frame and clamping structure. A clamping pressure is applied on the winding structure in order to ensure its mechanical stability and to prevent the windings from getting distorted by axial forces generated during operation and, more importantly, during short-circuits [15].

The next step of the process is drying of the active part. The transformer's cellulose based insulation (paper, pressboard, wood) absorbs moisture when exposed to the ambient. The amount absorbed depends on the temperature and RH. At 25 °C and 60% RH the moisture content can reach 7.5% [16]. This needs to be reduced to 0.5% so that the adverse effects caused by moisture, such as occurrence of partial discharges, are mitigated [4]. Processes such as vapour-phase drying are employed to dry the active part.

Post drying, the clamping pressure is re-tuned to the designed value in a process termed as *tightening* because the cellulosic materials shrink during the drying stage on account of losing moisture. The final assembly is performed next. The active part is fixed in the tank and the bushings and external accessories are also connected.

The transformer needs to be prepared for oil filling after final assembly. In order to achieve impregnation of the solid insulation by oil, a vacuum system is connected to the tank. Vacuum is held for a certain amount of time to allow proper evacuation of the air from within the tank and also from the pores in the insulation. Dried, hot oil that has been prepared separately is filled into the tank under vacuum. Vacuum is released after oil filling is completed.

This moment marks the start of the time interval known as *standing time*. Some amount of standing time is necessary for the oil to seep into the solid insulating materials and achieve proper impregnation [17]. Finally, the transformer is tested after standing time has elapsed.

Having become familiar with the transformer manufacturing process, the step to be targeted for optimization needs to be identified.

1-2 Standing time optimization and previous research

The logical target of an optimization initiative would be any activity that hampers resource utilization. Standing time, indicated in Figure 1-3, is intriguing from that point of view. Till the time a transformer is ready for testing, it occupies floor space which could otherwise be used to build another and consequently increase annual production capacity. Thus, it is beneficial to set the standing time to a minimum interval that still maintains the transformer's reliability.

Standing times (of similar sized transformers) may vary among manufacturers due to differences in processes and the knowledge gained from test results. Standing time can be multiple days, depending on the design. Extra caution on the part of the manufacturer may lead to overestimation of standing time since the cost of a high voltage, high power transformer runs into a few million Euro. This possibility of overestimation formed the basis of the standing time optimization project of which this research is a part. The objective of the project was to identify the factor(s) that govern standing time and to scientifically determine the minimum standing time necessary.

The following hypothesis was proposed for the work that preceded this research; *standing time is needed for high density cellulosic materials (pressboard and laminated wood) to be completely impregnated*. Shortening the interval would result in incomplete impregnation. Incompletely impregnated insulation could fail during testing or become vulnerable to failure during operation due to occurrence of PDs. PDs may arise due to presence of air-filled cavities in regions where oil has not yet penetrated. The hypothesis was refuted on the following grounds [18]:

1. Impregnation time constants obtained for the high density cellulosic materials were in hours rather than days and therefore did not warrant a long standing time.
2. Sizes of the naturally occurring cavities/voids found in these materials were too small to generate PDs based on the Paschen curve and the electric field stresses applied during the tests.
3. Completely dried but incompletely impregnated material did not show any PD activity at normal testing electric field stresses.

However, further investigations revealed that incompletely dried material exhibited PD activity immediately after impregnation with hot oil (70 °C). No PDs were observed on testing the same material after a standing time of a week (7 days).

1-3 Problem Statement

The results of the previous investigations indicate that *moisture and its associated dynamics, between oil and insulation material, can determine the duration of standing time*. This becomes the hypothesis proposed for this research.

The question then arises, where does this moisture come from? Referring to Figure 1-3, it is safe to assume that the active part is completely dried at the end of the drying step as the targeted moisture level is <0.5% [4]. The temperature of the active part is over 100 °C at that stage. Naturally, the active part begins to cool and convective air currents are generated.

Moisture is re-absorbed by the cellulosic materials depending on the environment in which tightening takes place and this is aided by the aforementioned convective currents. The amount of moisture absorbed also depends on the duration of the tightening activity. Some of the absorbed moisture may be extracted during the vacuum cycle due to low boiling point of water in vacuum. Post impregnation, the moisture migration process slows down because of the lower diffusion rate of moisture in oil [16, 19]. Thus, there is a possibility that some moisture remains trapped inside the insulation.

As mentioned before, the hypothesis is drawn on the basis of results obtained for pressboard and wood. Insulating paper is also used in a transformer as mentioned in Section 1-1-2. Although it is a low thickness material, the amount of paper used in a transformer is certainly not negligible. Moreover, paper is used in areas that are either very exposed to the ambient (tubes connecting windings to bushings) or are difficult to access (on conductors within a winding). These factors have a direct bearing on moisture absorption. Thus, the influence of paper on the post-impregnation standing time also needs to be investigated.

1-4 Research Questions

Based on the results of the previous investigations, mentioned in Section 1-2, it can be surmised that the disappearance of PD activity indicates the completion of standing time. The following questions arise when these observations are coupled with the hypothesis stated in Section 1-3. The aim of this research is to find an answer to these questions and check the validity of the hypothesis.

1. Can PDs attributable to moisture be observed in insulating paper for the electric field stress used during PD detection tests?
2. Does paper or low thickness cellulosic insulation material actually play a role in determining the standing time?
3. How does the duration of the vacuum cycle, prior to impregnation, influence the moisture migration process? Could a longer duration cause a significant reduction in standing time?

1-5 Thesis Outline

The remainder of the report is divided into five chapters covering the following aspects of the research:

Chapter 2 - Theoretical Backdrop

Use of paper in transformers, effect of moisture on properties of paper and factors affecting the rate of moisture migration, testing of transformers, use of PD detection and an overview of PDs along with PD in OIP are the topics discussed in this chapter.

Chapter 3 - Sample and Oil Preparation

This chapter contains the specifications of all samples that were used in the research. Additionally, the idea behind the sample design, selection of conditioning parameters and process of conditioning samples are also discussed. A section on the oil preparation process is also included.

Chapter 4 - PD Test Setups and Procedure

The test setups used during the course of the research are described in this chapter after an overview on PD detection is given. The oil impregnation process used for each sample is discussed along with the PD test procedure.

Chapter 5 - Results of the Investigations

This chapter presents the results obtained from the climate exposure experiments and the PD tests. The results are analysed in the form of discussion which are included in the chapter.

Chapter 6 - Conclusions and Recommendations

This chapter presents the conclusions drawn from the investigations conducted as part of this research and also includes some recommendations for studies that could be undertaken as follow-up.

Theoretical Backdrop

The takeaway from the discussion in Chapter 1 is that paper, moisture and PD occurrence are the principal elements in this research. Although the parts and materials used in the manufacture of an oil-filled power transformer have already been introduced, further discussion is required on the types of paper used and their locations within a transformer. This discussion forms Section 2-1. Section 2-2 deals with moisture in paper. Section 2-3 introduces the test plan of a transformer and explains why PD detection was chosen as the diagnostic technique. An overview of PDs is provided in Section 2-4.

2-1 Paper in oil-filled transformers

Solid insulating material, if used in a High Voltage (HV) transformer, must be easily impregnable [20]. Paper is such a material. Naturally, paper in this context refers to electrical grade paper. The electrical (insulating) properties of paper are dependent on its physical and chemical properties. Thus, varying the manufacturing process results in the production of different kinds of paper.

2-1-1 Types of paper and their location

The types of paper that can be used in a transformer are [21]:

- **Insulating (Kraft) paper**

It is produced in the form of a single layer wherein the desired density, thickness and moisture content are set by the temperature and pressure used during the rolling stage.

- **Thermally upgraded paper**

Heating causes degradation of paper resulting in breaking of the polymer chains due to the scission of hydrogen bonds. For greater thermal stability and reduced thermal degradation certain additives (stabilizers) are used during manufacturing, resulting in the production of thermally upgraded paper.

- **Crêped paper**

The crêped effect is specially added during the manufacturing process by way of an irregular increase in thickness in order to enhance the elongation property of the paper in the machine direction.

- **Presspaper**

In simple terms, it is a multi-layered arrangement of insulating papers.

- **Crêped presspaper**

- **Highly extensible paper**

Similar to crêped paper but processed in a way that it retains elasticity for a longer duration.

The specifications for insulating paper and for presspaper are stated in International Electrotechnical Commission (IEC) 60554 and IEC 60641, respectively [22, 23]. Additional coatings such as conductive layers can also be added to these papers in order to serve special functions.

Thermally upgraded presspaper and crêped presspaper are selected as material specimens in this research and small rolls of these types of papers are shown in Figure 2-1 and Figure 2-2, respectively. The datasheets describing the various properties of these papers are attached in Appendix B. On comparing datasheets, it is observed that the density of presspaper is greater than that of crêped presspaper. This fact is alluded to during the discussion of the results in Section 5-1.



Figure 2-1: Thermally upgraded presspaper



Figure 2-2: Thermally upgraded crêped presspaper

Having been introduced to the types of paper commonly used in oil-filled transformers, the focus now shifts to understanding the locations of these papers in a transformer. The active part of a transformer (seen from the HV side), shown in Figure 2-3, is revisited for this purpose. The winding tubes marked in the figure are wrapped using crêped presspaper whereas presspaper is used as insulation on the tap changer leads and cables. It can be clearly noticed that these regions are very exposed to the surroundings and thus, are very susceptible to moisture ingress. At the same time moisture egress is also not impeded.

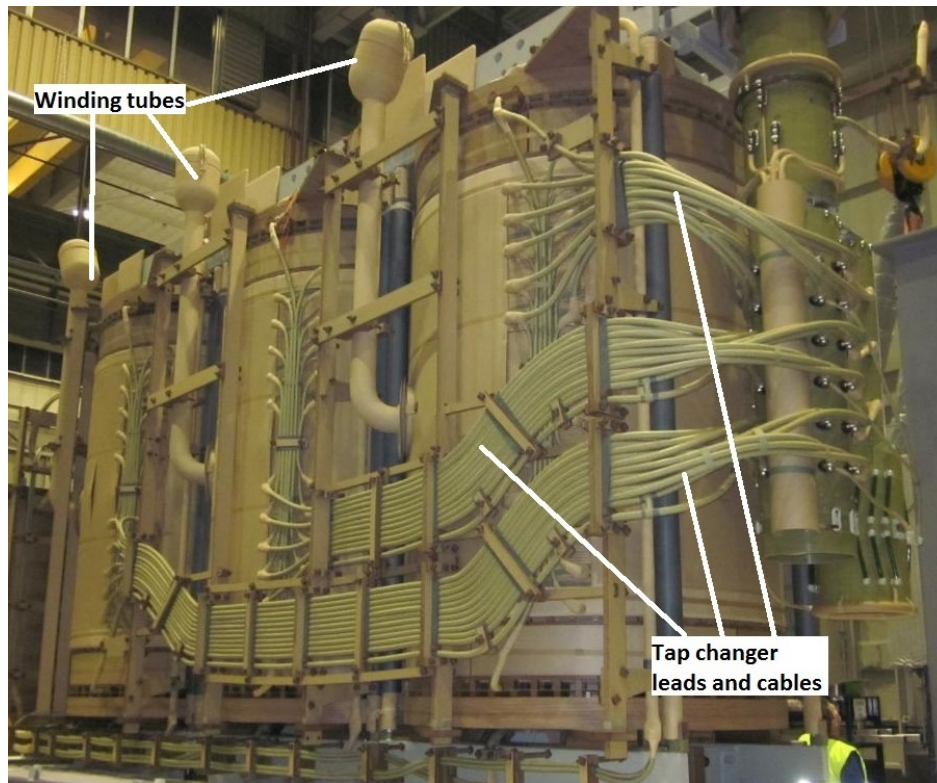


Figure 2-3: Active part of a transformer from HV side (Courtesy: Royal SMIT)



Figure 2-4: Front view of a winding (Courtesy: Royal SMIT)

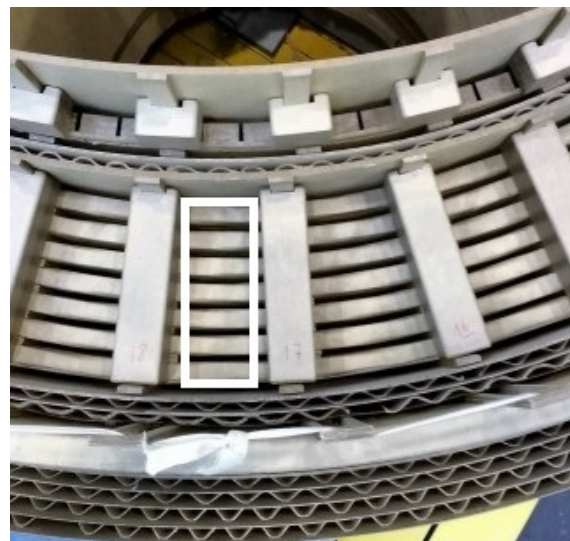


Figure 2-5: Top view of a section of a winding (Courtesy: Royal SMIT)

Figure 2-4 shows the front view of a winding composed of several turns of continuously transposed conductors (CTC) wherein each turn has been insulated using presspaper. Figure 2-5 is consulted in order to get an idea regarding the susceptibility to moisture ingress of paper used

in such regions. The box marked in the figure indicates the rows built from CTC. The gaps seen between the rows are the axial cooling ducts through which the convective air currents mentioned in Section 1-3 can flow. Thus, the axial surfaces of the paper wrap can interact with the surroundings with relative ease as compared to the surfaces between adjacent turns seen in Figure 2-4.

Crêped presspaper is also used for wrapping electrostatic stress control rings. Crêped texture is preferred because the shapes of these rings are customized to maintain a smooth electric field profile and the elongation property helps avoid damage at the bends [21]. Papers with a metal coating on one side, or a metal foil, are used in places where equipotential surfaces need to be created such as ends of windings and around the magnetic core [24].

2-1-2 Method of wrapping paper

The transformer designer decides the thickness of the insulation to be applied on each part. The process of wrapping paper on the object to be insulated is also termed as lapping. The dielectric strength of the lapped insulation depends upon the *registration* [25]. Registration indicates the amount of overlap between adjacent turns of the paper. 50% registration is illustrated in Figure 2-6 wherein it is clear that each turn covers half of its predecessor. 50% registration is commonly used by manufacturers.

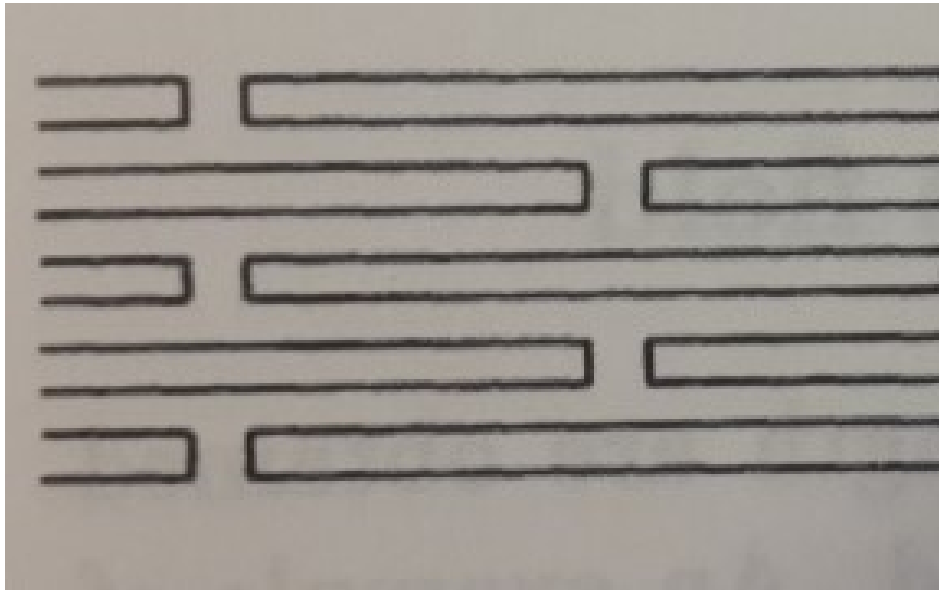


Figure 2-6: Schematic illustrating 50% registration [25]

2-2 Moisture in paper

Since moisture is the indicated problem, it is worthwhile to explore the impact of moisture on the dielectric properties of paper and what factors influence the rate of moisture absorption and extraction.

2-2-1 Effect of absorbed moisture on paper

Water, or moisture, is detrimental to the dielectric properties of any insulating material, be it solid, liquid or gas. The effect of water on the properties of a material depends upon the state in which water exists in that material. Paper is a hygroscopic/hydrophilic material. Water can exist in any of the following states insofar as paper, or cellulosic insulating material in general, is concerned [26]:

- vapour
- adsorbed as a monolayer
- adsorbed as polymolecular layers
- condensed in capillaries
- free, as an impregnating liquid

The states can also be broadly classified into *free water* and *bound water*. Free water manifests in the form of large clusters between the fibres of the paper or in the form of water vapour in the pores. Bound water occurs in the form of water molecules bonding with the hydroxyl (-OH) groups of the cellulose molecules. Referring to the aforementioned list, free water comprises of the vapour state, the condensed state and the free (impregnating liquid) state whereas the adsorbed states belong to the bound water category. The state adopted by water depends on the quantity of water available for absorption. Higher the moisture content, higher the likelihood of free water [26–28].

The absorption of water by cellulose occurs in three steps. The first two steps are actually adsorption processes and the condensation process constitutes the last step. Initially, water is adsorbed very quickly in the form of a monolayer [29]. Bound water, by itself, is observed up to a moisture content of 2% in non-impregnated paper after which free water properties are also expressed. In case of impregnated paper, bound water is observed only up to 1% moisture content [27]. Further supply of water leads to the formation of polymolecular layers. Condensation in the pores and capillaries of cellulose begins only after this stage and if more moisture is available. The monolayer structure persists up to a moisture content of 3-4% in paper. The minimum RH threshold for water to appear in the condensed form is stated as 60% [26].

Cellulose is comprised of both crystalline and amorphous phases. The crystals cannot get hydrated and therefore only adsorb water on the surface. This adsorbed water does not affect the properties of cellulose as mentioned in [29]. This observation is corroborated in [27] wherein the dielectric constant of bound water is determined to be $\epsilon_r=4$, which is nearly the same as the relative permittivity of paper. The changes in dielectric properties of cellulose are attributed to the moisture absorption in the amorphous zones wherein water is not tightly bound [29, 30].

This absorbed moisture causes a weakening of the dielectric strength of cellulose and makes it more susceptible to PDs [31]. Moreover, the state of water remains unaffected by impregnation as oil occupies spaces where water is not present [28].

2-2-2 Factors affecting rate of moisture absorption by dry paper

The rate at which moisture is absorbed by dry paper depends on the following factors [32]:

1. Surrounding conditions

(a) RH

(b) Temperature

They define the amount of moisture available for absorption; higher the RH and/or the temperature, greater is the moisture content. This creates a steeper gradient between the moisture content of paper and that of the surroundings which causes paper to absorb moisture faster and attain equilibrium sooner.

2. Circulation of the surrounding medium air/oil (natural or forced)

Moisture is absorbed faster if the circulation of air/oil is more efficient as a greater volume of the medium comes into contact with paper. Moreover, the medium is replenished with moisture from the surroundings at a faster rate.

3. Density of the paper

Denser the paper, the molecular structure is more closely packed and thus, the size of pores and capillaries are smaller. Thus, a longer duration is necessary for moisture to be absorbed.

4. Physical dimensions

(a) Thickness

Since absorption begins from the surface and proceeds inwards, thicker paper requires a longer time to absorb moisture.

(b) Surface area exposed

A larger exposed surface area of paper allows for a greater interaction with the surrounding and thus, moisture is absorbed faster.

5. Non-impregnated or Impregnated with oil

Oil impregnated paper absorbs moisture at a slower rate than non-impregnated as oil slows down the movement of water molecules. This is indicated in the calculations performed by the author in [33] which are based on the results observed in [16, 34]. Moreover, oil molecules occupy the spaces in the cellulose structure which minimizes the space available to water molecules [28].

RH and temperature of the surroundings are the major factors that determine the total amount of moisture absorbed by paper. The rest of the factors exhibit little to no influence on the final moisture content attained by paper [32].

The factors that affect the rate of extraction of water are almost the same. The additional factor that comes into play is the level of vacuum in case vacuum drying is employed. The absolute pressure of air determines the saturation temperature and consequently the amount of moisture that can be transported.

2-3 Transformer testing

PD occurrence is related to transformer testing. Therefore, an overview of equipment testing is given in Section 2-3-1 before discussing the test plan of a large oil-filled power transformer in Section 2-3-2.

2-3-1 Overview of equipment testing

The overall quality of the design and manufacturing process involved in the production of any equipment is determined by performing a set of tests. Generally speaking, the tests performed on any equipment can be categorized into *type tests*, *sample tests*, *routine tests* and *commissioning tests*.

Type and sample tests are generally destructive and therefore are conducted on one (type tests) or a few specimens (sample tests) to test the limits of a particular design. These tests are included in the testing plans of mass produced equipment. Routine tests are non-destructive in nature and are performed on each piece of equipment that is manufactured. Commissioning tests are performed, both, during and after erection of the equipment at site and culminate with placing the equipment in service [35].

Some of the routine tests are conducted after completion of specific stages of the manufacturing process, permitting timely corrective action to be taken, while some are conducted at the end [17]. A test plan is agreed with the client, also termed as purchaser, at the contract formulation stage which lists out the tests to be conducted in order to determine the acceptability of the equipment. The plan is largely dictated by the governing standards, such as IEC, which permit some modifications in the test parameters or the acceptance limits [36]. The tests that constitute the agreed plan are collectively termed as Factory Acceptance Tests (FAT).

The parameters of these tests (such as applied voltage, duration) are designed in such a way that successful completion of these tests almost guarantees that the equipment is fit for operation and will deliver the desired service life of >40 years [35]. The client authorises the dispatch of the equipment from the factory premises only after successful testing. This authorisation is often connected to a major payment milestone in the contract. From the purchaser's perspective, the results of these tests serve as a reference point for the on-site commissioning tests and subsequent periodic maintenance activities. Thus, the quality of the product and revenue for the business are both dependent on the equipment passing the FAT.

2-3-2 Typical test plan of an oil-filled transformer

IEC 60076 is the applicable standard for most of the single and three phase power transformers, including oil-filled transformers. The routine, type and special tests that can be conducted are described in part-1 of the standard. The tests that need to be performed vary depending upon the voltage rating of the transformer's windings. The distinction between transformers is based on U_m , which is the highest voltage for equipment applicable to a transformer winding [36,37]. The type tests mentioned in the standard (such as temperature rise tests) are not entirely destructive since transformers, particularly large oil-filled power

transformers, are customized for every order and really expensive which renders damaging them during testing illogical.

Dielectric tests are an integral part of the transformer testing scheme as they enable the evaluation of the insulation performance. This is the reason why successful FAT is an indicator of sufficient standing time. Part-3 of IEC 60076 specifies the guidelines for the dielectric tests, sub-divided into three ranges of U_m . It also specifies the sequence in which the tests are to be conducted, which is repeated here, with a note stating that the Induced voltage test with PD measurement (IVPD), if applicable, will be the last test [36].

1. Lightning impulse tests
2. Switching impulse tests
3. Applied voltage tests
4. Line terminal AC withstand test
5. Induced voltage withstand test
6. Induced voltage test with PD measurement

Thus, absence of PDs above a predetermined level during the IVPD implies completion of the dielectric tests and acceptance of the insulation quality. This is one of the reasons why PD detection is chosen to determine the sufficiency of the standing time.

Another reason is discussed here. Compared to the rest of the dielectric tests, time of voltage application during IVPD is the longest with just one step lasting one hour. In the other tests the voltage application duration is in seconds or a few minutes [36]. The amount of energy put into the transformer during the test is comparatively much larger due to its duration and also because it is an overvoltage test. This high energy input is sufficient to initiate discharge phenomena and consequently indicate most deficiencies in the insulation structure that could arise due to insufficient standing time. This claim is supported by the guideline followed by manufacturers which states that standing time is the minimum time necessary to avoid PD occurrence during FAT.

PD detection is the diagnostic technique most suited to determining if the standing time has been sufficient and thus, was used in this research. The test procedure, including the time sequence of voltage application, is covered in Section 4-4. The acceptance criteria, as defined in IEC 60076-3, are as follows [36]:

1. No collapse of the test voltage occurs
2. None of the PD levels recorded during the one hour period exceed 250 pC
3. PD levels measured during the one hour period do not exhibit any rising trend and no sudden sustained increase in the levels occur during the last 20 min of the test
4. Measured PD levels during the one hour period do not increase by more than 50 pC
5. PD level measured at a voltage level of $(1.2 \times U_r/\sqrt{3})$ after the one hour period does not exceed 100 pC

The test can be considered valid only if the measured background PD level does not exceed 50 pC at both the beginning and the end of the test.

2-4 PD due to moisture in oil-paper insulation

An overview of PDs is provided before discussing discharge activity associated with oil-paper insulation. PDs, as defined by Kreuger in [35], are breakdown phenomena that do not completely bridge the distance between electrodes. Prolonged discharge activity can lead to complete insulation breakdown. PDs can be classified into three categories [35]:

- **Internal discharges**

Generally associated with the presence of gas/air filled voids or cavities in solid dielectrics. Inception voltage of the discharge activity can be estimated by using the Paschen curve.

- **Surface discharges**

Initiated along interfaces wherein the interface is bound by liquid or gas. Tangential electric field stresses decide the inception voltage.

- **Corona discharges**

These discharges are initiated at sharp metallic points. They are unwanted as they interfere with the results of the PD test and therefore, sharp points and edges are avoided while preparing samples and designing test setups.

Being able to identify the type of discharge is beneficial as it acts as an aid in locating the defect/problem area within the equipment. An overview of the method used for detecting and measuring discharges is given in Section 4-1.

As discussed in Section 2-2-1, moisture decreases the dielectric strength of OIP insulation. This is more so when the transformer, and consequently the oil, is hot. Moisture starts to migrate from the paper into the oil as the temperature of the transformer increases. This is because the solubility of water in oil increases with temperature and at the same time the ability of paper to retain water diminishes. The migration is dictated by the equilibrium isotherms. Rapid moisture migration can lead to bubble formation and subsequent initiation of breakdown phenomenon. PDs may also be initiated by gas bubbles formed due to application of high electric field stresses on moisture contained in the paper. The aforementioned sources of PDs become active in case the moisture content in OIP is more than 3% [38].

Chapter 3

Sample and Oil Preparation

Crêped presspaper and presspaper are employed in the construction of an oil-filled transformer as mentioned in Section 2-1 wherein, their respective susceptibility to both moisture ingress and egress has also been discussed. As explained in Section 1-3, moisture can remain trapped in the paper post impregnation. Therefore, an investigation needs to be conducted in order to determine if, and when, PD activity will be observed in these conditions. If PDs are observed, the change in PD behaviour with increasing standing time also needs to be investigated.

This investigation was performed by way of sample testing. The samples were prepared and conditioned in a way that resembles the actual transformer manufacturing process. As explained in Section 2-1-2, paper is wrapped to a thickness defined by the design using 50% registration. The samples required to conduct this research were also prepared similarly.

Section 3-1 explains the geometries of the samples prepared during this research. The effect of clamping is dealt with in Section 3-2. Section 3-3 describes the basis for selection of the sample conditioning parameters. The process used to condition the samples is described in Section 3-4. Section 3-5 explains the method used to obtain dry, hot, PD free oil for impregnation.

3-1 Sample geometries

A two-pronged approach was adopted to conduct the investigation. On one hand, moisture ingress and egress processes with respect to paper were studied and on the other, the influence of standing time on PD behaviour in OIP was dealt with. This was achieved by adopting samples geometries that served their aforementioned purpose and were convenient to use too.

3-1-1 Samples for studying moisture ingress and egress

The time-frame under consideration in this research, as far as moisture ingress and egress are concerned, is from the end of the drying stage to the start of oil filling. This is because paper

is most susceptible to moisture migration when convective air currents are flowing and the paper has not been impregnated as explained in Section 2-2-2. Hence, moisture ingress was characterized by exposing samples to a particular climate that may be encountered on the shop-floor during tightening. The climate selection is discussed in Section 3-3. Exposure of samples to vacuum was the method used to understand moisture egress.

Figure 3-1 shows the substrate chosen for preparing these samples. The dimensions of the substrate are shown in Figure 3-2.¹ Crêped presspaper or presspaper wrapped on the curved surface of this cylindrical substrate constitutes a sample. The specifications of the samples prepared as part of this investigation are given in Table 3-1 and Figure 3-3 shows the samples. Three samples of each type were prepared to factor in variations caused due to wrapping by hand.

A substrate, different from that used for PD tests, was used because this investigation could then be conducted independently. Moreover, the substrate used for PD tests, as mentioned later, was custom designed for multiple tests. The size of the vacuum oven was not suited to placing samples of that size while maintaining sufficient separation between them.



Figure 3-1: Substrate for wrapping paper

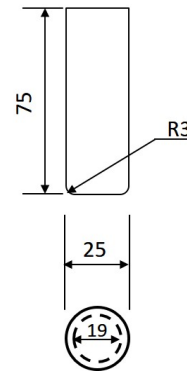


Figure 3-2: Dimensions of the substrate

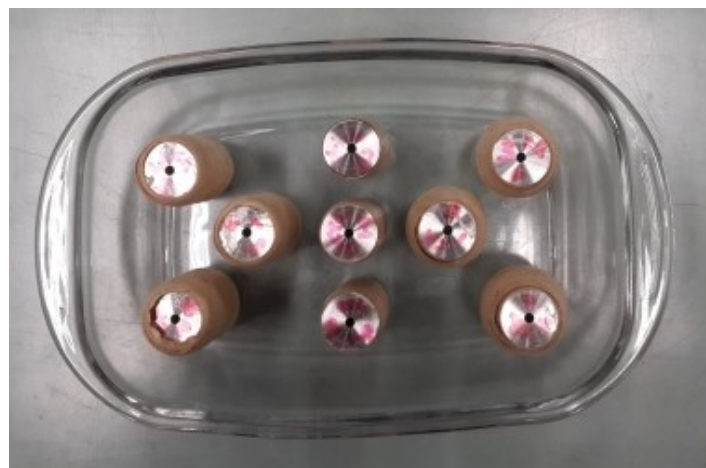


Figure 3-3: Samples for moisture ingress and egress study

¹All dimensions are in mm

#	Paper type	Wrapping thickness (mm)	Sample designation
1	Presspaper	1.4	PP.1 - PP.3
2	Crêped Presspaper	3.0	CR.3.1 - CR.3.3
3	Crêped Presspaper	6.0	CR.6.1 - CR.6.3

Table 3-1: Specifications of the samples for moisture ingress and egress study

The wrapping thickness chosen for the samples, as mentioned in Table 3-1, were based on the thickness used for the PD tests. The 6 mm crêped presspaper samples were included so as to observe the effect of wrapped layer thickness on the moisture migration rates. Crêped presspaper is used for wrapping layers of greater thickness as compared to presspaper as per manufacturer's data. For example, thickness of the wrapping on the HV tube section can be up to 10 mm.

3-1-2 PD test samples

The substrate chosen for preparing PD test samples is shown in Figure 3-4. It is a solid stainless steel bar 300 mm in length, 120 mm in width and 20 mm thick. All surfaces are well polished. The edges are rounded off with 10 mm radius of curvature to provide a profile suitable for wrapping paper and to avoid regions of electric field concentration. These bars were provided by Royal SMIT. Paper was wrapped on the bar up to the desired thickness. An example of a bar wrapped with crêped presspaper is shown in Figure 3-5. Such a wrapped bar is henceforth referred to as a *sample bar*.

The test setup, described in Section 4-2, is devised in such a way that the bar is connected to ground potential during the test for which an M4 sized hole is drilled into one of the 120 mm faces. The depth of the hole is made suitable for a banana plug type connector.



Figure 3-4: Substrate for PD test samples



Figure 3-5: Substrate wrapped with Crêped presspaper

The length of the bar allows multiple locations to be tested in a single impregnation which is desired since the PD behaviour needs to be observed for increasing standing time. The representative test locations are shown in Figure 3-6. This electrode placement also forms the basis of the clamping frame design which is described in Section 3-2. Each test location is termed as a *sample*. Thus, *one sample bar provides five samples*. The particulars of the sample bars prepared during the course of this research are given in Table 3-2. The schedule for testing each sample is discussed in Section 4-4.

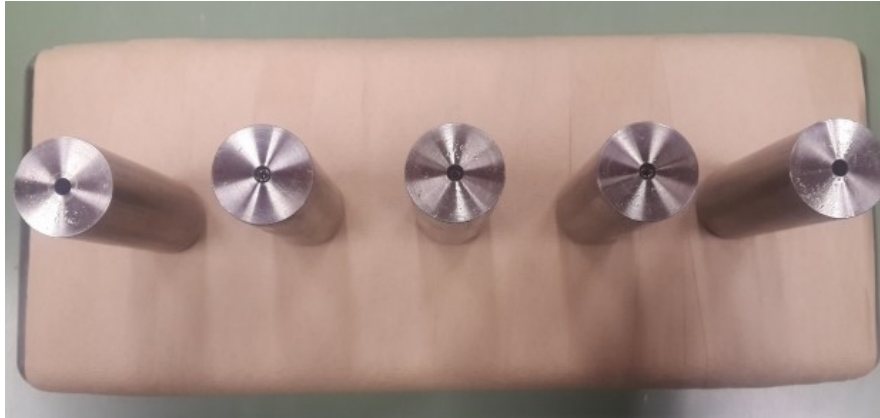


Figure 3-6: Representative electrode placement on a sample bar during PD testing

The average thickness was arrived at by taking eight measurements along the length of the sample bar. Pressurized callipers are used to measure the thickness of crêped presspaper wrapping in the factory on account of the elongation property. However, normal callipers with manual pressure were used for measuring thickness in the lab which is the reason behind the variation observed in the thickness of crêped presspaper samples.

Sample bar no.	Paper type	Avg. thickness (mm)	Sample designation	Wrapped at
1	Crêped Presspaper	2.5	1.1 - 1.5	SMIT
2	Crêped Presspaper	3.0	2.1 - 2.5	SMIT
3	Crêped Presspaper	3.0	3.1 - 3.5	SMIT
4	Crêped Presspaper	3.3	4.1 - 4.5	SMIT
5	Crêped Presspaper	3.1	5.1 - 5.5	SMIT
6 ^a	Presspaper	0.9	6.1 - 6.5	TU Delft
7	Presspaper	1.4	7.1 - 7.5	TU Delft
8	Presspaper	1.4	8.1 - 8.5	TU Delft
9	Presspaper	1.4	9.1 - 9.5	TU Delft
10	Presspaper	1.4	10.1 - 10.5	TU Delft
11 ^b	Presspaper	1.3	11.1 - 11.5	TU Delft

^a Trial sample

^b Variation produced due to wrapping by hand

Table 3-2: Particulars of the sample bars prepared during the research

Looking back at the manufacturing process illustrated in Figure 1-3, the steps following active part assembly are drying, tightening and vacuum pulling. In this document drying and tightening are collectively referred to as the conditioning process which is elaborated upon in Section 3-4. The applied vacuum cycle is explained in Section 4-3. The parameters and durations of these processes are selected and/or changed in order to observe the effects of the following factors on the PD activity, as dictated by the research questions mentioned in Section 1-4:

1. Changing duration of active part exposure to ambient

Moisture ingress is dependent, among others, on the RH and temperature of the surrounding air [39]. In case tightening is performed in an uncontrolled environment, changing ambient conditions are encountered over the course of the year. Thus, certain representative values must be chosen for testing purposes. These can be, for example, the highest, lowest or average RH observed during the year. The chosen temperature and duration of exposure can directly be correlated to the time interval between removal of the active part from the oven and completion of the tightening activity. The selection of ambient conditions, to which the samples were exposed, is discussed in Section 3-3.

2. Duration of vacuum prior to impregnation

Lowering the pressure reduces the boiling point of water and that is why moisture egresses from the paper. The prevailing temperature and the level and duration of the applied (stable) vacuum affect the amount of moisture extracted. This is because pressure and temperature of air determine its capacity to hold moisture and time allows the moisture migration process to occur. The vacuum level is fixed by the vacuum pump capacity and the temperature is near ambient by the time the tank assembly is completed. Thus, vacuum duration is the main factor affecting moisture egress and thus it was varied during the experiments conducted as part of this research.

3. Presence of clamping force

It is posited that the necessary clamping of the active part causes a reduction in the surface area exposed to the ambient, particularly in the case of the winding inter-turn insulation. This reduction in turn forms an impediment to moisture ingress and egress. The construction of some of the sample bars mentioned in Table 3-2 was modified, as explained in Section 3-2, in order to validate this assumption.

3-2 Effect of Clamping

As mentioned in Section 1-1-2, a clamping pressure is applied on the winding structure. As per manufacturer's data, the clamping pressure applied is in the region of 20 kg.cm^{-2} . This pressure needs to be applied on the laboratory sample bars as well in order to ascertain its impact vis-a-vis the assumption stated in Section 3-1-2.

A frame was designed which allowed the exertion of clamping force on the paper layers and also satisfied the objective of being able to conduct multiple PD tests on the same object. The frame components were made of the same laminated wood as used in transformer manufacturing.

Figure 3-7 shows the top view of the frame. The five holes seen along the centre line are the five test locations. These holes are 12 mm in diameter and 20 mm deep and are made to provide access for the connection between the HV electrodes and the test setup. A portion of the top surface of the HV electrodes can be seen inside these holes along with the M4 sized holes drilled into the flat face of each electrode. The depth of these M4 holes are suitable for a banana plug type connector. This sort of connection makes changing test locations very easy; simply remove the plug from one spot and insert it into the next! The HV electrode used is the same as that shown in Figure 3-1.

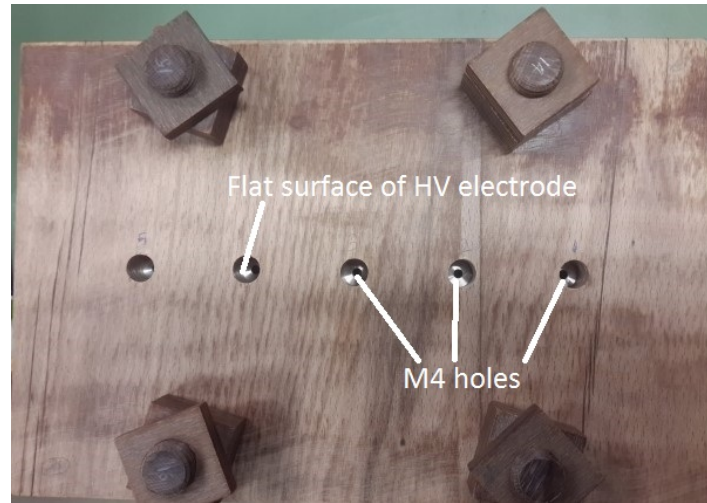


Figure 3-7: Top view of the clamping frame



Figure 3-8: Underside of the top block of a clamping frame

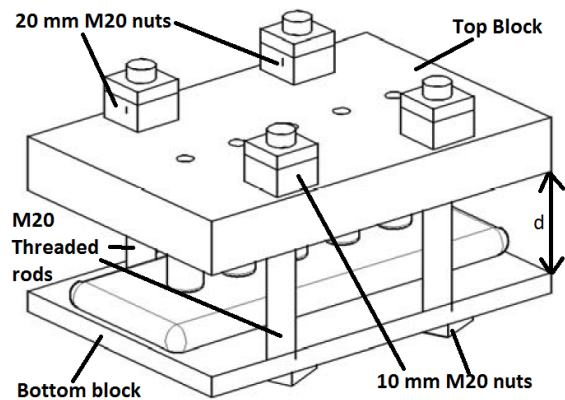


Figure 3-9: Schematic representation of the clamping frame with sample bar (Courtesy: Royal SMIT)

Figure 3-8 shows the underside of a top block after conducting a test. The five HV electrodes can be seen fixed in their respective positions. They are inserted into holes, of 25 mm diameter and 20 mm depth, cut on the underside of the top block. The depth grants stability to the electrode and prevents the frame from deforming due to the exerted force.

Figure 3-9 is the schematic representation of the clamping frame along with a sample bar. The holes in the 15 mm bottom block are threaded. The frame is held together using four 180 mm long, M20 sized threaded rods and secured using 10 mm thick nuts on the bottom and top and 20 mm thick nuts on the top as seen in Figure 3-9. The nuts are M20 too. The 10 mm nuts (top and bottom) perform the function of locking nuts. The force is mainly generated by tightening the 20 mm nuts at the top.

Setting the clamping force

A measuring system is needed in order to set the right clamping force. A load cell arrangement, shown in Figure 3-10, was devised so that the clamping force could be measured. The aluminium holder seen in the figure is made with an extension that fits the hole on the underside of the top block of the frame. The load cell (DS Europe - BC 303) is placed inside the aluminium holder first and then the brass stopper is put on top of it. The bottom of the brass stopper is profiled in the same way as the HV electrode so that the surface area in contact with paper remains the same. As the contact surface is of a circular cross-section, the area is calculated using Eq. (3-1):

$$Area = \pi (radius_{circle})^2 \quad (3-1)$$

The diameter of the circular face of the electrode in contact with paper is 19 mm (1.9 cm) (radius: 0.95 cm) as shown in Figure 3-2. Thus,

$$Area = \pi \times (0.95)^2 = 2.84 \text{ cm}^2$$

The instrumentation amplifier (Kyowa[®] - WGI-300C), used for reading the force measured by the load cell, displays the value in kilograms. Therefore, in order to obtain a pressure of 20 kg.cm^{-2} the force must be 57 kg for an area of 2.84 cm^2 .

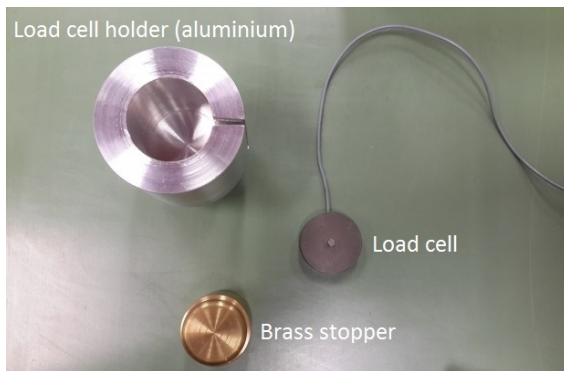


Figure 3-10: Load cell arrangement



Figure 3-11: Level check performed while setting clamping force

One of the HV electrodes is replaced by the load cell arrangement and the frame is assembled. Using a spirit level, as shown in Figure 3-11, the alignment of the top block is checked so that the electrodes remain flat against the paper. The 20 mm nuts are tightened while maintaining the alignment till the 57 kg value is attained. The distance 'd' between the bottom of the top block and the top of the bottom block, marked in Figure 3-9, is measured. This distance becomes the reference for further measurements.

The frame is disassembled, the load cell arrangement is swapped with another electrode and the frame is reassembled. The nuts are tightened till the distance 'd' measured previously is obtained. The corresponding force measurement is noted and compared. The process is similarly carried out for all remaining electrode locations. The spirit level is always used and

no location is kept empty during this procedure. Finally, the last electrode is fitted in place of the load cell arrangement and the frame is tightened till the distance 'd' is achieved. The object can now be conditioned and the conditioning process is discussed in Section 3-4.

Referring to Table 3-2, the sample bar numbers to which the clamping frame was applied were 3, 4 and 7 to 11.

The drawings pertaining to this frame design are attached in Appendix A.

3-3 Selection of sample conditioning parameters

As mentioned in Section 3-1, the RH and temperature need to be chosen for conditioning the sample bars. The best way to arrive at those conditions is to create a long term record of the ambient conditions prevailing in the area where the tightening activity takes place on the factory floor. Higher the RH of air, higher is its moisture content and thus, more moisture is available to ingress into the paper. Thus, a value of 75% was chosen as the humidity level in consultation with production engineers so that a worst-case scenario can be studied. Such a scenario may be encountered by only a few transformers each year. If no PD activity occurs at this RH condition then it will not occur at lower levels of RH as there will be lesser moisture in the paper prior to impregnation.

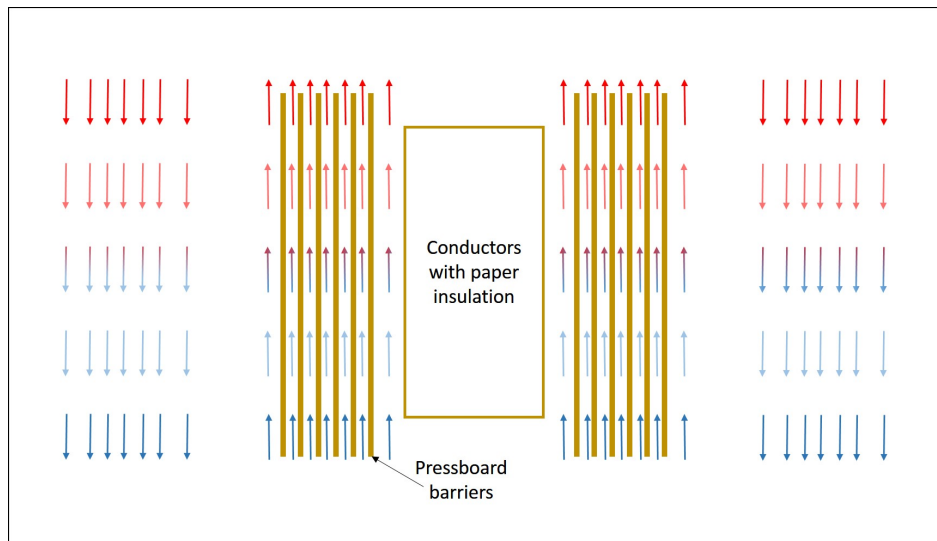


Figure 3-12: Simplified schematic representation of the convection air currents

The post drying activities play a major role in the selection of the temperature that was eventually used for sample conditioning. The active part is at $>100\text{ }^{\circ}\text{C}$ when taken out of the oven after drying. It is moved to the location where tightening is to be performed. Convection air currents begin to flow due to the temperature difference between the active part and the surrounding atmosphere. These currents are schematically illustrated in a simplified manner in Figure 3-12. The active part is cooled in the process while at the same time moisture in the air is also absorbed by the solid insulation. Cooler, denser ambient air enters the structure at the bottom which accelerates the cooling of the bottom section. Thus, the temperature varies

over the height of the active part. 60 °C was the temperature chosen for sample conditioning as per the data provided by the manufacturer.

Therefore, the ambient conditions used for conditioning the samples in order to simulate the tightening process occurring in a worst case scenario (implying maximum moisture ingress) were 60 °C and 75% RH.

3-4 Sample conditioning process



(a) External view of the drying oven



(b) Assembled frame kept for drying

Figure 3-13: Drying samples in the oven

The conditioning of the samples used for moisture ingress and egress studies is explained in Section 5-1 whereas the conditioning of the PD test sample bars is discussed here.

Preparing the samples as explained in Section 3-1 is similar to building a transformer winding. If the clamping frame discussed in Section 3-2 is included, the resulting object is almost like an active part. Similar to the active part in the manufacturing procedure, the samples need to be dried too. They were dried in an oven as shown in Figure 3-13 wherein, Figure 3-13a shows the external view of the drying oven and Figure 3-13b shows an assembled frame and components of another frame kept for drying.

80 °C and atmospheric pressure were used during the drying phase which is different from that used in the industry. Thus, the amount of moisture removed from the laboratory samples by drying is lesser than that removed in the factory, provided the process time remains the same. This condition is again representative of a worst-case scenario. The duration of the drying step was varied, with longer times allotted generally to sample bars with clamping frame. Some variations were caused due to activity scheduling constraints. The drying times used for each sample bar are summarized in Table 3-3. Sample bar 4 was dried in preparation for another test but was then saturated during the climate exposure stage to convert it into a saturated sample.

After drying comes the tightening phase. The samples need to be exposed to the ambient conditions selected in Section 3-3 to simulate a particular scenario encountered during tightening. This was achieved by utilizing a climate chamber (Espec - PR-3F) which is shown in

Figure 3-14a. The conditions (60 °C, 75% RH) were set on the machine using the interface. Humidity in the chamber is produced by boiling de-mineralised water which is taken from a tank fitted underneath the chamber thus, the tank was filled periodically. The samples were placed in the chamber, as shown in Figure 3-14b, for a particular duration.

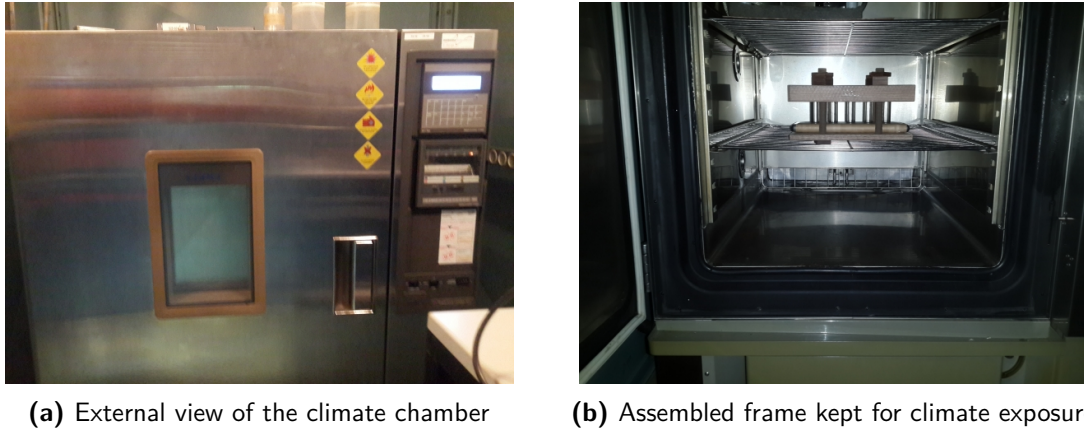


Figure 3-14: Conditioning samples in the climate chamber

Sample bar no.	Clamping frame	Drying duration (h) 80 °C, 1 atm.	Climate exposure duration (h) 60 °C, 75% RH	Vacuum duration (h): 10 mbar, ambient temp.
1	No	72	4	24
2	No	144	24	4
3	Yes	140	24	4
4 ^a	Yes	93	24	-
6	No	96	24	4
7	Yes	144	24	4
8	Yes	140	24	4
9 ^a	Yes	-	7	-
10 ^b	Yes	Exposed to ambient		
11	Yes	121	24	4

^a Saturated sample

^b Ambient exposed sample

Table 3-3: Conditioning parameters and durations applied to each sample bar

Since this phase was intended to represent the tightening duration, two time frames were considered namely, 24 hours and 4 hours. 24 hour time frame was chosen to represent a condition wherein, the time interval between removal of the active part from the oven and placing it inside the tank is practically the largest. Thus, the amount of moisture absorbed would be the greatest. The 4 hour time frame represents a kind of ideal/theoretical situation, as per the manufacturer, wherein tightening is carried out very rapidly and consequently, least possible amount of moisture ingresses into the material.

Table 3-3 lists the climate exposure and vacuum durations applied to each sample bar. Tightening is followed by assembly inside the tank and the vacuum cycle. Thus, the conditioned

samples (dried and climate exposed) were taken out of the chamber after exposure duration completion and placed in the testing tank for further processing which is explained in Section 4-3.

3-5 Oil preparation

The oil that is to be filled in the transformer must first be made suitable for the impregnation process. Having taken the utmost care in drying the solid insulation and evacuating and degassing its pores under vacuum to aid proper impregnation, it would be counter-productive to use wet oil or oil with gaseous contents. The viscosity of transformer oils decreases with increase in temperature. Lower viscosity allows the oil to flow better and seep into smaller pores and capillaries which benefits the impregnation process [18]. The oil used for impregnation during the manufacturing process is thus, heated, dried and degassed and so was the oil used during the course of this research.

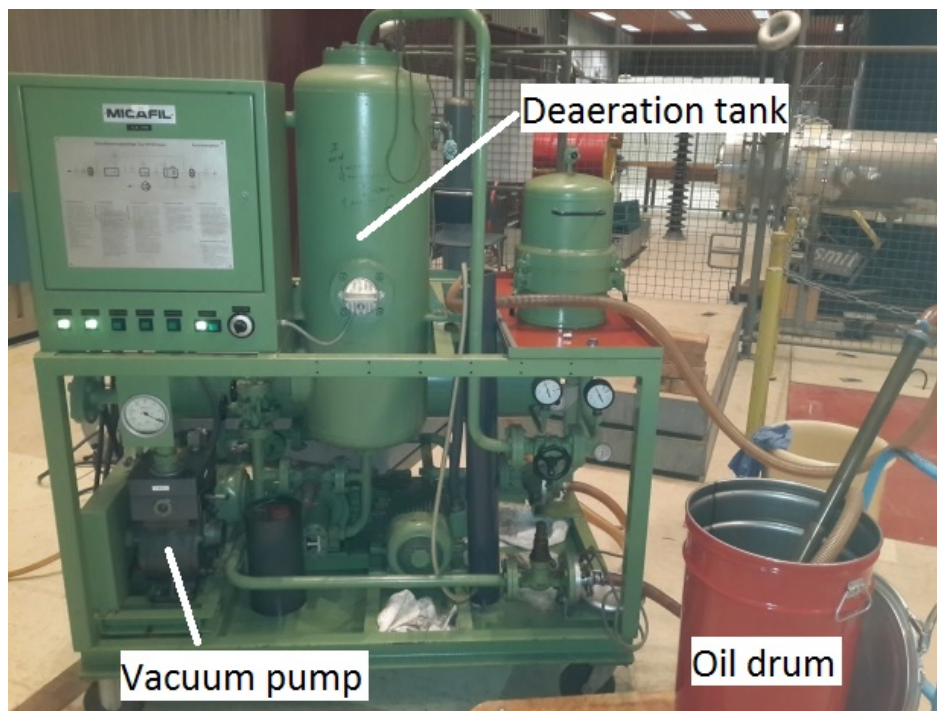


Figure 3-15: Oil preparation skid (Heating element at the rear)

The equipment used for the pretreatment of oil in the laboratory is shown in Figure 3-15. Nynas[®] Nytro Taurus was the oil used in the experiments and the oil preparation skid is Micafil² Type VH022. The deaeration tank and the vacuum pump perform the drying and degassing function. The heating element located at the rear of the skid enables the required temperature to be attained. Oil was circulated through the skid until it had a moisture content less than 5 ppm and a temperature of 70 °C as these are the conditions used by the manufacturer. The authors in [17] also report a similar oil temperature (75 °C). The skid also has filters to remove particulate impurities.

²Micafil is now Micafluid AG

Vaisala HUMICAP[®] Hand-held Moisture and Temperature in Oil Meter - MM70 was used for measuring the humidity of the oil. The temperature limit for MM70 is 60 °C thus, a T-type thermocouple and an RS 1314 Dual Thermometer were used for measuring the oil temperature beyond 60 °C.

The dried, degassed and hot oil was filled into the oil drum and then moved to the testing area for impregnation. This preparatory process was carried out prior to the impregnation of each sample bar. The impregnation process is described in Section 4-3.

PD Test Setups and Procedure

As explained in Section 2-3-2, PD detection is the diagnostic technique of choice in this research. Therefore, a setup needs to be devised to test the samples for PDs. The essential theory about PD detection, or discharge measurements, is discussed in Section 4-1 before delving into the details of the practical setups used in this research in Section 4-2. The process used to impregnate PD test samples with oil is described in Section 4-3. Section 4-4 explains the procedure that was followed while conducting the PD tests.

4-1 Measuring discharges

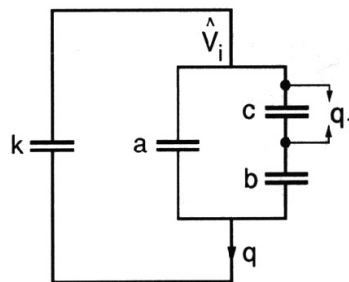


Figure 4-1: Apparent charge measurement [35]

PD detection during the IVPD test on transformers is to be carried out using the technique mentioned in IEC 60270, which is the *apparent charge* measurement method [36, 40]. This method can be conceptualized as shown in Figure 4-1. An external impedance (k) is connected in parallel to the test object depicted herein by the abc series-parallel equivalent circuit. In the abc circuit a represents the bulk of the test object, b represents the portion of insulation in series with the defect and c represents the defect itself [35].

The test voltage is applied across the sample and the charge displacement through k is measured instead of the charge displacement through c . It has been demonstrated by Kreuger

in [35] that the discharge magnitude measured in this manner is representative of both the volume of the discharging defect and the energy dissipated by it.

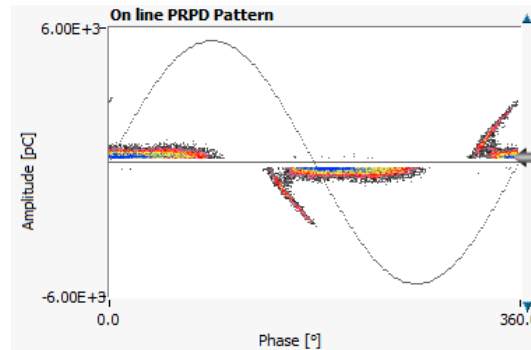


Figure 4-2: Example of a PRPD pattern - internal discharge

Classical detection is one of the basic methods of performing these apparent charge displacement measurements, the alternative being *time resolved detection*. Time resolved detection allows the user to visualize the actual shape of the PD pulse [35]. As this is not the primary target of this research, classical detection is preferred.

In classical detection the discharge magnitudes are measured and plotted over a power frequency (50/60 Hz) reference sine wave at points corresponding to the measured phase of the respective discharge. Thus, resulting in a Phase-Resolved Partial Discharge (PRPD) pattern as illustrated in Figure 4-2. The pattern observed in the figure is characteristic of an internal discharge. Classical detection can be achieved using two techniques namely, *straight detection* and *balanced detection* [35].

A straight detection circuit is employed herein as the additional features, such as locating the discharge source, provided by balanced detection are not essential in this case as the test object is quite small. Moreover, the tests are performed in laboratory conditions wherein each test setup is placed in a grounded cage which reduces the influence of external noise.

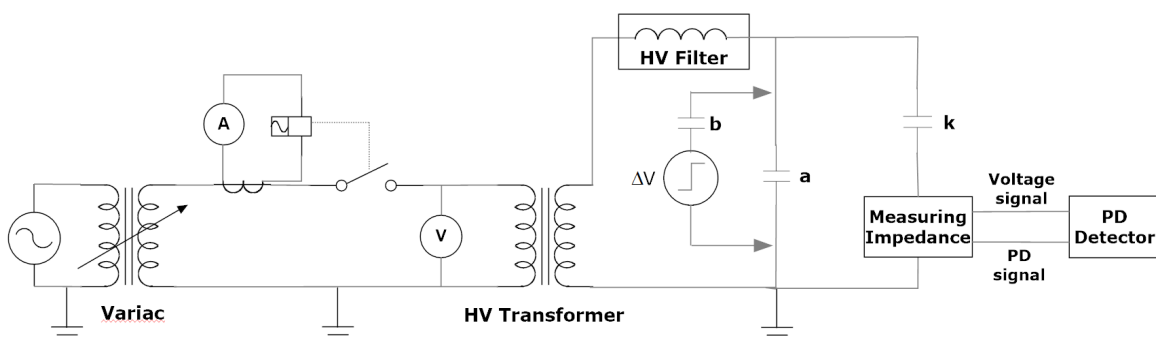


Figure 4-3: Schematic circuit for straight detection

The schematic diagram of a straight detection circuit is shown in Figure 4-3. The major parts of the circuit are as follows:

1. **Variac** and **HV transformer** (test transformer) to generate the required test voltage

2. **HV Filter** to prevent noise from the source from entering the PD detection circuit and also to protect the HV source from the high frequency discharges
3. Test object (designated as a)
4. Coupling Capacitor (designated as k) - external impedance which provides the path for external charge displacement measurement
5. **Measuring impedance** - Impedance network that feeds the PD and reference voltage signals to the PD detector
6. Detection Unit - The following inputs are obtained from the measuring impedance:
 - PD signal
 - Reference voltage signal

The PD signal received from the measuring impedance is given a value (in pC) by means of a known calibrating signal. This signal is generated using a calibrator comprising of a voltage source (marked as ΔV) and a capacitance (demarcated as b). The PD and reference voltage signals received may be visualized on the following display equipment depending on the capabilities of the employed detection unit:

- Oscilloscope
- Software interface

Having established *straight detection* as the PD detection scheme of choice in this research and having provided a brief overview of it, the discussion can proceed to the practical implementations of this scheme beginning with the test setups.

4-2 Test setups

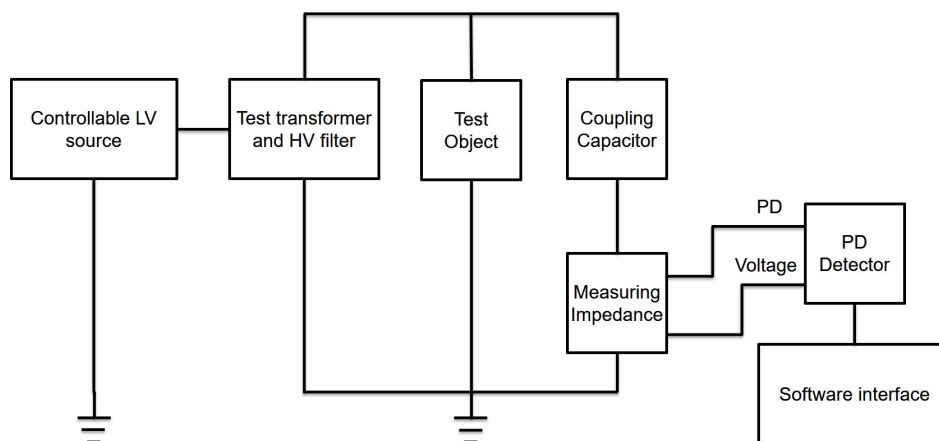


Figure 4-4: Block representation of straight detection circuit used in the experiments

In order to better visualize the setup, the straight detection circuit schematic shown in Figure 4-3 is converted into the block representation shown in Figure 4-4.

The **controllable Low Voltage (LV) source** block comprises of the following components:

- **1- ϕ LV variable voltage transformer (variac)** - control the test voltage level by varying the input to the test (HV) transformer
- **Protection and metering device** - This multi-purpose device provides the following facilities:
 - On/Off push buttons to connect/disconnect grid input to the variac
 - Measurement of applied voltage and current drawn by the test setup (LV side measurement)
 - Overcurrent trip function to stop voltage injection in the event of heavy discharges or sample breakdown. The current setting can be varied to adjust the sensitivity.
- **Net-filter** - filter out disturbances existing in the grid supply

Techimp[®] PDBase II was the **PD detector** employed in the experiments wherein the visualization of the PD and reference voltage signals is achieved using a software interface.

The **measuring impedance** used in the test setups is shown in Figure 4-5. It consists of a capacitive divider network that provides two ratios for the reference voltage measurement namely, 1000/1 and 10000/1. The ratios are network capacitance dependent and thus, the actual ratio needs to be measured and then fed into the software interface. The in-built current transformer provides the PD signal.

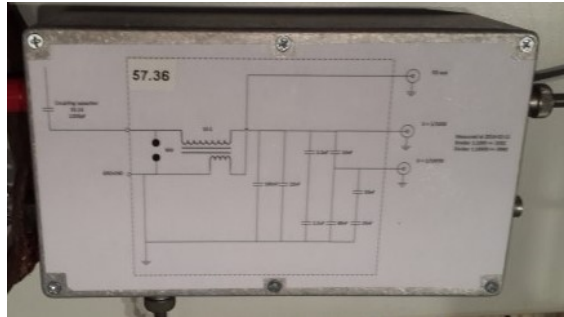


Figure 4-5: Measuring impedance used in the experiments

Two test setups, differing in test voltage generation capabilities, were used during the course of this research. The protection and metering device, net-filter, HV filter, measuring impedance and PD detector were common to both setups. The HV filters were mounted in field graded regions atop the respective transformers.

Component	Setup 1	Setup 2
Variac output	0-280 V, 8 A	0-270 V, 20 A
Test (HV) transformer voltage ratio	$(34500/\sqrt{3})/(110/\sqrt{3})$	150000/220
Coupling capacitor	40 kV, 1000 pF	140 kV, 1200 pF

Table 4-1: Differences in component ratings between the two test setups

Table 4-1 shows the differences between the ratings of the components namely, the variac, test (HV) transformer and coupling capacitor, used in the two setups.

4-2-1 Test tank description

In reality, impregnation and testing occur in the same vessel - the transformer tank. A transformer tank is subjected to vacuum prior to impregnation as shown previously in Figure 1-3. The test tank shown in Figure 4-6 is actually a vacuum chamber and thus, can be compared to an actual transformer tank. A provision for looking inside the tank is made available in the form of two viewing windows on one side. The tank is fitted with a door to allow easy access to the interior and also has the following connections to the surroundings that are marked in Figure 4-6:

- **Vacuum break/vacuum measurement valve (1)** - A quick coupler port is provided along with a manual valve. Tank vacuum level measurements are taken from this port using a hand-held digital gauge (Druck Limited - DPI 700). Release of vacuum, post oil filling, is also achieved through this port.
- **Oil fill/drain valve (2)** - A manual valve with an attached pipe is provided. The valve is used to control the oil flow rate mainly during the filling operation.
- **Air outlet to vacuum pump (3)** - This connection is also provided through a manual valve. Air from the tank is drawn out by the vacuum pump through this valve. The valve is kept fully open on account of the vacuum pump having an additional isolation valve which prevents loss of vacuum when the pump is not operational.

Figure 4-7 shows the internals of the tank located behind the door. The test object is placed inside the bucket. The test object can be considered to represent the active part of the transformer. The bucket has an opening at the bottom which serves as an oil filling and draining port. This port is connected to the oil fill/drain valve through a vacuum resistant seal. A stud is provided in the side wall of the bucket which provides the connection between the test object and earth. Both of these features are seen in Figure 4-8. The tank is connected to the vacuum pump as shown in Figure 4-9.

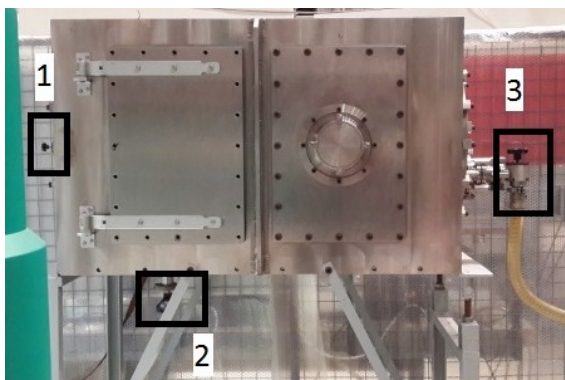


Figure 4-6: Test tank - external view

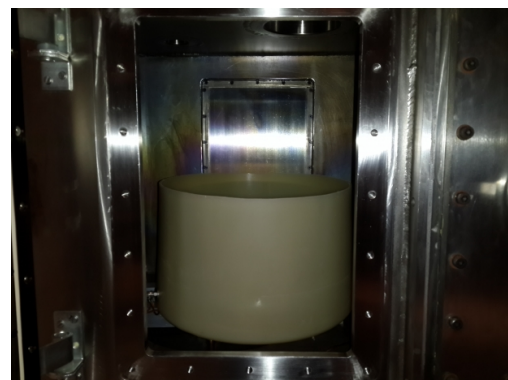


Figure 4-7: Test tank - internal view

The outer side of the stud is connected to the tank wall and the tank itself is connected to the earthing grid of the lab. The test tank, vacuum pump and part of the test setup are all situated inside a grounded cage.

Part of the test setups are also placed inside the test tank.



Figure 4-8: Oil filling and draining port (centre) and stud for connection of test object to earth (left)



Figure 4-9: Test tank to vacuum pump connection with tank air outlet valve marked

4-2-2 Setup 1

The test transformer and coupling capacitor used in setup 1 were kept inside the test tank. Setup 1 was used for testing samples with and without the clamping frame. The differences between those two scenarios were in the length of the test electrode (20 mm-without, 75 mm-with) and in the mechanism used to connect it to the test transformer. The connector and test electrode used for testing samples without clamping are shown in Figure 4-10. A horizontal sliding mechanism comprising of two interconnected T-pieces was mounted on the horizontal pipe in order to facilitate selection of the test locations; the mechanism is shown in Figure 4-11a.



Figure 4-10: Connector and electrode used for samples without clamping

Figure 4-11b shows the connection between the test transformer, test object and coupling capacitor used for testing samples with clamping. The LV input to the test transformer was brought out of the tank, via terminals affixed on both sides of a tank mounted flange, and subsequently connected to the variac. The measuring impedance was placed on top of the tank and the connection to the coupling capacitor made via an adapter.

4-2-3 Setup 2

The test transformer and coupling capacitor used in setup 2 were placed outside the tank as shown in Figure 4-12. The horizontal copper pipe, seen in Figure 4-12b, was mounted on an insulator. The bent pipe in the foreground formed the connecting link between the test transformer and the horizontal pipe. The sliding mechanism remained the same as in setup 1 but the flexible link was made suitable for higher voltages.

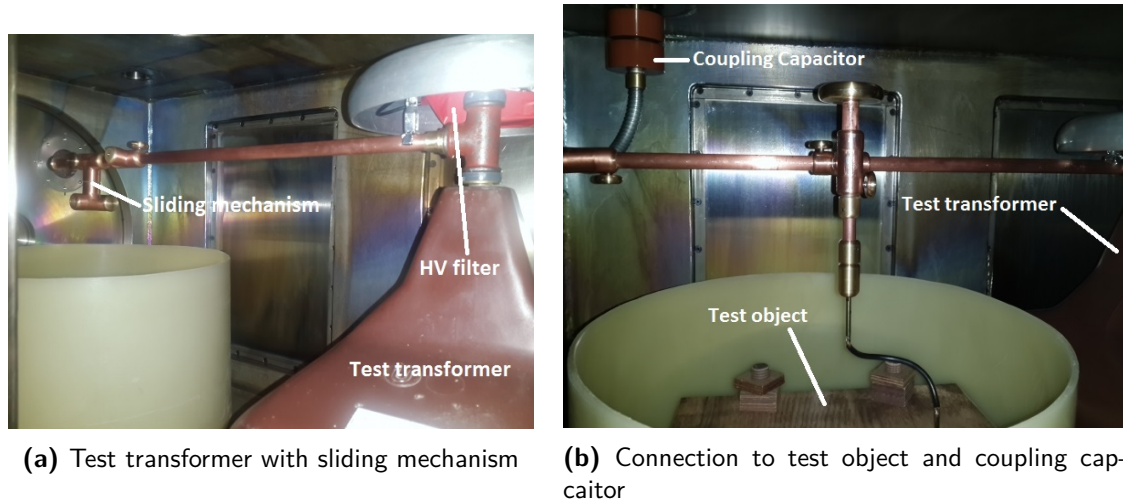


Figure 4-11: Test transformer, test object and coupling capacitor connection - setup 1

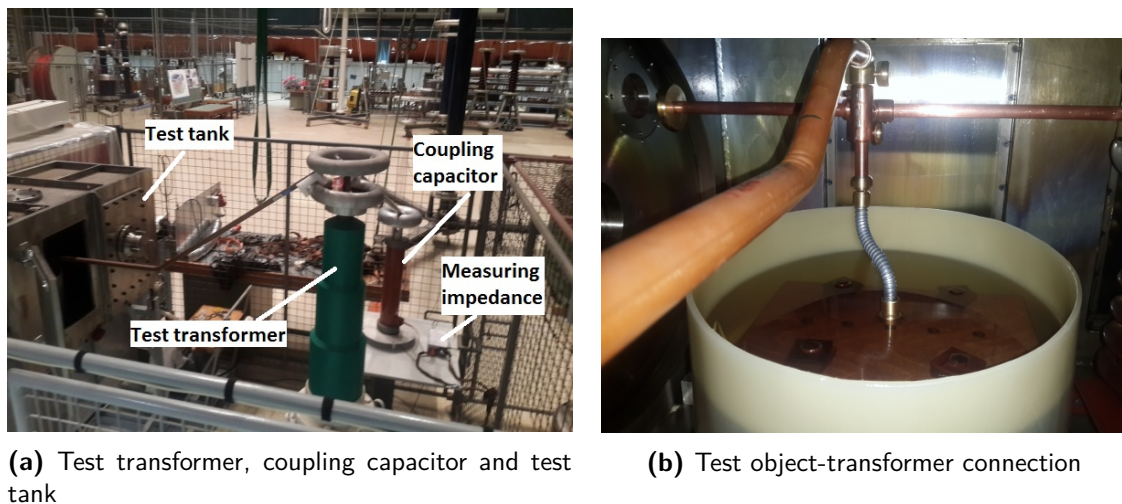


Figure 4-12: Test transformer, test object and coupling capacitor connection - setup 2

For the purpose of PD testing, it is essential that the setup itself does not become a source of PDs. Thus, each test setup was tested for PDs. The **first** setup was found to be **PD free** up to **21 kV (1- ϕ voltage)** and the **second** was PD free up to **49 kV (1- ϕ voltage)**.

With a PD free setup available, the test object is introduced in it. The ground point of the test object is connected to the earth stud by means of an insulated wire link. Such a link was used so as to ensure corona does not appear on the ground potential side. The first test location is selected and the oil impregnation process initiated.

4-3 Oil impregnation process

The door of the tank is closed after placing the conditioned test object inside the bucket and ensuring proper connection to earth. The oil fill/drain and vacuum break valves, marked in

Figure 4-6, are also closed. The vacuum pump is started and operated till a stable vacuum level of 10 mbar is attained. The pump is operated periodically during the prescribed vacuum duration to allow for any vapours to be evacuated and to maintain the vacuum level.

The drum containing the hot, dry and PD free transformer oil (70 °C, <5 ppm), obtained as explained in Section 3-5, is used as the source for oil filling. The vacuum pump is kept in operation at the end of the prescribed vacuum duration. As seen in Figure 4-13, oil is drawn into the bucket using the oil fill/drain valve and the connected pipe with vacuum as the driving force. Oil is filled up to a level such that the entire test object and a part of the flexible link are submerged which corresponds to an approximate height of 6 cm in case of samples without clamping and 19 cm in samples with clamping.

The rate of oil flow is controlled such that oil filling occurs smoothly thus, minimizing air bubble formation. Control is exercised by observing the filling process through the viewing windows. Filling oil from the bottom up also aids in reducing bubbles. As explained by the authors in [41], air bubbles are potential sources of PDs. Their presence can interfere with the results of the tests and must therefore be minimized. Thus, to remove bubbles that may have been formed, vacuum is maintained for a fixed time interval after attaining the necessary oil level which can be termed as the *degassing interval*. This process is demonstrated in Figure 4-14. A degassing interval is also applicable during transformer manufacturing as mentioned by the authors in [17].



Figure 4-13: Oil filling in progress

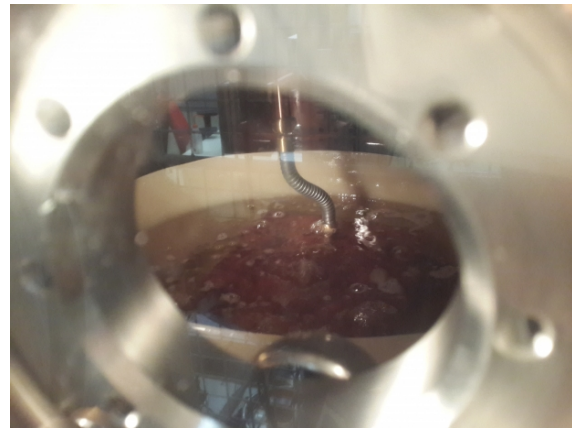


Figure 4-14: Air bubbles in oil during degassing interval

At the end of the degassing interval the vacuum is slowly released using the vacuum break valve. The complete release of vacuum is considered as the moment of impregnation and marks the beginning of the *standing time*.

This process was followed for the impregnation of all sample bars tested as part of this research. The PD behaviour of each sample bar was tested according to the procedure explained in Section 4-4.

4-4 Test Procedure

The sample bar has been designed to allow five PD tests to be conducted as explained in Section 3-1-2. Tests on each impregnated sample bar are performed as per the schedule given in Table 4-2. Table 3-3 is modified and represented in the form of Table 4-3. Table 4-2 and Table 4-3 together provide an overview of the PD testing program.

Location No.	Scenario
1	Day 0 ^a
2	Day 1
3	Day 2
4	Day 3
5	Day 4

^a Immediately after impregnation

Note: Day mentioned herein refers to a working day

Table 4-2: PD test program - Testing schedule for each impregnated sample bar

Sample bar no.	Clamping frame	Drying duration (h) ^a	Climate exposure duration (h) ^b	Vacuum duration (h) ^c
Crêped presspaper				
1	No	72	4	24
2	No	144	24	4
3	Yes	140	24	4
4 ^d	Yes	93	24	-
Presspaper				
6	No	96	24	4
7	Yes	144	24	4
8	Yes	140	24	4
9 ^d	Yes	-	7	-
10 ^e	Yes	Exposed to ambient		
11	Yes	121	24	4

^a Dried at 80 °C, 1 atm.

^b Exposed to air at 60 °C, 75% RH

^c Vacuum parameters - 10 mbar (abs.), ambient temp.

^d Ambient exposed sample

^e Saturated sample

Table 4-3: PD test program - Specifications of sample conditioning parameters

The flowchart shown in Figure 4-15 describes the activities that constitute the testing of a single location.

The PD signal calibration is performed using Seitz Instruments¹ - Calibrator Type CAL 141 as a source. The calibrator is connected across the test object, i.e., one terminal connected

¹Seitz Instruments is now part of the Onsite High Voltage group (Onsite HV Holding)

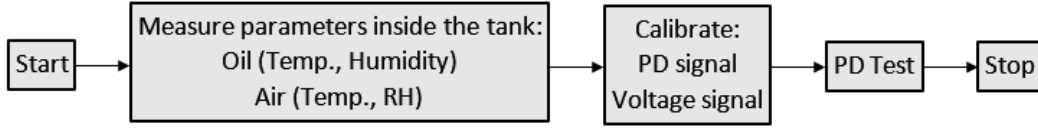


Figure 4-15: Activities to be performed while testing each location

to the flexible link and the other terminal to ground. A fixed charge, say 10 pC, is injected and the same is configured in the software interface (PDBaseII v1.01.16).

The voltage signal is calibrated by injecting a fixed voltage. The measurement on the HV terminal is performed using a probe that has a ratio of 1000/1 (Testec[®] TT-HVP40). The measured voltage is fed into the interface. This takes into account, both, the measuring impedance and the network capacitance effect mentioned in Section 4-2.

The PD test on each location is conducted as per the procedure specified in Section 11.3 of IEC 60076-3 in order to mirror the test performed on an actual transformer. The one hour PD measurement level is specified as $(1.58 \times U_r/\sqrt{3})$ [36]. The parameter (U_r) for the tests conducted as part of this research is calculated using Eq. (4-1).

$$U_r = \frac{\sqrt{3}E_{test}t_s}{1.58} \quad (4-1)$$

where:

$$\begin{aligned}
 U_r &= \text{Rated voltage of a winding (kV) [36]} \\
 E_{test} &= \text{Test field stress level as per design/test data (kV/mm)} \\
 t_s &= \text{Thickness of the paper sample (mm)}
 \end{aligned}$$

The voltage profile used during the tests is shown in Figure 4-16. Table 4-4 lists out how the voltages at each step are calculated and also the time duration of each step. Background noise measurements are recorded at the beginning and end of the test as mentioned in Table 4-4.

Step No.	Step Description	Duration	Test Voltage
1	Background measurement	1 min	$(0.4 \times U_r/\sqrt{3})$
2	Intermediate measurement	1 min	$(1.2 \times U_r/\sqrt{3})$
3	Test level	5 min	$(1.58 \times U_r/\sqrt{3})$
4	Enhancement level	1 min	$(1.8 \times U_r/\sqrt{3})$
5	Test level	60 min	$(1.58 \times U_r/\sqrt{3})$
6	Intermediate measurement	1 min	$(1.2 \times U_r/\sqrt{3})$
7	Background measurement	1 min	$(0.4 \times U_r/\sqrt{3})$

Table 4-4: Test voltage calculation and duration of voltage application

During the course of the tests the following parameters are recorded in case any continuous discharges are observed:

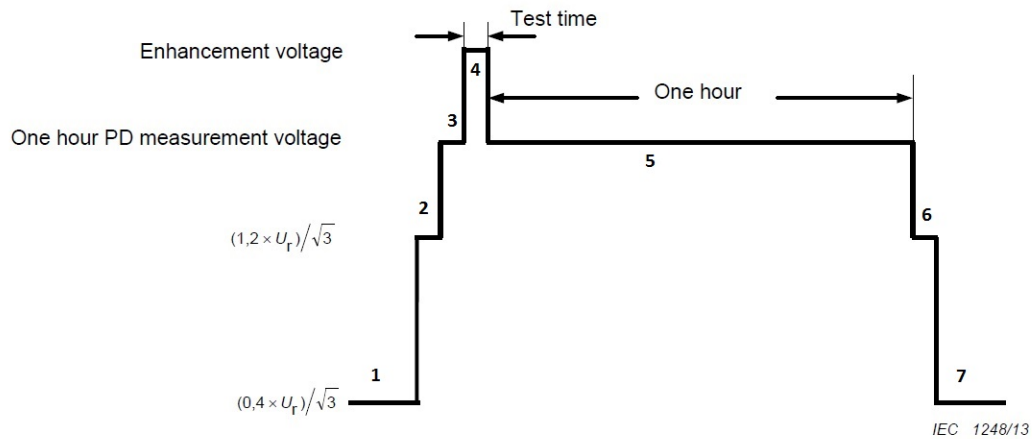


Figure 4-16: Time sequence for the application of test voltage for PD test (base image - [36])

- **Partial Discharge Inception Voltage (PDIV)** - At what voltage do the PDs start
- **Partial Discharge Extinction Voltage (PDEV)** - At what voltage do the PDs stop
- **PD magnitude** - To estimate the severity of the discharge activity
- **PRPD patterns** - To analyse the type of discharges

The door of the tank is closed after the completion of the test on the chosen location so as to minimize the interaction with ambient. In the case of test setup 2 the bent pipe is removed and kept aside in order to achieve this. The next test location is connected to the setup using the sliding mechanism and the test procedure described in Figure 4-15 is repeated. The locations that are not under test are kept floating.

Each sample bar was tested in this manner and the PD behaviour over the course of the standing time was observed and noted. The results of these tests are described in Section 5-2.

Results of the Investigations

The results of the climate exposure and vacuum duration tests are discussed in Section 5-1 and the results of the PD tests in Section 5-2.

5-1 Climate exposure and vacuum duration test

The paper samples, prepared as explained in Section 3-1-1, were dried overnight (16 hours) in an oven at 80 °C and atmospheric pressure. The weight of the paper wrapped on the substrate (W_{paper}) was calculated using Eq. (5-1). Eq. (5-2) was the general expression used to compute the % change in weight during the process.

$$W_{paper} = W_{sample} - W_{substrate} \quad (5-1)$$

$$\% \text{ change} = 100 \times \frac{(W_{final} - W_{initial})}{W_{initial}} \quad (5-2)$$

Sample type	Initial weight (g)	Weight after drying (g)	% change in weight
Presspaper (1.4 mm)	8.68	8.04	-7.39
Crêped Presspaper (3 mm)	14.04	12.93	-7.92
Crêped Presspaper (6 mm)	18.15	16.76	-7.66

Table 5-1: Average weight of each sample type before and after drying at 80 °C, 1 atm.

The results of the drying process are summarized in Table 5-1 wherein, the weights mentioned are the average of the three samples belonging to each type. The same connotation is applicable to the values mentioned in Table 5-2 and Table 5-3 as well.

In this situation (Table 5-1) the drops in weight are due to loss of moisture. As the drops range from 7.39% to 7.92%, the paper samples can be considered as *fully dried*. This claim is based

on the fact that maximum moisture content in paper is 8% by weight, as mentioned in the supplier's (Weidmann) datasheets shown in Appendix B. For the purpose of representation, it is considered that the fully dried condition corresponds to a moisture content of 0.5% by weight. This is based on the typical post-drying moisture content in paper mentioned by the authors in [16].

The dried samples were then exposed to the 60 °C, 75% RH environment for a duration of 24 hours in the climate chamber. The conditioned samples were subsequently placed in a vacuum oven at 25 °C, 10 mbar (abs.) pressure for a duration of 48 hours. The selection of 48 hour vacuum duration was based simply on it being double of the 24 hour stable vacuum period used in the transformer manufacturing process. The effect of an extended vacuum duration on the standing time can be studied on this basis (Research Question 3).

Figure 5-1 and Figure 5-2 show the samples placed in the climate chamber and the vacuum oven, respectively.



Figure 5-1: Paper samples placed in climate chamber



Figure 5-2: Paper samples placed in the vacuum oven (10 mbar (abs.), 25 °C)

Eq. (5-2) was used to compute the changes in weight during the climate exposure and vacuum cycle durations wherein, the weight after drying (from Table 5-1) was taken as $W_{initial}$. Thus, the change in weight can be considered as the average moisture contained in the paper. Average refers to the distribution of moisture over the thickness of the material as far as individual samples are concerned. Table 5-2 and Table 5-3 show the average moisture content of each sample type at the end of the climate exposure and vacuum cycles, respectively.

Sample type	Weight after drying (g)	Weight after climate exposure (g)	% moisture content
Presspaper (1.4 mm)	8.04	8.72	7.77
Crêped Presspaper (3 mm)	12.93	14.01	7.67
Crêped Presspaper (6 mm)	16.76	18.12	7.50

Table 5-2: Avg. moisture content (% w/w) of each sample type after climate exposure

The change in moisture content with respect to time during the climate exposure and vacuum cycle periods are shown in Figure 5-3 and Figure 5-4, respectively. As seen in Figure 5-3, average moisture content after 7 and 23 hours of exposure is nearly the same.

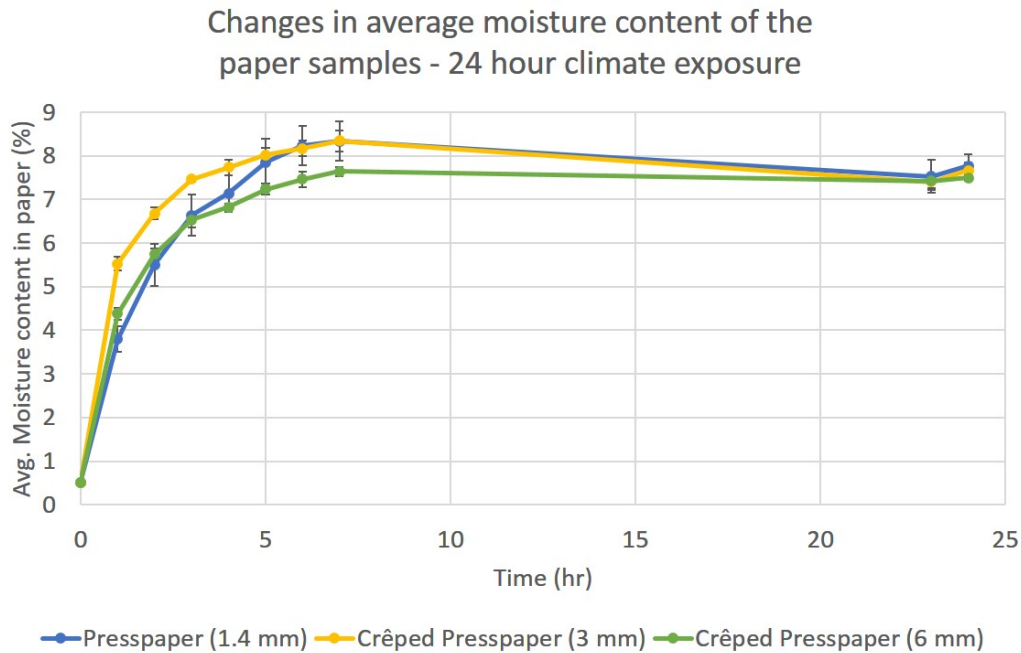


Figure 5-3: Changes in avg. moisture content of paper during climate exposure

Sample type	Weight after drying (g)	Weight after vacuum cycle (g)	% moisture content
Presspaper (1.4 mm)	8.04	8.12	0.99
Crêped Presspaper (3 mm)	12.93	13.09	1.21
Crêped Presspaper (6 mm)	16.76	16.98	1.28

Table 5-3: Avg. moisture content (% w/w) of each sample type after vacuum cycle

Consider Figure 5-3. The overshoots observed in case of presspaper (1.4 mm) and crêped presspaper (3 mm) in relation to crêped presspaper (6 mm) can be explained as follows. The climate chamber was opened each time the samples had to be weighed. Due to differences in climatic conditions inside and outside the chamber, wet spots appeared on the surface of the samples due to condensation. These spots augmented the weight slightly. The effect was more pronounced in the lighter samples because the weights of the drops were more comparable with the base weight of the paper and thus, the % change was higher. The slight rise at the end (23 h vs. 24 h) was also due to the same phenomenon. Since no measurements were conducted overnight (between 7 and 23 h) the condensation effect was not observed and the moisture distribution gained more uniformity.

Figure 5-4 shows that the average moisture contents at $t=48$ h and $t=72$ h are virtually the same. Thus, the weight of the sample, consequently the moisture content, stabilizes within 24 hours of stable vacuum application (which is started at $t=24$ h). The oscillations observed in the tails of the curves are due to errors in measurements. 0.01 g corresponds to 0.13% in the case of presspaper (1.4 mm) and 0.01 g is the least count of the weighing scale used. Thus, small errors in measurements are magnified when translated to percentages.

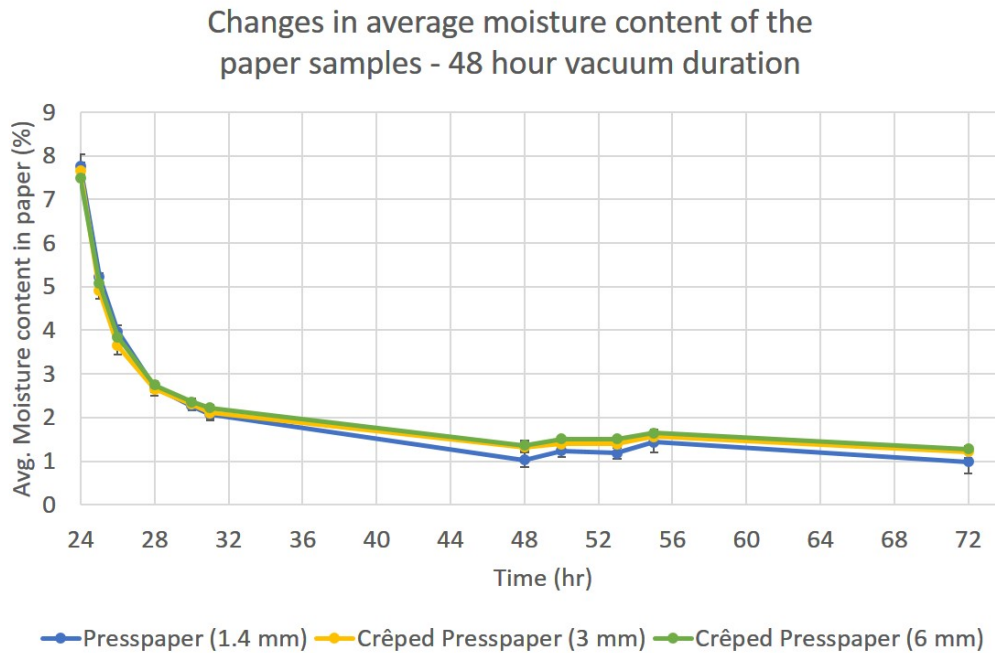


Figure 5-4: Changes in avg. moisture content of paper during vacuum cycle

Discussion

The following can be observed, with respect to the moisture absorption and extraction processes, in Figure 5-3 and Figure 5-4:

1. As mentioned in Table 5-2, the average moisture content in both types of paper after 7 hours of climate exposure is approximately 8.0% which is virtually the same as the aforementioned saturation value. Thus, *saturation occurs nearly 7 hours into the exposure duration.*
The average moisture content drops to approximately 2% after 7 hours of vacuum in both types of paper. 24 hours of stable vacuum (10 mbar (abs.) at 25 °C) is sufficient to dry the paper.
2. Moisture ingress and egress in presspaper is slower as compared to crêped presspaper.
3. Crêped presspaper (3 mm) samples absorb and lose moisture faster as compared to the crêped presspaper (6 mm) samples.

Thus, the following can be surmised from these observations which is also corroborated by the authors in [19] and the attached datasheets (Appendix B):

1. Moisture ingress and egress in paper is inherently fast when compared to the time durations involved in the activities constituting the building of a transformer.
2. Saturation level of moisture is independent of the type of paper, i.e., crêped presspaper or presspaper

3. Moisture ingress and egress is slower in denser materials, with presspaper being denser as mentioned in Section 2-1-1.
4. Moisture ingress and egress is faster in thinner materials

Samples were kept in ambient conditions after the vacuum cycle, represented in Figure 5-5, so that the rate of moisture ingress in this situation could be compared with that of the climate exposed condition. Figure 5-6 shows the result of the exercise wherein, it is observed that the samples attain an average moisture content of 7.5% in 75 hours for temperatures between 22.5 °C and 25.1 °C and RHs between 54.5% and 68.5%.



Figure 5-5: Samples placed in ambient conditions after vacuum cycle

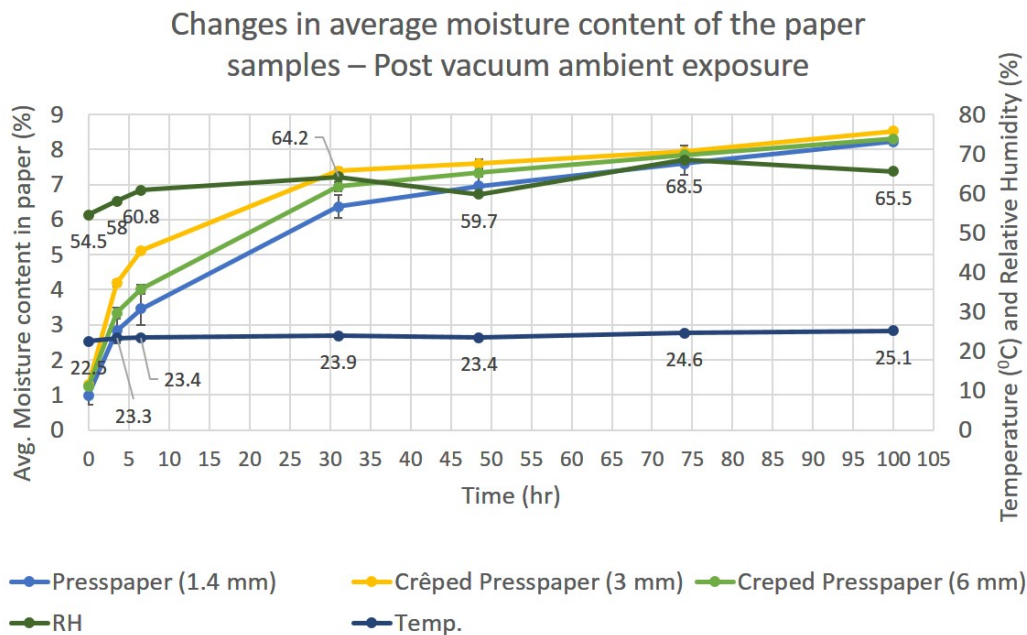


Figure 5-6: Changes in avg. moisture content of paper during post vacuum ambient exposure

The trends pertaining to the rate of moisture ingress observed in the fixed climate exposure tests are also seen in this situation. Moreover, there is no condensation effect observed as the samples do not encounter a sudden change in climate.

5-2 PD test results

The test voltage that is to be applied on the test object must be known prior to the start of a PD test. As explained in Section 4-4, U_r determines the PD test voltage in case of transformers. Since samples of materials are tested in this research, the test voltage is derived from data describing the electric field stresses experienced by the particular material during actual tests. This data is generally available in the form of electric field plots. It is also useful to recall that the cellulosic insulation has been impregnated by oil prior to the start of the PD test.

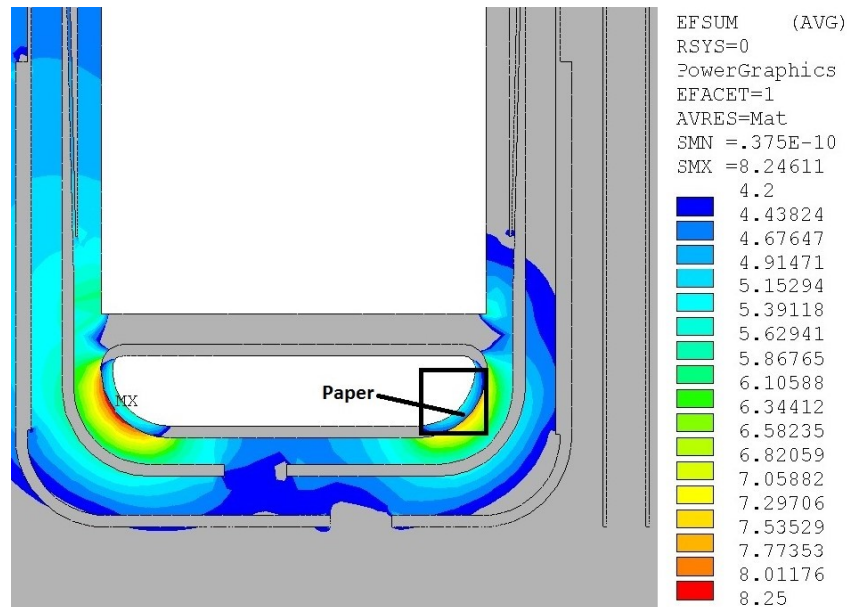


Figure 5-7: Electric field plot of part of a transformer winding (courtesy: Royal SMIT)

Figure 5-7 shows an electric field plot of part of a transformer winding. The conductors are indicated by the white spaces. Focussing on the marked zone, the field stress encountered by the paper layers closest to the conductors is nearly 6 kV/mm and reduces to 5 kV/mm (approx.) in the layers closest to the OIP-oil interface. The 8 kV/mm field stress occurs in oil that surrounds the paper.

The higher field stress in oil is consistent with the result obtained by applying the equations, mentioned by Kreuger in [25], that govern the behaviour of fields at the interface between two dielectrics. The result being that the field is concentrated in the low permittivity material which in this case is oil. **Thus, 6 kV/mm was chosen as the test field stress for OIP** and sample bars without clamping were tested initially.

5-2-1 Sample bars without clamping

Paper insulation is used in areas of a transformer's active part that are not subjected to the clamping force such as the use of crêped presspaper on the tubes that link the windings to the bushings as explained in Section 2-1-1. Thus, sample bars 1, 2 and 6, i.e., two cases of crêped presspaper and one of presspaper, were tested without clamping.

Out of these, sample bars 1 and 2 were subjected to tests first. They were conditioned and subjected to vacuum for the time durations given in Table 3-3 after which they were impregnated with oil. The weight of each sample bar was measured at the beginning and end of each part of the conditioning process. In order to determine the weight of paper wrapped on the metal bar the initial weight of the bar must be known. Since the bars were received from Royal SMIT in wrapped condition, the weights of the bare metal bars were measured after having completed the test and unwrapped the OIP.

Weights of both the sample bars measured after completion of drying and after climate exposure are listed in Table 5-4 along with the weights of the bare metal bars. The calculation of moisture contained in the paper is based on Eq. (5-1) and Eq. (5-2) wherein, the bare metal bar represents the substrate.

Sample bar no.	Wt. of bare metal bar	Wt. after drying	Wt. after climate exposure	% moisture (w/w) in paper
1	5423.2 g	5546.5 g	5555.8 g	7.5
2	5424.8 g	5550.8 g	5560.3 g	7.5

Table 5-4: Weights of sample bars 1 and 2 pre and post climate exposure

Test setup no. 1 and 25 mm long HV electrodes were employed and the tests were conducted according to the schedule mentioned in Table 4-2. An example of testing sample bars without clamping is shown in Figure 5-8 wherein, sample 1.3 (sample bar 1 - location 3) is under test.



Figure 5-8: Testing of sample 1.3 in progress

The aforementioned field stress of 6 kV/mm was used for testing these sample bars. The test voltage levels used, calculated in accordance with Table 4-4 and Eq. (4-1), for both sample bars are listed in Table 5-5. The test voltages are different due to the difference in the thickness of the wrapped paper layer. Results pertaining to sample bar 1 are used as illustrative examples for explanation.

Step Description	Test voltage	
	Sample bar 1	Sample bar 2
Background measurement	3.8 kV	4.6 kV
Intermediate measurement	11.4 kV	13.7 kV
Test level	15 kV	18 kV
Enhancement level	17.1 kV	20.5 kV

Table 5-5: Test voltages used for sample bars 1 and 2

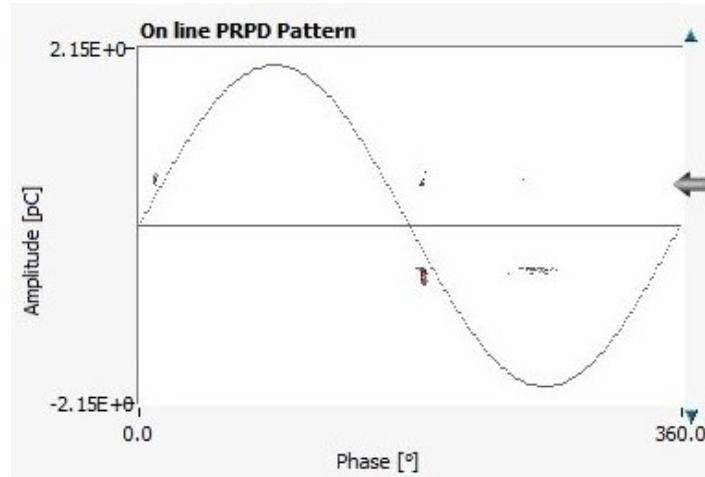


Figure 5-9: Burst of discharges observed during testing of sample 1.1 at 13.8 kV

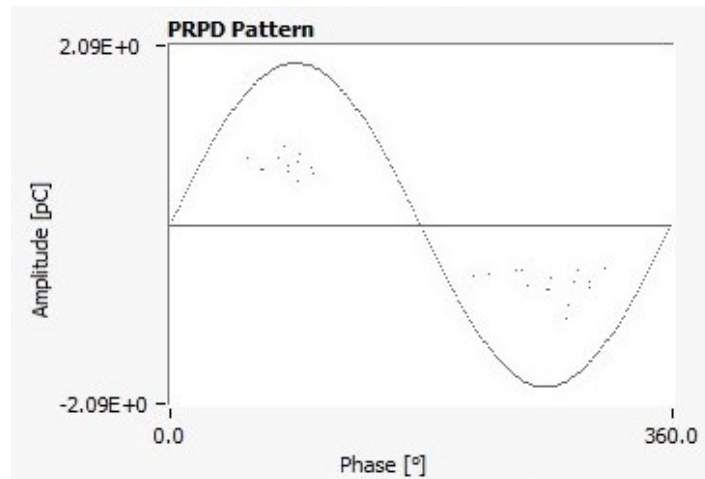


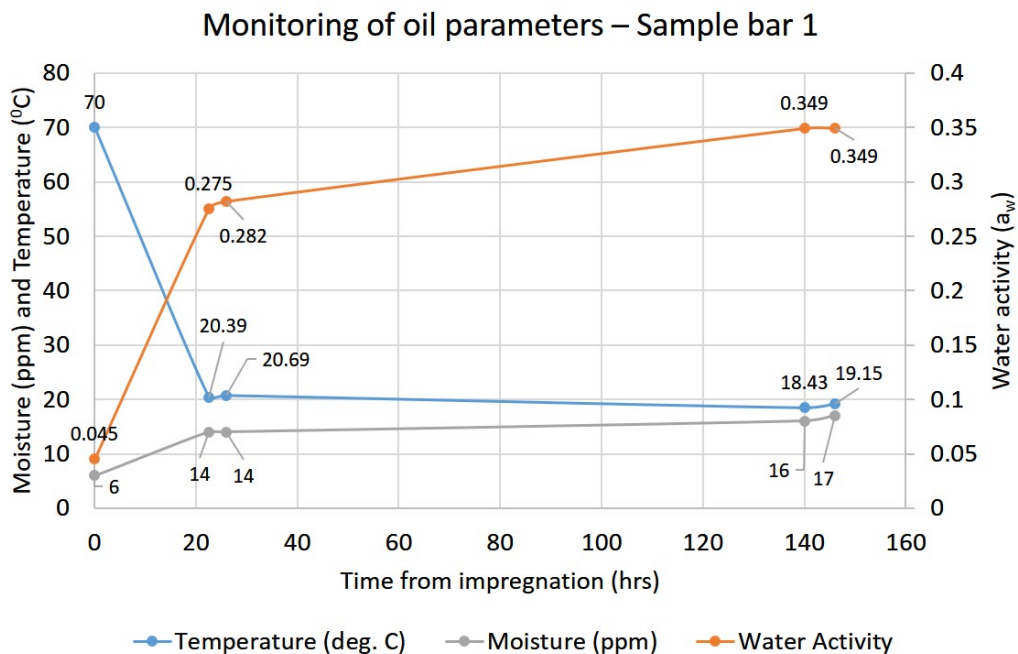
Figure 5-10: Burst of discharges observed during testing of sample 1.2 at 18 kV

Sample bars 1 and 2

The PD tests conducted on sample bar 1 resulted in **no PD activity** being observed in any of the five samples (five locations) tested therein. The claim of no PD activity is based on the following arguments:

- Although some bursts of discharges were observed during the testing of samples 1.1 (Day 0) and 1.2 (Day 1), the magnitude of these bursts were near the 1 pC mark which is a low value considering that the background noise measured was 0.2 pC. Examples of the observed burst discharge activity are shown in Figure 5-9 and Figure 5-10.
- Occasional bursts of discharges, even of high magnitude, can be neglected as mentioned in IEC 60076-3 [36].

Increasing the test voltage to 18 kV, corresponding to an electric field stress of 7.2 kV/mm, also did not yield any discharge activity.



Note: Time lapse represents non-working days

Figure 5-11: Monitoring of oil parameters during testing of sample bar 1

The temperature, absolute humidity (moisture) and a_w (water activity or relative saturation) of the oil in the bucket were also noted during the test, the record of which is shown in Figure 5-11. These parameters were measured so that moisture migration between OIP and oil could be observed.

Figure 5-11 re-emphasizes the fact that relative saturation is temperature dependent whereas the absolute humidity is not. Moisture remaining the same (e.g. 14 ppm), as the temperature varies (20.39 °C to 20.69 °C) the a_w changes too (0.275 to 0.282). The variation seen in this case appears anomalous though, since a rise in temperature should result in a fall in the a_w , absolute humidity remaining the same. This can be explained by the fact that the least count of the device is 1 ppm for absolute humidity measurements and thus, rounding off errors could result in such observations for minor variations in temperature.

Although transformer oils are not hydrophilic, hot and dry oil has a tendency to absorb water as mentioned by the authors in [16]. Moreover, as oil cools down the moisture should go

back into the paper as it has a greater affinity for water. Thus, a positive spike, post impregnation, in the humidity of oil would be expected but that does not appear in the measurement record. An increase in the moisture content of oil, consequently in the relative saturation, is seen instead. This observation is deliberated upon after the results of sample bar 6 has been presented.

With occasional bursts of up to 5 pC, samples 2.1 to 2.5 did not show any significant PD activity either. The record of the oil parameters for sample bar 2 is shown in Figure 5-12.

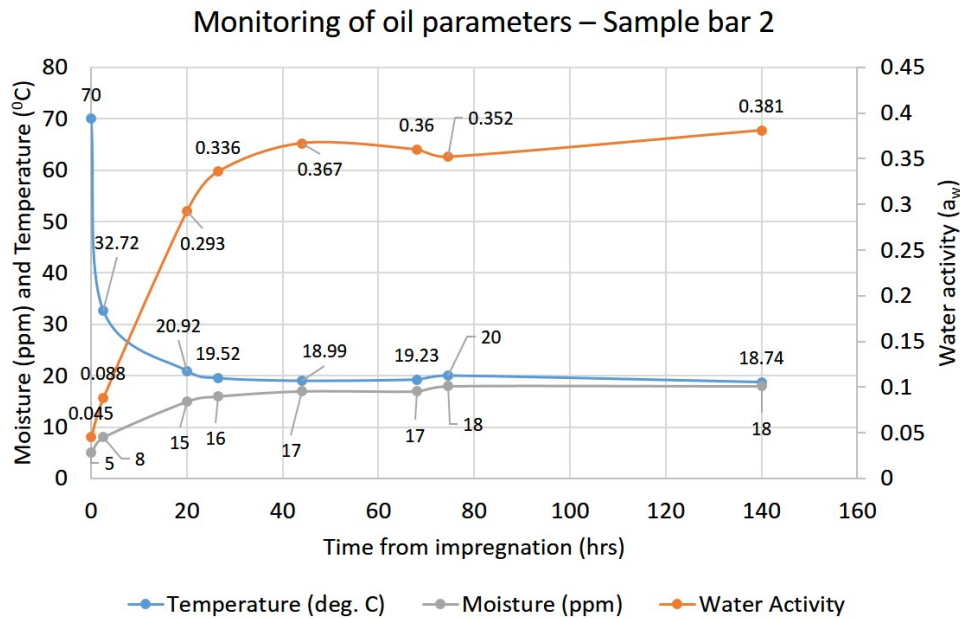


Figure 5-12: Monitoring of oil parameters during testing of sample bar 2

Sample bar 1 was unwrapped after the completion of the test and the bare metal bar was washed and cleaned. This bar then became the substrate for sample bar 6 which was wrapped at TU Delft. Similarly, sample bar 2 became sample bar 7.

Results of tests on Sample bar 6

As far as stochastic processes are concerned, considering a greater number of samples results in a more reliable conclusion. PD phenomenon is also a stochastic process as mentioned by Brunt in [42]. Although ten is not a large sample size, it was decided to increase the test field stress to the values mentioned in Table 5-6 based on the results obtained for sample bars 1 and 2.

Paper type	Thickness range	Field stress
Presspaper and Crêped presspaper	< 2 mm	12 kV/mm
Crêped presspaper	2 mm to 3 mm	10 kV/mm
Crêped presspaper	> 3 mm	10 kV/mm

Table 5-6: Revised testing field stresses for different types and configurations of paper

Step Description	Test voltage
Background measurement	2.7 kV
Intermediate measurement	8.2 kV
Test level	10.8 kV
Enhancement level	12.3 kV

Table 5-7: Test voltages used for sample bar 6

Sample bar no.	Wt. of bare metal bar	Wt. after drying	Wt. after climate exposure	% moisture (w/w) in paper
6	5423.2 g	5492.5 g	5497.4 g	7.1

Table 5-8: Weight of sample bar 6 pre and post climate exposure

Sample bar 6 was tested using the revised field stresses. The test voltages applied at each step of the PD test are listed in Table 5-7 and the weights of the sample bar during the conditioning process are given in Table 5-8. The results obtained were similar to that of sample bars 1 and 2. No PD activity of significance was observed.

The record of the oil parameters for sample bar 6 is shown in Figure 5-13.

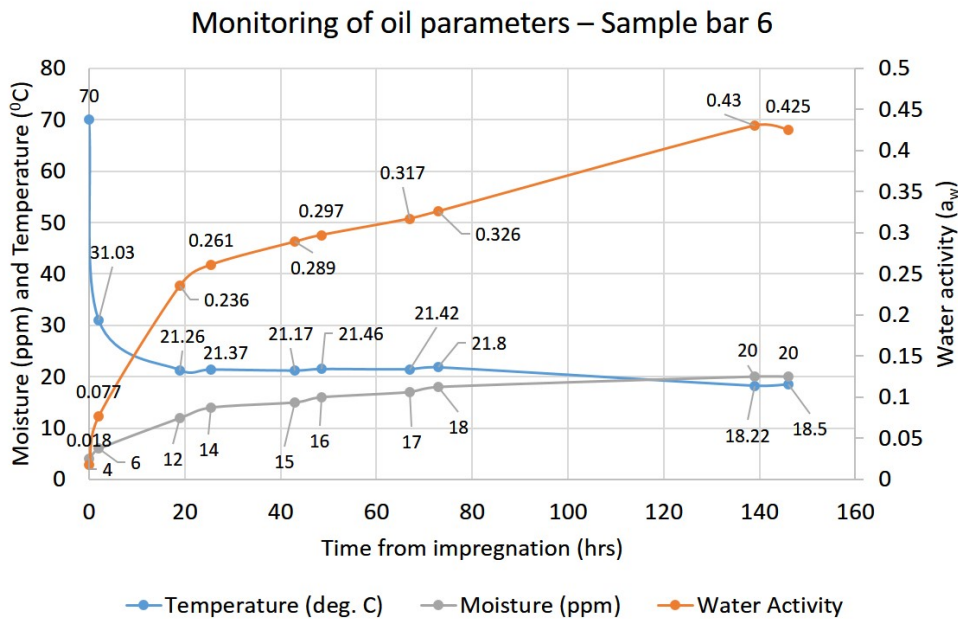


Figure 5-13: Monitoring of oil parameters during testing of sample bar 6

Discussion

In summary, no PD activity was observed during the tests conducted on sample bars 1, 2 and 6. Correlating the conditioning parameters used for preparing the samples with the curves obtained for moisture ingress and egress processes (Figure 5-3, Figure 5-4) allows the

aforementioned observation to be explained. According to the ingress and egress curves, the moisture content of sample bar 1 would be close to 1% as the exposure time of 4 hours is insufficient to cause saturation and at the same time the vacuum duration of 24 hours is long enough to remove most of the moisture. The moisture content of sample bars 2 and 6 would be approximately 2.5% based on 24 hour climate exposure and 4 hour vacuum duration.

On impregnating with hot oil more moisture egresses from the paper into the oil. Hot oil being less viscous also penetrates the pores and capillaries better and thus, paper is impregnated almost completely since the individual layers and the wrapping as a whole are thin. PDs are not seen at the applied field stresses as impregnation causes an increase in dielectric strength of paper and reduction in number/sizes of voids which in turn raises the breakdown strength according to the Paschen criteria [25].

The moisture egress is reflected in the increased humidity of oil. Moreover, hot oil also absorbs moisture from the air inside the tank which is why the humidity of oil increases post impregnation. The diffusion time constant of water in OIP is in the region of weeks for temperatures below 40 °C as mentioned by the authors in [43]. Thus, the process of moisture re-entering paper is very slow. Therefore, the humidity of oil remains almost at the same level and fluctuations are dependent on variations in humidity of the surrounding air. This trend is, in fact, observed in all cases which is why the oil parameter records for the rest of the samples are located in Appendix C.

The results of PD tests on sample bars with clamping are discussed further.

5-2-2 Sample bars with clamping

Sample bar 7 was the first to be tested. It was conditioned according to the parameters given in Table 3-3 prior to oil impregnation. The oil parameter measurements are shown in Figure C-1. Figure 5-14 shows an example of testing a sample bar within a clamping frame wherein, sample 7.2 is being tested.



Figure 5-14: Testing of sample 7.2 in progress

The weight of the sample bar was not measured separately as that entailed dismantling and then reassembling the clamping frame which would disturb the conditioning process. Moisture was absorbed by the frame components (made of wood) and the sample bar.

Table 5-9 lists out the stage-wise test voltages applied. Just as in sample bars 1, 2 and 6, no PDs of significance were observed in samples 7.1 to 7.5 with the exception of sample 7.4. Discharges such as those shown in Figure 5-15 were observed in that case. Figure 5-15a depicts PDs observed during the voltage ramp up phase whereas Figure 5-15b shows discharges seen during the one hour test phase. The maximum magnitude of discharge observed during the test was approximately 7 pC which can be gleaned from Figure 5-15b.

Step Description	Test voltage
Background measurement	4.3 kV
Intermediate measurement	12.8 kV
Test level	16.8 kV
Enhancement level	19.1 kV

Table 5-9: Test voltages used for sample bar 7

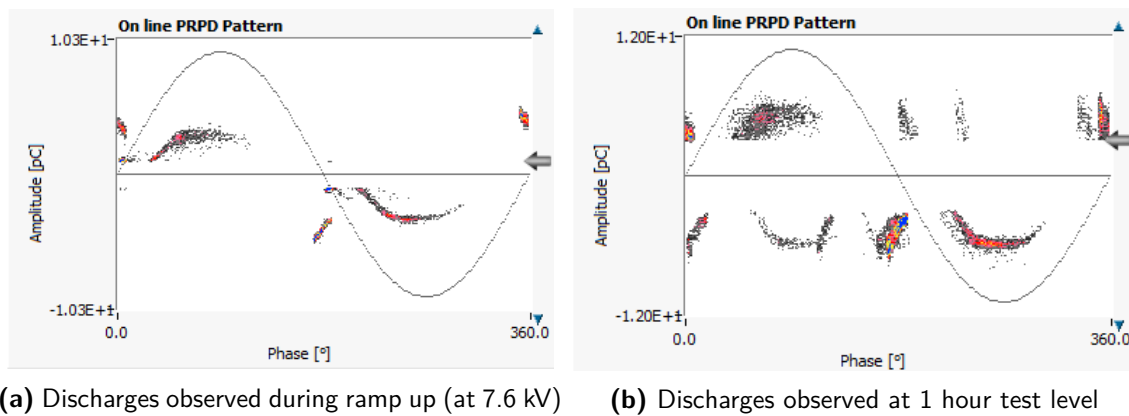


Figure 5-15: Discharges observed during testing of sample 7.4

As these discharges incepted at a field stress of 5.4 kV/mm (7.6 kV), which is within the initial test field stress of 6 kV/mm, further investigation into the source of these discharges was necessary despite the magnitude being low. The discharge pattern seen in Figure 5-15a resembles patterns pertaining to discharges occurring within the insulating material structure (internal discharges) such as in cavities or voids [44].

Sample 7.5 was tested after 7.4 but no discharges were observed. 7.4 was tested again after 2 days. The discharges initiated at nearly the same voltage with similar patterns being observed. It was then exposed to the enhancement voltage for a longer duration. On reducing the voltage back to the test level no further PD activity was observed. Two more tests were conducted on the same sample. The PDs restarted at the enhancement level in the first test and then died out in the second test.

The sample bar was checked for visual signs of discharges after dismantling the frame and during the unwrapping process but nothing was observed.

The peculiar pattern seen in Figure 5-15b was investigated and it was determined that there was a problem with the detection software which caused the synchronizing voltage signal to distort for a period of time. This distortion is illustrated in Figure 5-16.

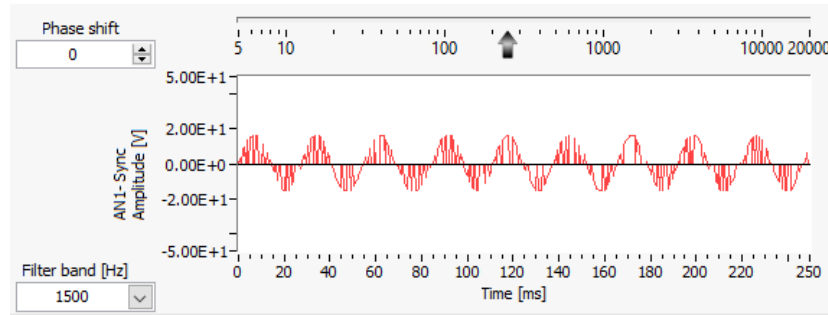


Figure 5-16: Distortion seen in the synchronizing voltage signal

Sample bar 8 was prepared, conditioned and tested in the same way as sample bar 7 in order to check the reproducibility of the result. However, none of the five samples showed any PD activity. The oil parameter measurements are shown in Figure C-2.

Discussion

The author in [45] mentions that the porosity of paper fibres within a single sheet reduces on application of mechanical pressure. The same could be envisaged in case several layers are pressed together which actually happens when clamping force is applied. From a microscopic point of view the end fibres of neighbouring layers interact with each other to form a new contact and change the overall pore pattern. Moreover, the surface area of paper exposed to the surroundings is physically reduced due to the obstruction caused by the HV electrodes which generate the clamping force. The only way moisture can ingress into these zones is through the neighbouring layers of unclamped paper. Thus, in effect the rate at which moisture is absorbed in the compressed zone (test sample region) would be reduced.

Sample bars 7 and 8 were exposed to the conditioning climate for the maximum duration of 24 hours and subjected to the minimum vacuum period of 4 hours. If these time parameters are cross-referenced with the moisture ingress and egress trends pertaining to presspaper observed in Figure 5-3 and Figure 5-4, an average moisture content of 2.6% could be expected in the exposed regions.

The reduced moisture absorption rate in the compressed regions would imply that saturation values are unlikely to be achieved locally despite the exposure duration being high. A short vacuum period implies that whatever moisture has been absorbed in these regions is not removed completely.

Following on from the discussion on the results obtained for sample bars 1, 2 and 6, impregnation by hot oil would assist in removal of more moisture from the compression zones as an oil film will be formed between the HV electrode and the top layer of paper. Moreover, the convection currents that occur due to oil cooling down naturally would cause the periodic renewal of the oil film and consequent removal of moisture from the region. The time taken to fill oil in the bucket, coupled with the degassing interval, proves to be enough to allow the PDIV to increase beyond the test field stress applied.

The PD activity observed in sample 7.4 is thus deemed an exception and cannot be attributed to moisture or its migration. Had that been the case a similar phenomenon would have been

expected during the testing of sample bar 8. Prolonged high voltage application on the discharge site may have caused it to burn out or burst and repeating the test might have caused the discharge path to lengthen or branch out, reminiscent of the treeing phenomenon explained in [35].

It is plausible that had sample 7.4 been tested first, PDs would still have been observed. In that case the inference would have been that discharges are seen immediately post impregnation after which they seize, i.e., one day standing time is sufficient.

The fact that no PDs were observed in samples with clamping, coupled with the absence of PD activity in sample bars 1, 2 and 6, pointed at the necessity to investigate the field stress pattern actually being applied on the sample. This was mainly to determine whether the electrode profile being used was suitable or if it was more perfect than desired. The investigation was performed by means of field simulations which are described in Section 5-2-3.

5-2-3 Field simulation study

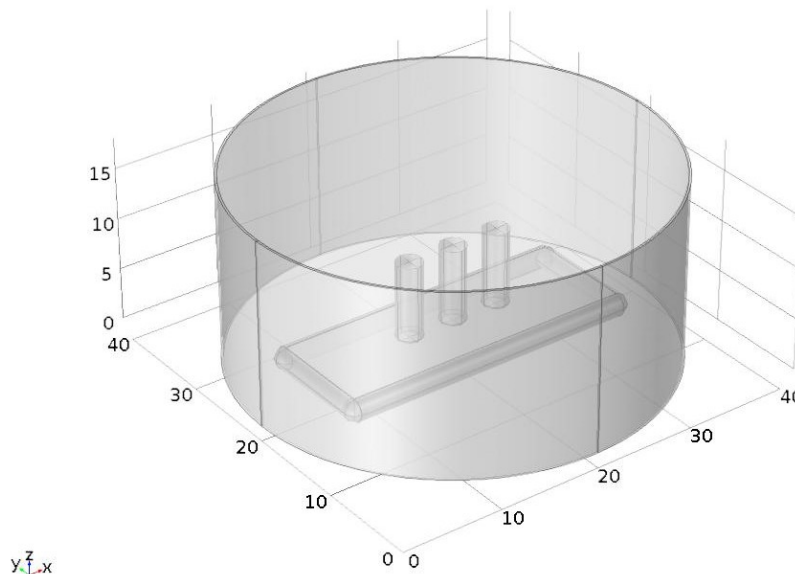


Figure 5-17: Object model used in the simulation (axis orientation - bottom left)

Simulations were performed using COMSOL Multiphysics® v5.1 and stationary studies were carried out since the steady-state behaviour of fields was to be observed. The clamping frame was omitted as the field stress it experienced was not the primary focus of the study. The model was created on the basis of the following material specifications:

HV electrode - Stainless Steel

Transformer oil - $\epsilon_r=2.3$

LV electrode - Stainless Steel

OIP - material with $\epsilon_r=4.0$

The complete object model used in the simulation is shown in Figure 5-17. Three 75 mm long HV electrodes are included to check for any mutual influences. The outer cylinder mirrors the bucket placed in the test tank and is used to portray the oil medium. The bar underneath the HV electrodes depicts a wrapped sample bar.

A 1 mm thick paper layer is placed on the LV electrode and a 0.1 mm oil film is inserted between the bottom surface of the HV electrodes and the top of the paper layer. 12 kV is applied to the middle electrode.

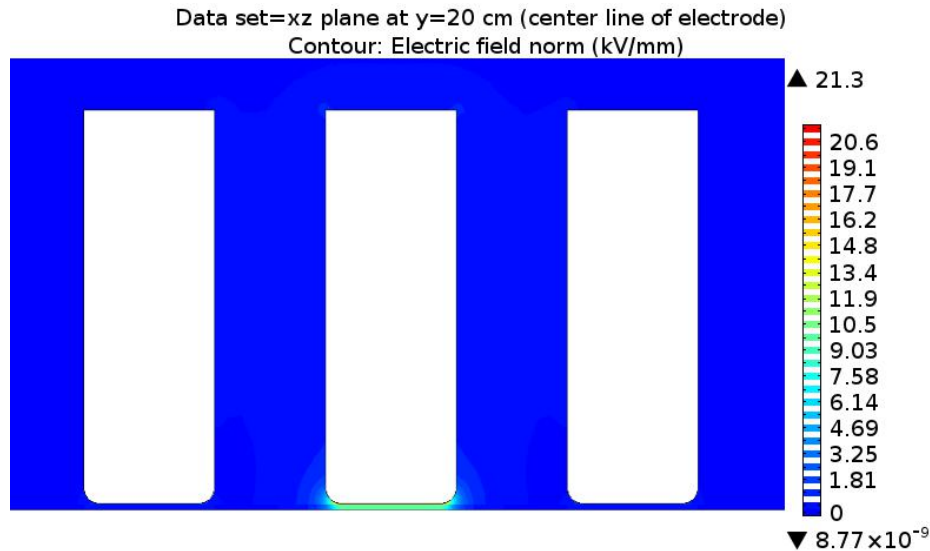


Figure 5-18: Field stress pattern (normal component) - 0.1 mm oil film, 1 mm paper layer, 12 kV applied voltage

Figure 5-18 shows the normal component of the electric field encountered when the entire object is sliced by an xz-plane through the centre ($y=20$ cm). It can be seen that the field is almost zero in the bulk of the oil. The neighbouring electrodes help to shape the field pattern but the field exists only in the vicinity of the energized electrode. The electrode can thus be considered as an axisymmetric object and the field distribution can be studied on that basis.

Figure 5-19 zooms in on the bottom left corner of the energized electrode, albeit rotated 90° to the right. The thickness of the oil film has an impact on the field distribution. Thinner the oil film, lesser is the voltage drop up to the start of the paper layer which results in a higher field stress in the paper. This explains the 11 kV/mm field stress seen in the flat portion of the HV electrode. Had the oil film not been considered the field stress in the paper would have been 12 kV/mm.

It must be remembered that the field stress at the point where the electrode begins to curve away from the paper is affected by the size of the mesh used during modelling and may therefore be overestimated. Focussing on the two lines marked in Figure 5-19, the normal components of the field at the oil - OIP interface are about 6 kV/mm and 15 kV/mm along lines 1 and 2, respectively. Both of these values are equal to or more than the actual field stress applied during tests. Thus, the normal component of field generated by the electrode is acceptable.

Surface discharges are governed by tangential field stresses. For the HV electrode profile used in these experiments, tangential fields are produced in the curved sections. Figure 5-20 shows the x-component of the electric field. The magnitude of the x-component of the field at the oil - OIP interface along the marked line is about 3.5 kV/mm.

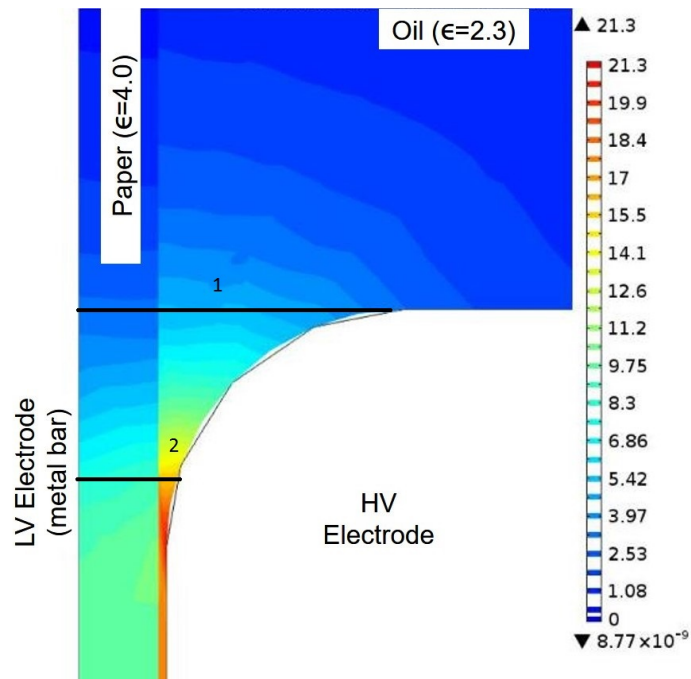


Figure 5-19: Field stress pattern (normal component) - zoomed in

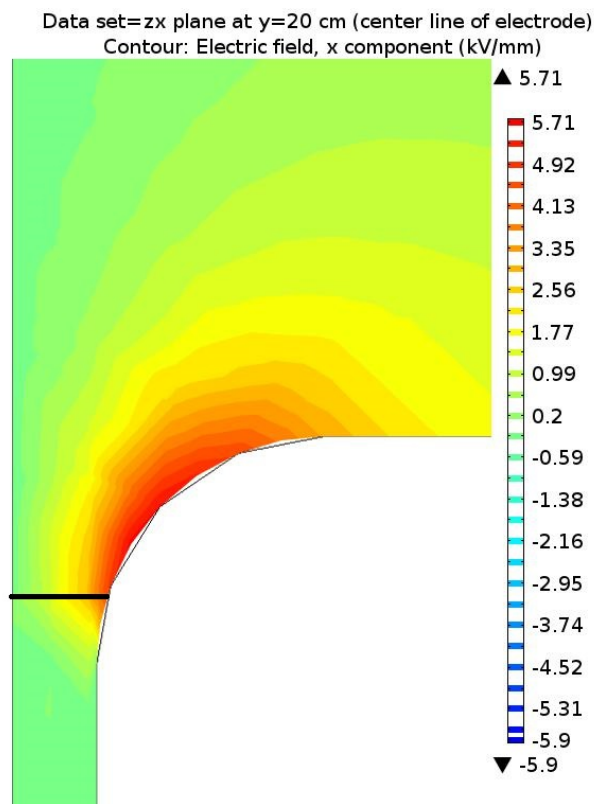


Figure 5-20: Field stress pattern - x component

Interfaces parallel to the field breakdown at lower voltages when compared to interfaces that are perpendicular to the field due to the inevitable presence of impurities such as dust particles or surface irregularities [25]. Thus, equipment designers attempt to keep the tangential stresses down to a minimum. The x-component value of 3.5 kV/mm is more than 50% of the normal component of the field stress used during actual tests, which is significant. The HV electrode profile is therefore considered suitable from this perspective too.

Since even the worst among worst case scenarios (maximum climate exposure, minimum vacuum time, maximum field stress) failed to generate any PDs, an investigation into determining the PDIFs for paper conditioned like sample bar 7 (24cc/4vac) and for paper saturated with moisture was undertaken.

5-2-4 Tests to determine PDIF

Two sample bars each of presspaper (no. 9 and 11) and crêped presspaper (no. 3 and 4) were prepared as part of this exercise. As mentioned in Table 3-3, sample bars 9 and 4 were conditioned to be saturated samples and sample bars 11 and 3 were conditioned like sample bar 7. The procedure used to determine PDIV is the one described in IEC 60270:2001 [40]. Gradual voltage increase was executed by raising the voltage in steps of 1 kV/mm and including a wait time of 1 min at each step.

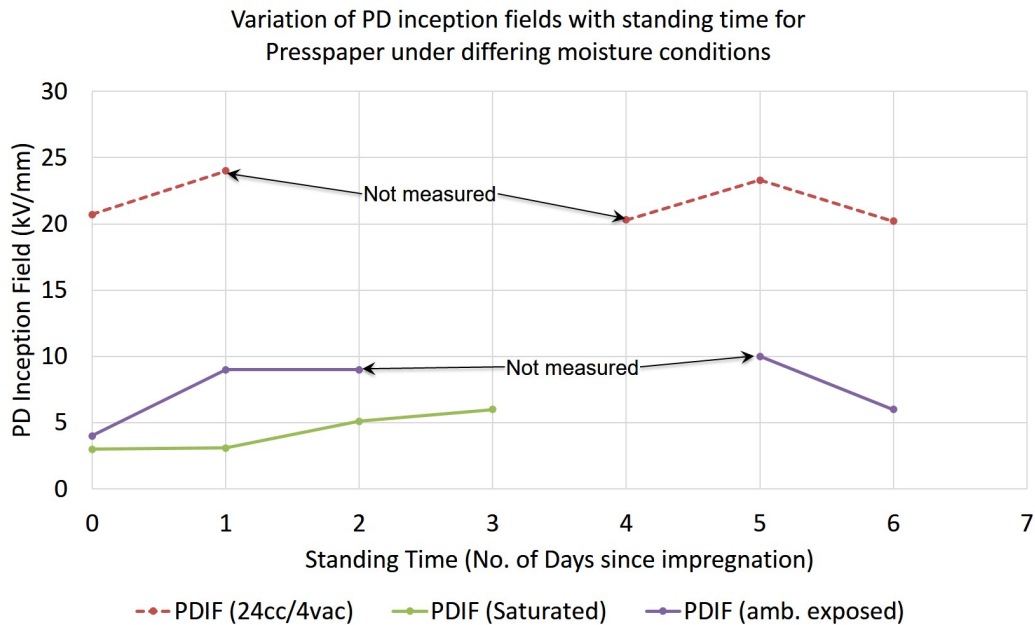


Figure 5-21: PDIF variation with standing time for presspaper with differing moisture content

The results of the tests conducted on sample bars 9 and 11 are shown in Figure 5-21. In case of saturated sample bar 9, sample 9.1 broke down at 3 kV/mm. This was initially indicated by the tripping of the protection device. The apparatus was reset and the test restarted. The breakdown was confirmed by the PRPD pattern, shown in Figure 5-22, obtained at just 2 kV after restarting the test.

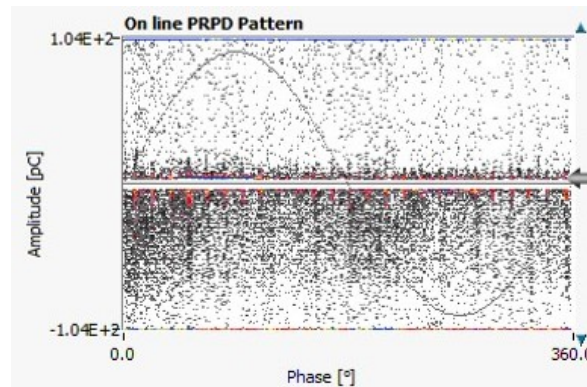


Figure 5-22: PRPD pattern obtained at breakdown of sample 9.1

Sample 9.5 was tested immediately after 9.1 in order to determine whether the breakdown was due to moisture or some other defect. Sample 9.5 also broke down at nearly 3 kV/mm. Thus, the first point on the PDIF curve actually represents two measurements. Figure 5-23 clearly shows the punctures caused by the breakdown events. While unwrapping the sample it was observed that the punctures went right through up to the LV electrode.



Figure 5-23: Punctures in sample bar 9 caused by the breakdown events

The other three samples (9.2 - 9.4) showed PD activity without breakdown and their PDIFs were between 3.5 kV/mm and 5.6 kV/mm as shown in Figure 5-21. An increasing trend in the PDIF with increasing standing time is also observed therein. Thus indicating that standing time does have an effect on the PD behaviour. Figure 5-24 shows a PRPD pattern obtained at 6.8 kV when testing sample 9.2. The arc in the pattern is a characteristic of an internal discharge and the peak of the arc represents a discharge of 200 pC.

The PDIFs obtained for the samples tested in sample bar 11 are all in excess of 20 kV/mm which is three times higher than the test field stress considered initially. Once the PDs incept the discharges are extremely heavy with magnitudes in the nano-coulomb (nC) range. An example of a PRPD pattern showing such a situation is given in Figure 5-25 wherein the discharges are actually larger than the full scale of the display (6 nC). However, no clear trend in PDIF with respect to increasing standing time is observed.

Another sample bar, no. 10, was prepared and left exposed to ambient conditions which meant that the moisture content in the paper would be lesser as compared to the saturated condition. It was therefore expected that the PDIF for these samples would be higher than the

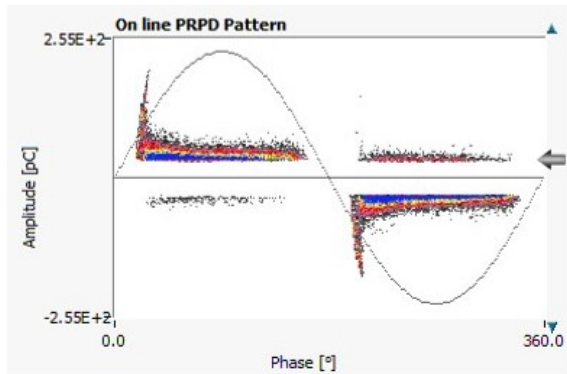


Figure 5-24: PRPD pattern obtained while testing sample 9.2 (at 6.8 kV)

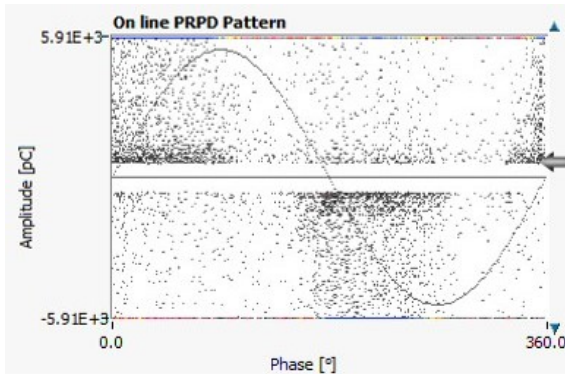


Figure 5-25: PRPD pattern obtained while testing sample 11.2 (at 31.2 kV)

PDIF obtained for saturated samples. As seen from the trend in Figure 5-21, the expectation was met. The curve for ambient exposed samples lies above the curve for saturated samples. However, the effect of standing time on the PDIF cannot be seen as the value increases initially and then drops.

The oil parameters measured during the testing of sample bars 9, 10 and 11 are shown in Figure C-3, Figure C-4 and Figure C-5, respectively.

The high intensity discharges observed during the tests on sample bar 11 were clearly visible in the form of carbonized regions on the paper. This is illustrated in Figure 5-26.



Figure 5-26: Carbonization caused by heavy discharges on sample bar 11

An important aspect needs to be kept in mind while discussing the results of the PDIF tests performed on crêped presspaper. As mentioned in the datasheets attached in Appendix B, the elongation property of crêped presspaper is vastly different from that of presspaper. It is in fact close to 30 times greater when comparing the values given for elongation in machine direction. When clamping force is applied on crêped presspaper it causes a depression to be created underneath the electrode surface. Figure 5-27 illustrates the phenomenon quite clearly. A similar zone also appears in the case of presspaper but it is barely discernible as evinced by the outline of the electrodes seen in Figure 5-23.

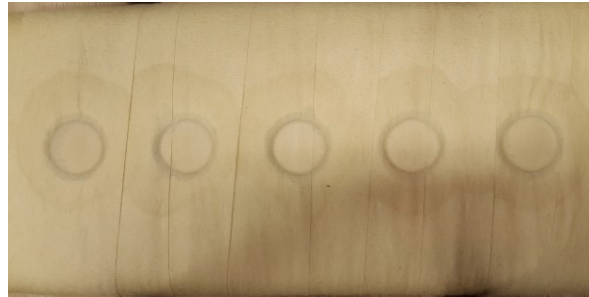


Figure 5-27: Depression caused by clamping force in crêped presspaper

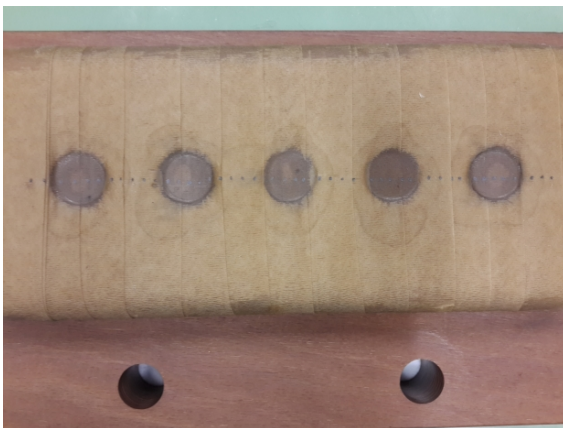


Figure 5-28: Measurement spots marked on the sample bar



Figure 5-29: Measuring depth of the depression using a dial gauge

The effective thickness of the paper layer under test is no longer the same as that measured after wrapping. Since determining the PDIF is the primary concern, the correct thickness of the paper layer is needed for the calculation. The depth of the zone was measured using a Mahr's Micromar - depth micrometer and correlated using a Compac Jet 512K dial gauge.

In the case of dial gauge measurements, several spots were marked on the sample bar as shown in Figure 5-28. To understand the method used for calculation the following needs to be considered. The points marked in the region between the depressions can be referred to as *peak points* and the points marked in the depressions as *valley points*. The readings corresponding to each peak and valley points are noted with respect to an arbitrary zero. An example of dial gauge measurement is illustrated in Figure 5-29.

An average of all peak points is calculated so as to obtain a single value for the peak (Pk_{avg})

and similarly the valley points are averaged to get a single value for the valley (Vl_{avg}). The average depth of depression (D_{avg}) is determined using Eq. (5-3). The effective thickness of the paper (t_{eff}) is calculated using Eq. (5-4), where t_s is the thickness of the paper layer mentioned in Table 3-2.

$$D_{avg} = Pk_{avg} - Vl_{avg} \quad (5-3)$$

$$t_{eff} = t_s - D_{avg} \quad (5-4)$$

The D_{avg} obtained for sample bar 4 was 1.8 mm. The individual depths measured for the five compression zones were within 5% of 1.8 mm and thus, that was the depth considered for the sample bar as a whole.

The PD test results give information regarding the PDIV. However, the exact profile of materials lying between the two electrodes must be known in order to calculate the PDIF. Since a 0.1 mm oil film has been considered previously, the same assumption is retained to maintain consistency. The field simulation performed in Section 5-2-3 is repeated with the following changes:

- Paper layer modelled - 3.3 mm thick
- 1.8 mm depression added
- 20 kV applied voltage

The results of the simulation are shown in Figure 5-30. Without the depression and the oil film, the field stress on the paper under the flat portion of the HV electrode would have been 6.1 kV/mm but including them causes an increase in the field stress and it becomes nearly 11 kV/mm. Thus, this factor of field magnification, caused due to clamping, was applied to the PDIFs obtained for samples 4.1 to 4.5. A similar factor was also determined for samples 3.1 to 3.5.

The corrected PDIFs for both sample bars 3 and 4 are shown in Figure 5-31 wherein, an overall trend of PDIF increasing with standing time can be observed. While testing sample bars 11 and 3, 1 hour tests at the revised field stress values were conducted prior to raising the voltage and subsequently determining the respective PDIF. Thus, supporting the observation that no PDs are observed for 24cc/4vac exposure with a greater sample size.

The oil parameters measured during the testing of sample bars 3 and 4 are shown in Figure C-6 and Figure C-7, respectively.

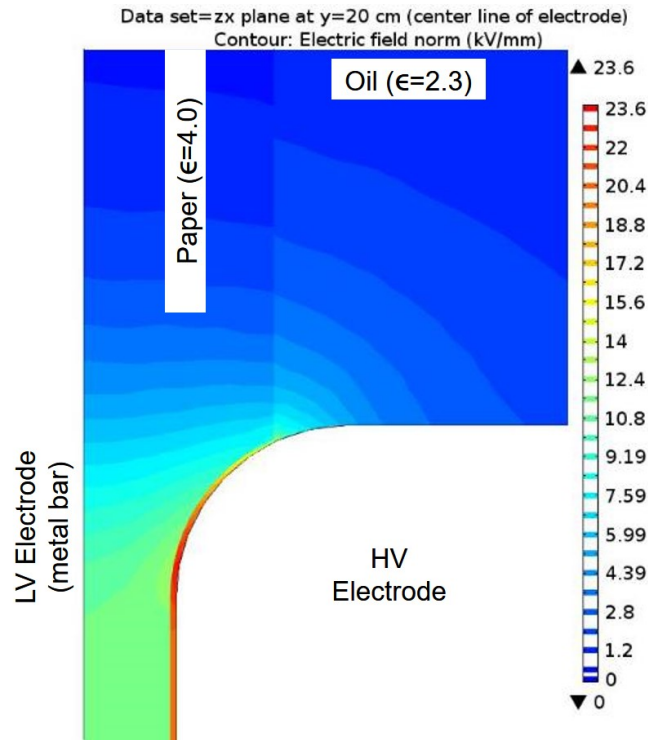


Figure 5-30: Field stress pattern - 3.3 mm paper layer, 1.8 mm depression, 20 kV applied voltage

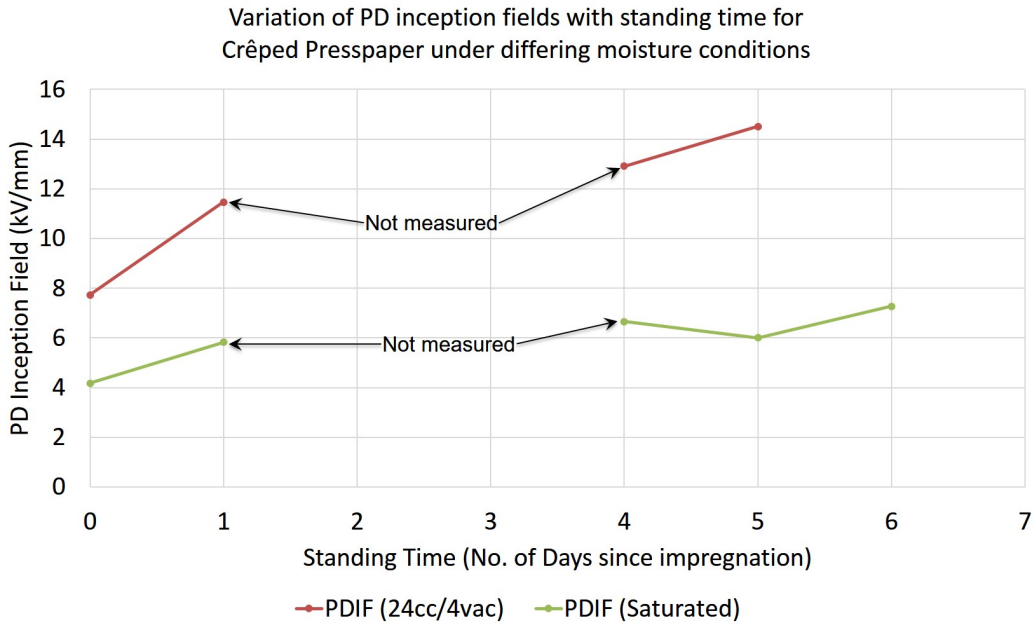


Figure 5-31: PDIF variation with standing time for crêped presspaper with differing moisture content

Discussion

The nature of the curve describing the behaviour of oil humidity with time remains the same for sample bars 3, 4, 9, 10 and 11. The humidity of oil rises post impregnation and is followed by a plateau. Where the scenarios for sample bars 4, 9 and 10 differ from the rest are in the amount of moisture contained initially in the paper. Being saturated samples, moisture is much higher. Thus, even though some moisture will egress out of the paper due to hot oil there will still be some that remains within the paper. This moisture gets trapped by the oil during the impregnation process which leads to PD activity.

The RH of air inside the test tank was also monitored during the tests conducted on samples with clamping. The measurement point was just above the surface of the oil inside the bucket. Tempcontrol P670 Temp was used for the measurements. This record was created in order to check if RH of air inside the tank influences the humidity of oil. The following data was considered:

- The final value of oil humidity reached during each PD test.
- Conditioning durations to which the respective sample bars were subjected
- The range of RH of air encountered over the duration of each sample bar test

Sample bar no.	Conditioning duration (cc/vac)	Final oil humidity (ppm)	Range of RH of air (%)
7	24 h/4 h	15	25 - 33
8	24 h/4 h	17	36 - 48
11	24 h/4 h	24	51 - 70
3	24 h/4 h	21	50 - 60
10	Exposed to ambient	26	38 - 55
9	Saturated	28	45 - 55
4	Saturated	28	45 - 63

Table 5-10: Conditioning duration, oil humidity and RH of air - sample bars with clamping

Table 5-10 lists out the data. The moisture in oil is maximum in the case of saturated sample bars followed by the ambient exposed sample bar and then 24cc/4vac sample bars in decreasing order. As seen previously, susceptibility to PDs also decreases in the same order which demonstrates that moisture does indeed have an effect on PD behaviour. Comparison between the three 24cc/4vac presspaper sample bars (7, 8 and 11) indicates that RH of air also has an influence on the final moisture content with higher moisture levels encountered under higher RH conditions.

Conclusions and Recommendations

Although oil-filled transformers using paper as insulating material have been in operation for more than a century, studies are undertaken even today to evaluate the efficiency of design and production processes. Scientific investigations aid in this regard by identifying the area(s) of improvement and/or providing information about how the proposed improvement(s) affects the overall output. The work carried out in this research is an example of the latter.

This research was conducted as part of a project that aims at reducing the post impregnation standing time of oil-filled power transformers. The main aim of this research was to study the influence of moisture in insulating paper on standing time. To this effect, PD tests were conducted in order to determine if PDs would be observed in OIP for selected process conditions and durations that may be faced during manufacturing. These tests were also used to look for changes in PD behaviour with increasing standing time. Moisture ingress and egress processes related to insulating paper were also studied for those selected process conditions.

The tests performed on paper samples with clamping also gave an insight into the behaviour of laminated wood. The clamping frame was made of thick blocks of laminated wood with the top and bottom blocks being 40 mm and 15 mm thick, respectively. Although dimensions may vary, thick blocks of wood are also used in active parts of transformers. Moisture is absorbed from the surface inwards. Moisture that has percolated into the central regions may not be extracted by the applied vacuum, due to the distance it has to travel to reach the surface, which would then be trapped during the impregnation process.

20 mm of each HV electrode is embedded inside the top block and the bottom block lies underneath the sample bar. Looking back at the electric field simulation results shown in Figure 5-18, it is observed that the **field stress** in those regions is very **low** (≤ 1 kV/mm). Thus, no PDs were observed despite moisture being trapped as the **PDIV was not reached**. A similar scenario is encountered in transformers where **laminated wood** is used in regions that experience low field stresses. **Thus, an investigation into the influence of wood on standing time was not necessary.**

The research questions are tackled in Section 6-1 followed by some recommendations for further research in Section 6-2.

6-1 Conclusions

The research questions posed in Section 1-4 are answered here:

1. *Can PDs attributable to moisture be observed in insulating paper for the electric field stress used during PD detection tests?*

A scenario pertaining to ambient conditions (60 °C, 75% RH) was employed in the investigations which only a few transformers might actually experience. The amount of moisture available for absorption during the tightening phase will be less, in majority of cases, due to lower humidity and/or lower temperature.

Considering an overall duration of 24 hours between the end of drying and the end of final assembly, which is enough to saturate paper, and a subsequent 4 hour period of vacuum results in a net moisture content of about 2.6% in both types of papers, based on the moisture ingress and egress curves.

No PDs were observed in presspaper samples conditioned as per the aforementioned scenario at test field stresses of 12 kV/mm, regardless of the use of clamping force. The PDIFs observed were ≥ 20 kV/mm. In case of crêped presspaper, PDIF immediately after impregnation was 8 kV/mm but rose beyond the revised test stress value of 10 kV/mm after 1 day. However, saturated samples of presspaper and crêped presspaper exhibited PD activity, some resulting in breakdown, even at 3.5 kV/mm.

In reality vacuum is maintained at least for 24 hours in order to cater to the huge volume of a transformer tank and the sheer bulk of solid insulation used in it. Moisture egress studies showed that 24 hours of stable vacuum (10mbar (abs.), 25 °C) reduced the avg. moisture content in both papers from saturation to about 1%. Thus, an increase in the PDIF is expected due to lower moisture content. Moreover, the electric field stress that OIP is subjected to during IVPD is in the region of 6 kV/mm for high power HV transformers which is lower than the PDIFs obtained during the tests.

Thus, PD activity attributable to moisture will not be observed in paper for the electric field stresses applied during an IVPD test unless the moisture content is close to saturation. However, PDs due to other sources may be observed as in the case of sample 7.4.

2. *Does paper or low thickness cellulosic insulation material actually play a role in determining the standing time?*

No PDs were observed, at conventional test field stresses, even immediately after impregnation. Thus, paper or low thickness cellulosic insulation material does not play a role in determining the standing time. Based on the observation it can be claimed that no standing time is required if varieties of presspaper are the only solid insulation material used in a transformer and PD detection the only test performed.

3. *How does the duration of the vacuum cycle, prior to impregnation, influence the moisture migration process? Could a longer duration cause a significant reduction in standing time?*

A period of vacuum applied prior to impregnation has a drying effect on the material. Longer the duration of the vacuum cycle, more is the amount of moisture extracted.

This is true only up to a certain minimum for a fixed set of conditions. This was seen in the results of the moisture egress tests where 1% moisture content was attained in 24 hours and the value remained the same even after 48 hours of vacuum. The ambient temperature determines the rate at which moisture can be extracted.

Considering only presspaper and créped presspaper, the standard 24 hour vacuum cycle is sufficient to dry the insulation assuming the conditions of vacuum and temperature remain the same. A longer duration is therefore not necessary.

The ambient temperature considered in this research was 25 °C which is representative of summer months. It is possible that, depending on heating arrangements at the shop-floor, a lower temperature is encountered during cooler seasons. In that situation drying at the same level of vacuum would be less effective. However, the amount of moisture absorbed during tightening will also be lesser mainly due to lower RH. Thus, the net effect would almost be the same.

Controlling the amount of moisture entering the insulation is the ideal method to reduce standing time. This can be achieved using the following:

- Performing the tightening activities in a climate chamber like environment wherein the RH is very low. Thus, there will be less moisture available in the environment for the material to pick up
- Speeding up the tightening process to allow lesser time for moisture to be picked up

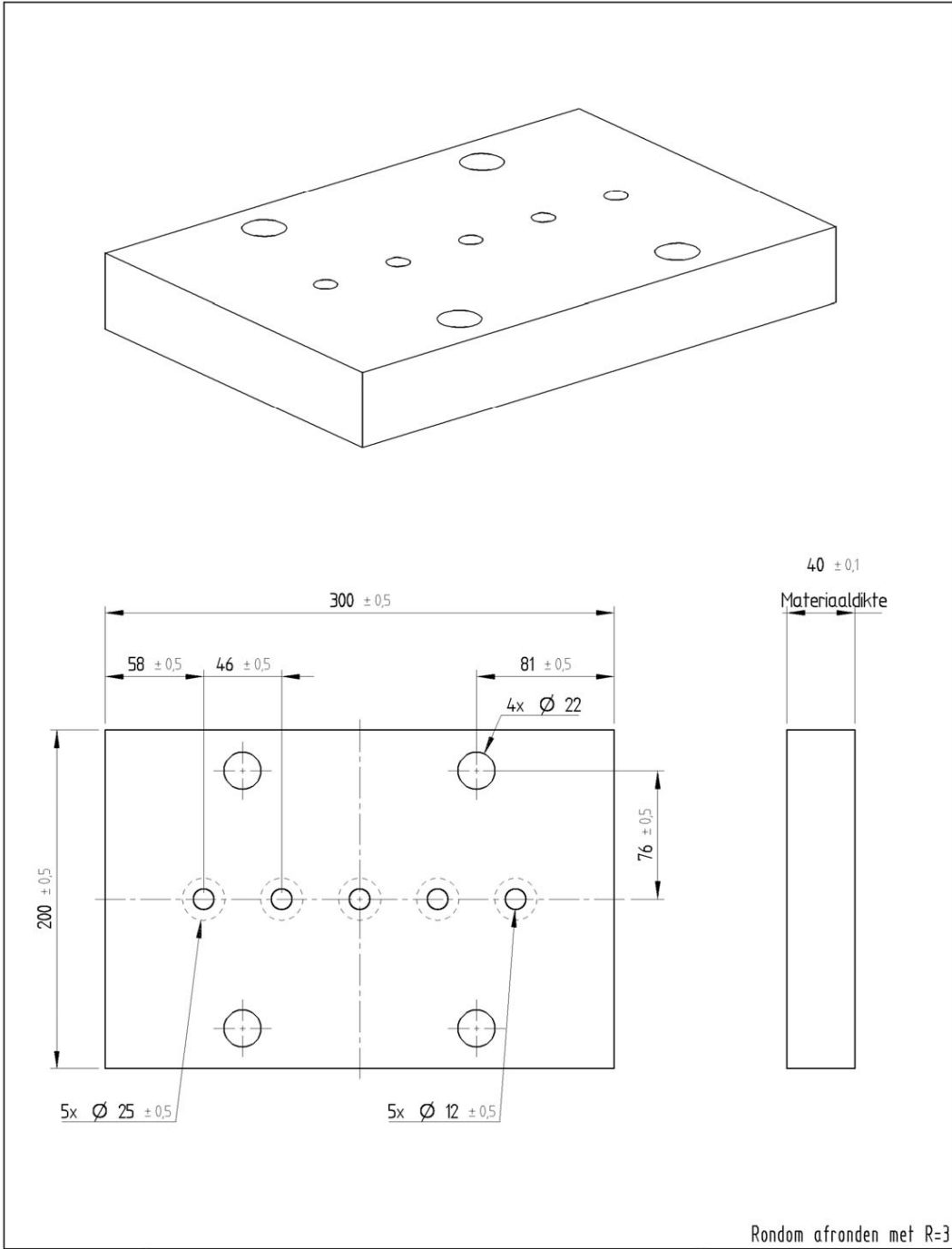
6-2 Recommendations for further research

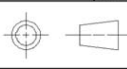
1. All tests that form a part of this study have been conducted on samples and are therefore applicable to those dimensions. Actual transformer constructions are much larger, more complex and involve interaction with other materials. Therefore, these results need to be translated from sample level to real-life constructions in order to formulate guidelines directly applicable to the manufacturing process. A study could be undertaken on how to achieve this translation.
2. Samples were tested for PDs directly after impregnation despite the PD test being the last in an actual FAT program. It is possible that tests such as impulse tests and heat run tests have an impact on the moisture content of both oil and paper which can change the PD behaviour and consequently affect the required standing time. An investigation could be conducted to study the effect of the testing sequence.
3. All the observations are valid for Nynas[®] Nytro Taurus oil. These results may not be applicable in case the oil is changed because the new oil may have different properties such as the relation between temperature and viscosity. This can impact the film thickness and moisture migration process. A study could be initiated which investigates other varieties of insulating oils.
4. A quantitative study could be conducted to understand the variation in porosity caused by the application of clamping pressure and consequent impact on the local moisture ingress and egress.

Appendix A

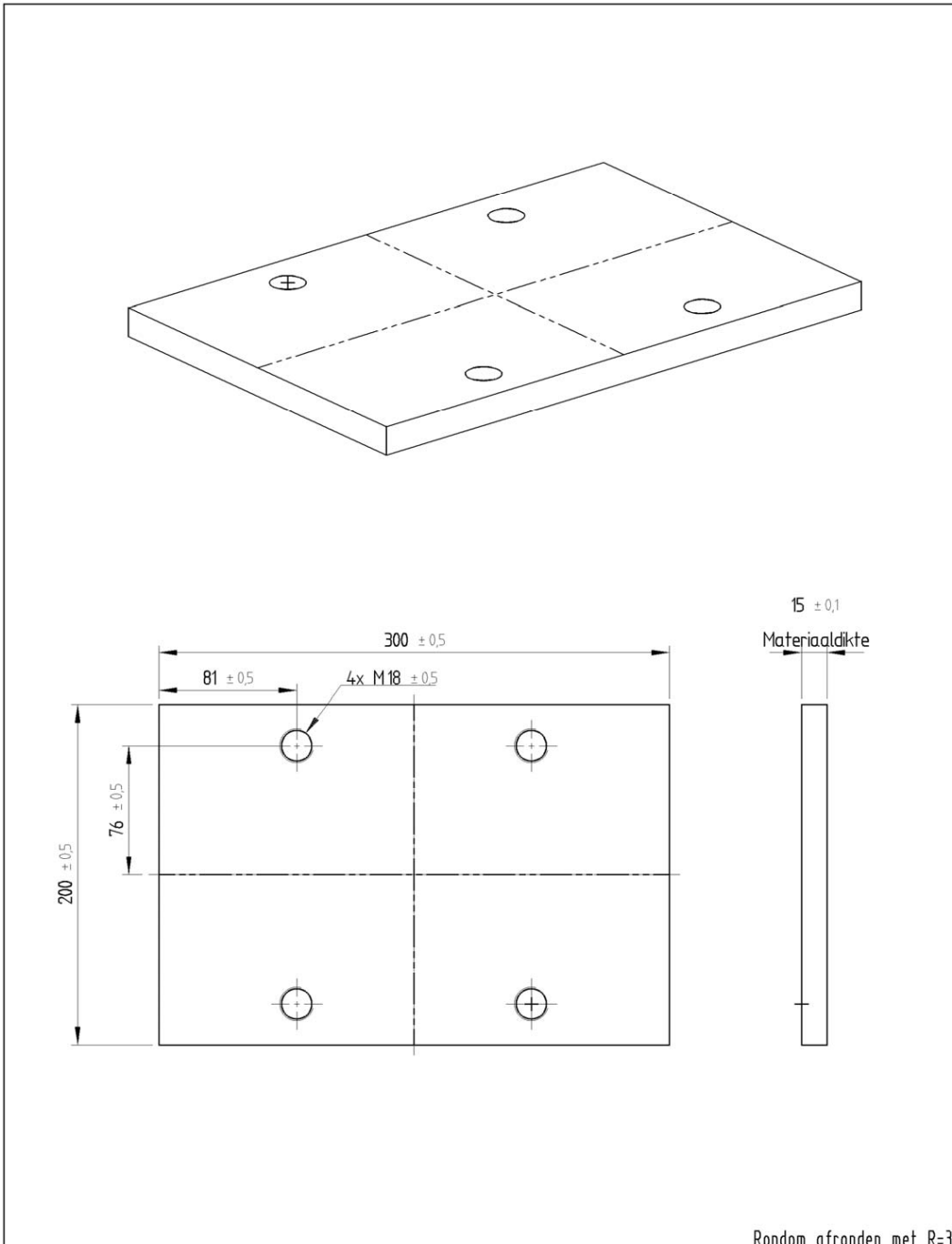
Clamping Frame

The design drawings (courtesy: Royal SMIT) pertaining to the clamping frame are included in Appendix A. The features of the top block are shown first followed by the bottom block and then the clamping frame as a whole including the HV electrodes and the sample bar.

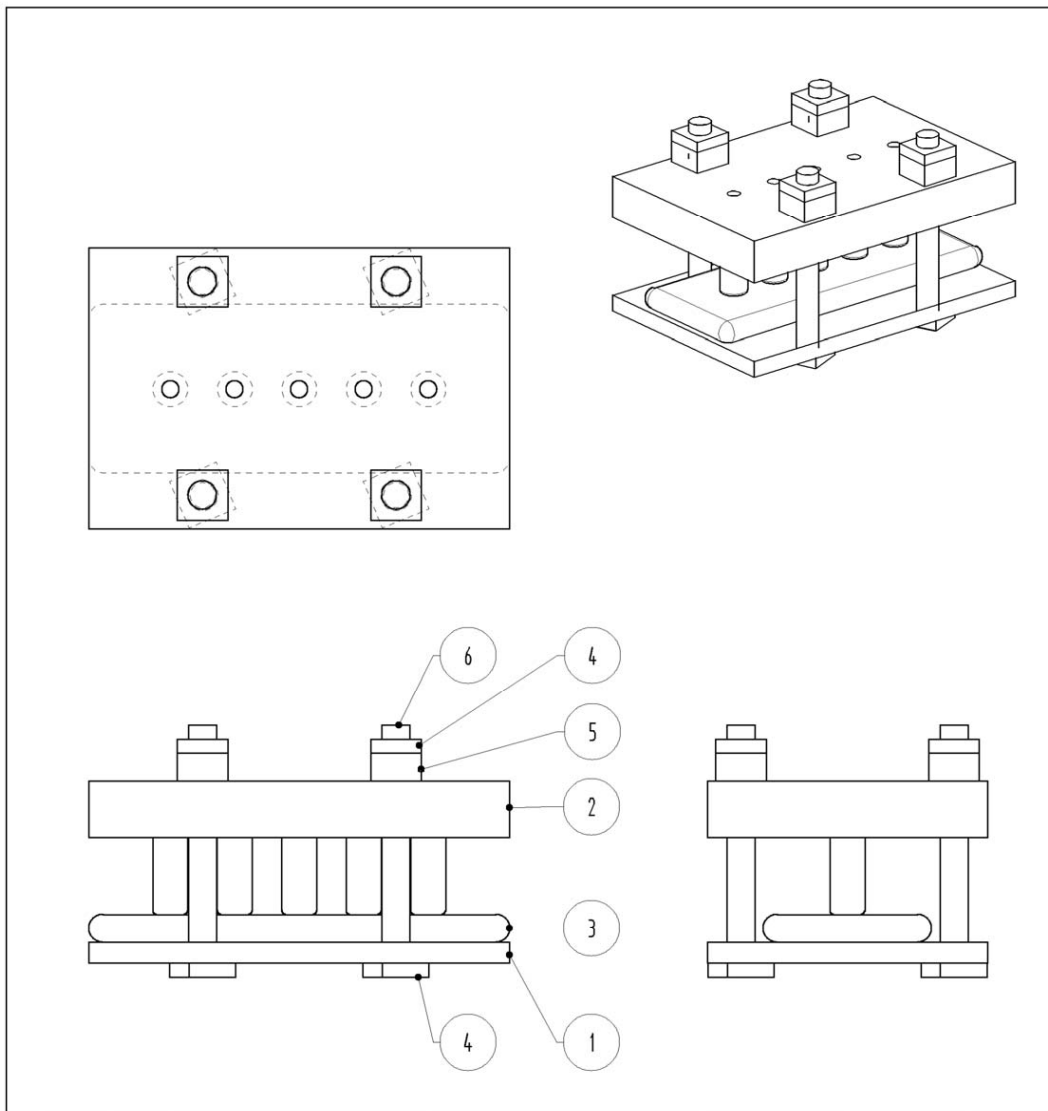


Smit 29.4.01-09.006e		Description of modification			Modified by	Date
DO NOT MEASURE FROM DRAWING		Material	Project number	Article number	Drawn	04-Mar-2016
		KP20224		P1002860	Checked	08-Mar-2016
		Name			Projection	Form
		Block				A4
					Drawing number	Rev
					1169655-001	A

Copyright © Royal SMIT Transformers B.V.



Smit 29.4.0.01-09.006e		Description of modification		Modified by	Date
DO NOT MEASURE FROM DRAWING		-		-	-
Material	Project number	Article number	Drawn	R.Guldenaar	04-Mar-2016
KP20224		P1002860	Checked	R.Guldenaar	08-Mar-2016
Name			Projection	Form	
Block					A4
Drawing number				Rev	
1169607-001				A	



6	4	279753	Threaded rod	KP	M20x180	KP20214	1000817
5	4	279860	Square nut		M20x20	KP20224	HF2005
4	8	279859	Square nut		M20x10	KP20224	HF2004
3	1	1110885	Electrode	-		X2CrNiMo17-12-2	P1110885
2	1	1169655	Block			KP20224	P1002860
1	1	1169607	Block			KP20224	P1002860

Pos	Count	ID nr	Name	Description	Type	Material	Art nr
Smit 29.4.0.01-09.006e		Description of modification			Modified by	Date	
DO NOT MEASURE FROM DRAWING		Material	Project number	Article number	Drawn	R.Guldenaar	07-Mar-2016
		n.a.			Checked	R.Guldenaar	08-Mar-2016
		Name 1169663			Projection		Form A4
		1169663			Drawing number	1169663-001	
						Rev A	

Copyright © Royal SMIT Transformers B.V.

Appendix B

Datasheets of insulating paper

Datasheet for Presspaper - Weidmann

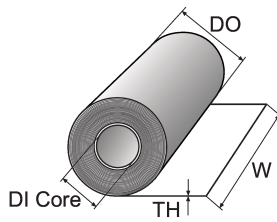
Datasheet for Creped presspaper - Weidmann

WEIDMANN

Presspaper thermally upgraded

E3ET060.RP

Product description
Presspaper thermally upgraded



Product properties

Norm	IEC 60641-3-2, type P.4.1 A		
------	-----------------------------	--	--

Product information

Master size: 3400mm

Standard widths: 850mm, 1135mm, 1700mm or 3400mm

For additional properties, please see additional information in table below.

Existing article can be taken from the chart for product-variants.

Minimal order quantity: 1 rol

Alternative ordering unit: kg

Product parameter

	Description	Unit	Range of value	Constraint	Tolerances		Comment
					Min	Max	
TH	thickness	mm	$0.076 \leq TH \leq 0.5$	0.076mm, 0.127mm, 0.18mm, 0.25mm, 0.38mm or 0.50mm	-10%	+10%	
GRM	grammage	g/m ²		Calculated characteristic			
DO	diameter outside	mm	$280 \leq DO \leq 1000$	Standard 280mm or 370mm			
DI Core	diameter inside core	mm	$70 \leq DI \text{ Core} \leq 154$	Standard 76mm			
W	width	mm	$10 \leq W \leq 160$ $160 < W \leq 300$ $300 < W \leq 3400$	Tolerance >500 mm see Comment	-0.5mm -0.8mm -1mm	0mm 0mm 0mm	W = 501mm to 600mm -1.5mm/-0mm and W = 601mm to 3400mm +/- 1%
L	length	m		Calculated characteristic			

Additional information

Property	Unit	Range of thickness in mm	Value
Apparent density	g/cm ³		1
Tensile strength, machine direction	Mpa	≤ 0.2	115

WEIDMANN

Property	Unit	Range of thickness in mm	Value
		> 0.2	110
Tensile strength, cross machine direction	Mpa	≤ 0.2	50
		> 0.2	39
Elongation, machine direction	%	≤ 0.2	2
		> 0.2	2.4
Elongation, cross machine direction	%	≤ 0.2	7.2
		> 0.2	7.5
Moisture content	%		< 8.0
Ash content	%		0.3
Conductivity of aqueous extract	mS/m		2.2
pH of aqueous extract			7
Nitrogen content	%		1.8
Electrical strength in air unfolded	kV/mm	≤ 0.2	10
		> 0.2	7
Electrical strength in oil	kV/mm	≤ 0.2	70
		> 0.2	50

Please contact us for values outside the specified ranges. The specified tolerances are valid for measurements taken at WEIDMANN or after conveyance and warehousing under conditions appropriate for the material. Customers are advised to add appropriate additional tolerances in case of extreme environmental conditions at the place of warehousing or processing of the material.

Ordering code

E3ET060.RP /TH/GRM/DO/DI Core/W/L

Product variants

	TH (mm)	GRM (g/m ²)	DO (mm)	DI Core (mm)	W (mm)	L (m)
E3ET060.0178R0119	0.18	178	280	76	1000	305.26

Disclaimer

Subject to change without prior notice

PDF generated on: 2015-11-28 22:00:42

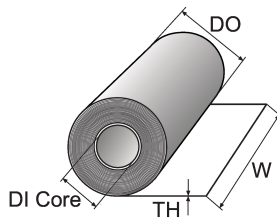
WEIDMANN

35 DICY

E3CCLA0.RP

Product description

Low density insulating base paper



Product properties

Base Paper Thickness:	3 mil (0.076 mm)	Elongation:	50%
Density:	Low density base paper	Upgrade:	Thermally upgraded
Surface:	Non-Calendered		

Product information

Minimal order quantity: 1 rol

Alternative ordering unit: kg

Product parameter

	Description	Unit	Range of value	Constraint	Tolerances		Comment
					Min	Max	
TH	thickness	mm		Typical Value 0.330mm			Please refer to the table below for additional information
GRM	grammage	lbs/3000ft ²		Typical Value 0.28 g/cm ²			Please refer to the table below for additional information
DO	diameter outside	mm	$50.8 \leq DO \leq 965.199$				
W	width	mm	$5.994 \leq W \leq 1473.199$	Tolerance is for Trimmed Rolls	-0.792mm	+0.792mm	The tolerance for STW Rolls is ± 0.396 mm
L	length	mm		Calculated characteristic			
DI	diameter inside	mm	$25.4 \leq DI \leq 152.399$	Standard Core ID's: 25.4mm, 28.575mm, 31.75mm, 38.099mm, 50.8mm, 76.199mm, 101.6mm and 152.399mm			

Additional information

Property	Test Method	Units	Typical Value	Minimum Value	Maximum Value
Thickness	ASTM D374, Method E	inch	0.013	-	-

WEIDMANN

Property	Test Method	Units	Typical Value	Minimum Value	Maximum Value
		mm	0.330	-	-
Tensile Strength - MD	ASTM D202	lbs/inch	20	11	-
		kN/m	3.50	1.93	-
Tensile Strength - CD		lbs/inch	-	-	-
		kN/m	-	-	-
Elongation - MD	ASTM D202	%	65	50	70
Elongation - CD		%	-	-	-
Basis Weight (Grammage)	ASTM D202 (ASTM D646)	lbs/3000ft ²	57.0	-	-
		g/m ²	93	-	-
Density	Calculated	g/cm ³	0.28	-	-
		kg/m ³	280	-	-
Finch Edge Tare (5/8 inch wide)	-	lbs	-	-	-
Finch Edge Tare (15.9mm wide)		kg	-	-	-
Tensile Energy Absorption (T.E.A.)	On going quality assured by tensile and elongation conformity		-	-	-
Ash Content	Supplier certification of base paper (ASTM D586)	%	<1	-	-
Moisture Content	ASTM D644	%	6.0	4.0	7.0
Insuldur Content	Calculated	%	-	-	-
Nitrogen Content	ASTM D982	%	1.9	-	-
Dielectric Strength - Air	ASTM D202 (ASTM D149)	V/mil	100	-	-
		kV/mm	3.9	-	-
Dielectric Strength - Oil	ASTM D202 (ASTM D149)	kV/mil	0.77	-	-
		kV/mm	30.3	-	-
Impulse - Oil (1 layer)	ASTM D2413 prep	kV/mil	-	-	-
	ASTM D3426 test	kV/mm	-	-	-
pH of aqueous extract	TAPPI T435, ASTM E70 or IEC 605542	pH	-	-	-
Conductivity of aqueous extract	ASTM D202	mS/m	-	-	-
Yield	Function of basis weight	Sq.ft/lb	53	-	-
		m ² /kg	11	-	-
Hill Count	Physical count under 10x magnification	No. per inch (25.4mm)	-	-	-
Please contact your WEIDMANN representative for additional technical details, or to inquire if our products meet your company's internal specifications.					

Please contact us for values outside the specified ranges. The specified tolerances are valid for measurements taken at WEIDMANN or after conveyance and warehousing under conditions appropriate for the material. Customers are advised to add appropriate additional tolerances in case of extreme environmental conditions at the place of warehousing or processing of the material.

Ordering code

E3CCLA0.RP /TH/GRM/DO/DI/W/L

Disclaimer

Subject to change without prior notice

PDF generated on: 2015-11-28 22:00:42

Appendix C

Oil parameters measured during PD tests

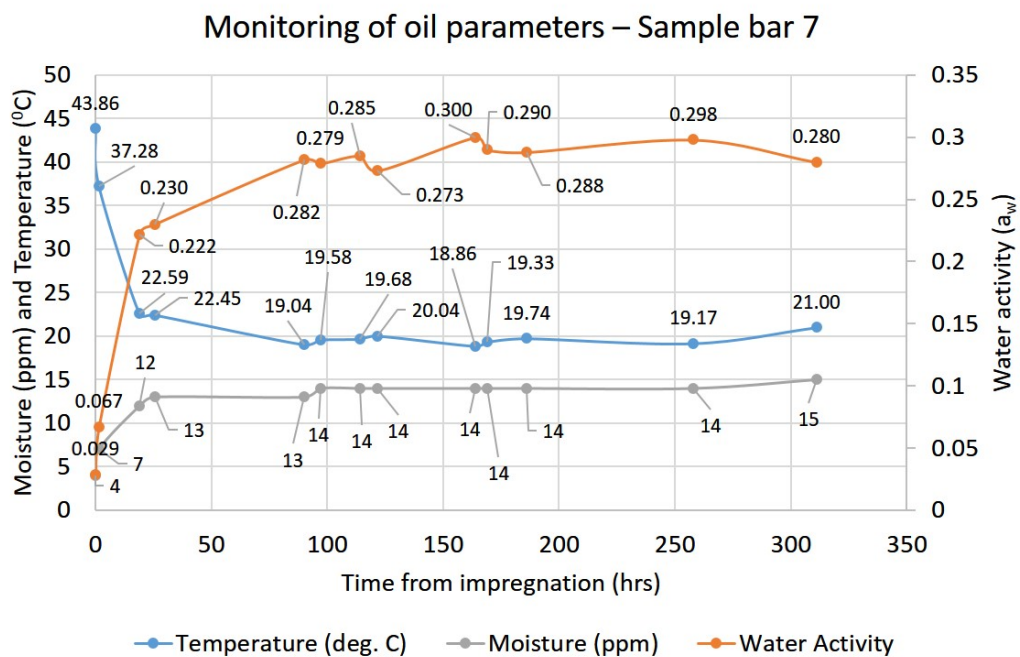


Figure C-1: Monitoring of oil parameters during testing of sample bar 7

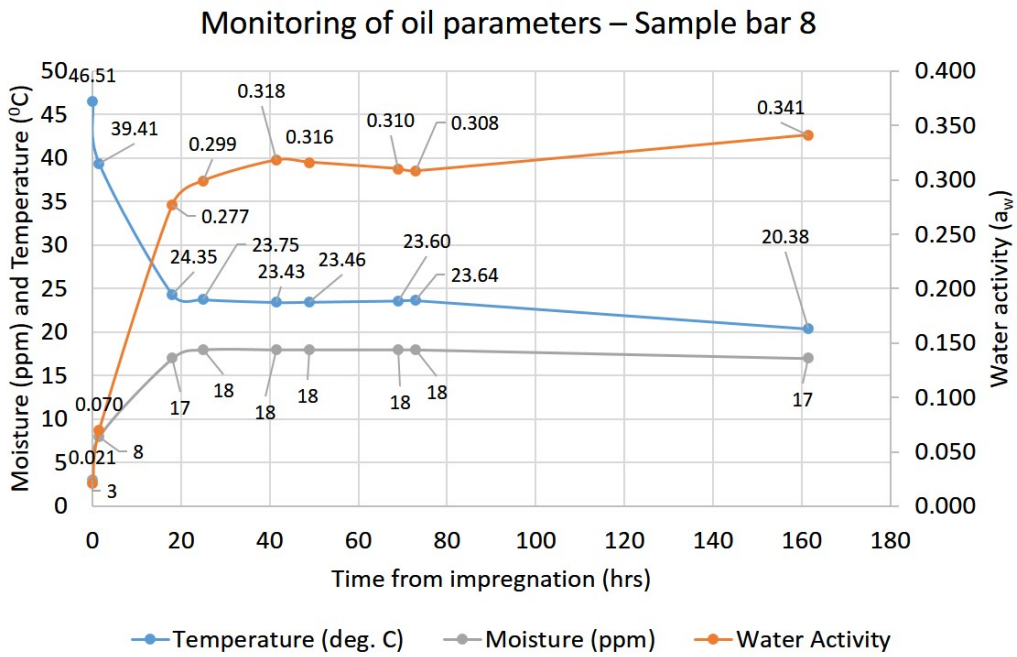


Figure C-2: Monitoring of oil parameters during testing of sample bar 8

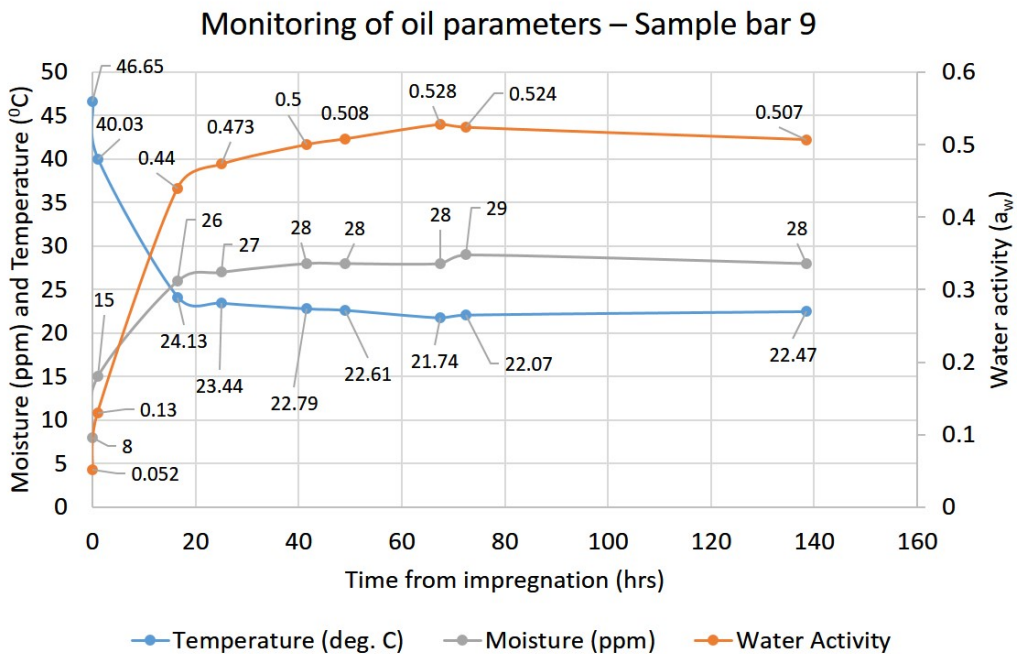


Figure C-3: Monitoring of oil parameters during testing of sample bar 9

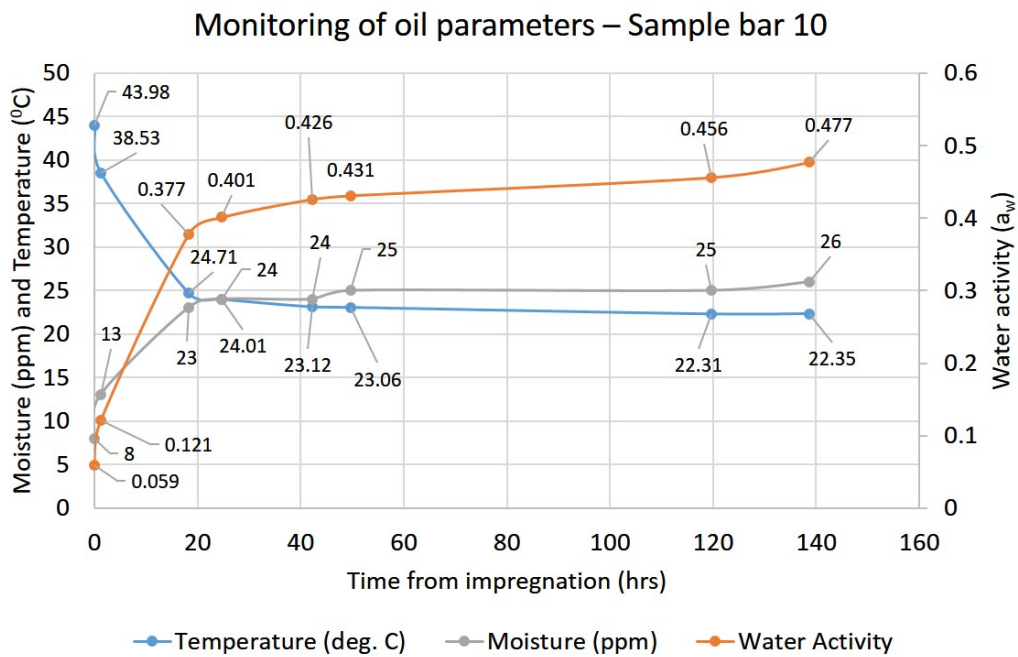


Figure C-4: Monitoring of oil parameters during testing of sample bar 10

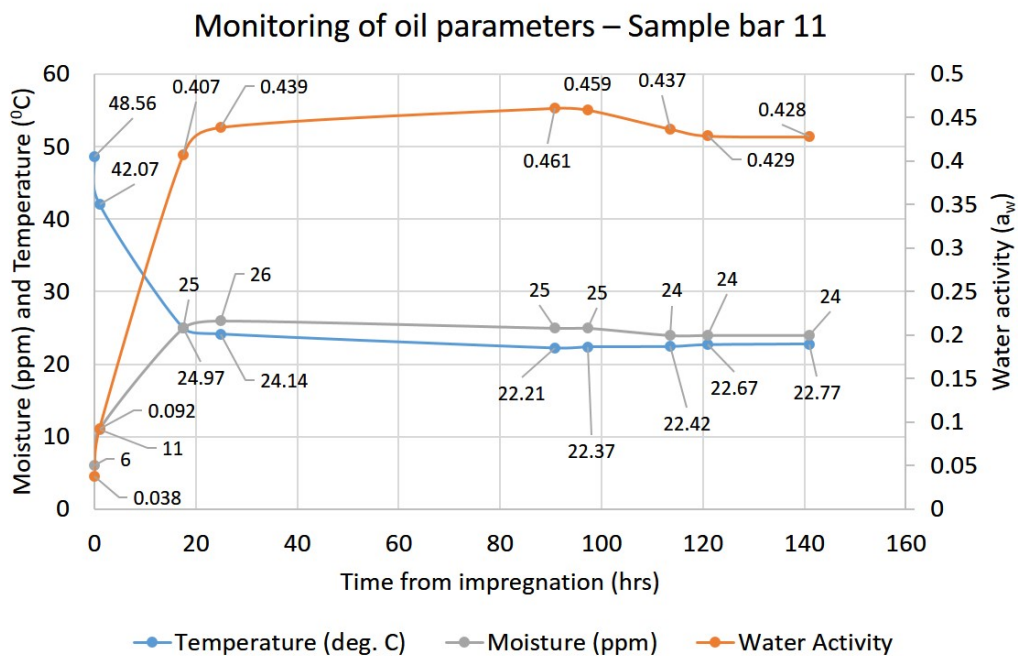


Figure C-5: Monitoring of oil parameters during testing of sample bar 11

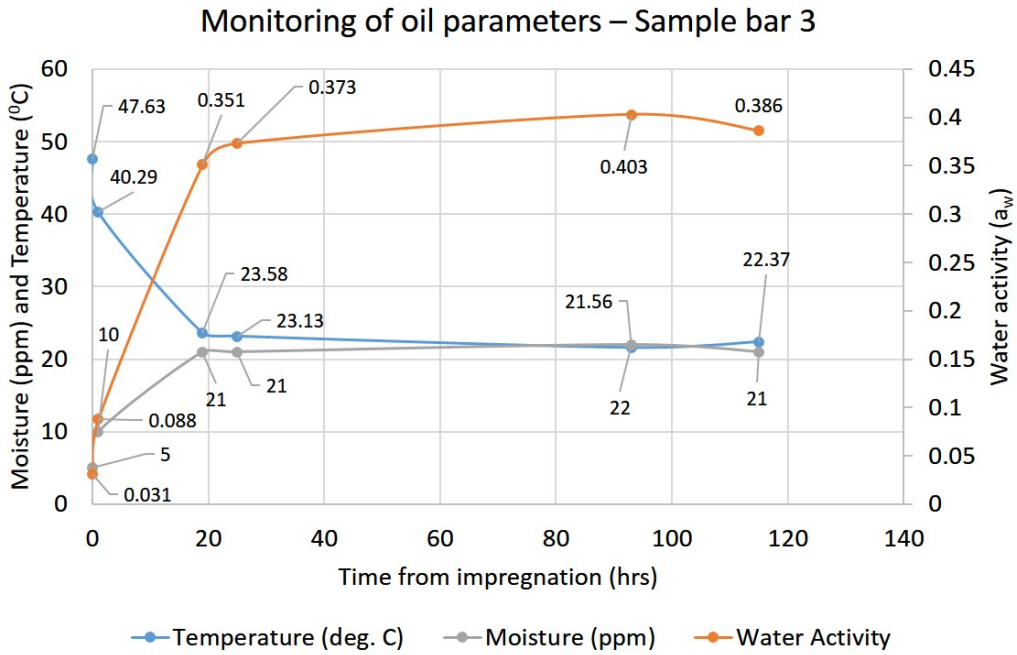


Figure C-6: Monitoring of oil parameters during testing of sample bar 3

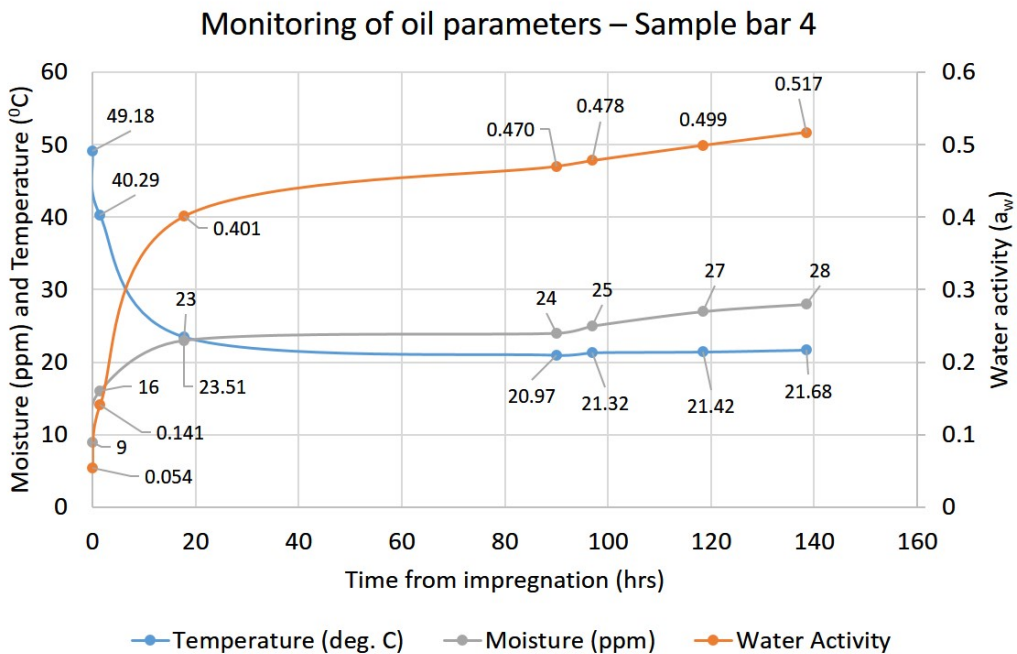


Figure C-7: Monitoring of oil parameters during testing of sample bar 4

Bibliography

- [1] S. Jeszenszky, "History of Transformers," *IEEE Power Engineering Review*, vol. 16, no. 12, pp. 9–, Dec 1996.
- [2] "International Electrotechnical Vocabulary, Chapter 421: Power transformers and reactors," visited on 25-02-2016. [Online]. Available: <http://www.electropedia.org/iev/iev.nsf/display?openform&ievref=421-01-01>
- [3] H. Erdman, A. S. for Testing, and Materials, *Electrical Insulating Oils*, ser. ASTM STP 998. ASTM, 1988, no. 998.
- [4] D. J. Allan, "Power transformers-the second century," *Power Engineering Journal*, vol. 5, no. 1, pp. 5–14, Jan 1991.
- [5] CIGRE WG 37.27, "Ageing of the system. Impact on planning," Technical Brochure 176, December 2000.
- [6] "Strategic asset management of power networks," White Paper, International Electrotechnical Commission, October 2015.
- [7] B. Gorgan, P. V. Notingham, J. M. Wetzler, H. F. A. Verhaart, P. A. A. F. Wouters, A. Van Schijndel, and G. Tanasescu, "Calculation of the remaining lifetime of power transformers paper insulation," *Proceedings of the International Conference on Optimisation of Electrical and Electronic Equipment, OPTIM*, pp. 293–300, 2012.
- [8] *Classification of Transformers Family*, ser. Transformers Magazine, vol. 1, no. 1, 2014, visited on 25-02-2016. [Online]. Available: <http://www.transformers-magazine.com/issue1/item/639-classification-of-transformers-family.html>
- [9] P. R. Barnes, J. W. Van Dyke, B. W. McConnell, and S. Das, "Determination Analysis of Energy Conservation Standards for Distribution Transformers," Oak Ridge National Laboratory, Tech. Rep., July 1996. [Online]. Available: <http://cta.ornl.gov/cta/Publications/Reports/ORNL-6847.pdf>

- [10] “fluorinated greenhouse gases and repealing Regulation (EC) No 842/2006,” Regulation (EU) No 517/2014 - Official Journal of the European Union, European Parliament and the Council, April 2014.
- [11] “Mitsubishi Electric Power Products Inc. - SF6 Gas Insulated Transformers,” visited on 22-03-2016. [Online]. Available: <http://www.meppi.com/Products/Transformers/Pages/SF6Gas.aspx>
- [12] G. Camilli, “Gas-insulated power transformers,” *Proceedings of the IEE - Part A: Power Engineering*, vol. 107, no. 34, pp. 375–382, August 1960.
- [13] D. F. Warne, *Newnes Electrical Power Engineer’s Handbook*, 2nd ed. Elsevier, 2005, ch. 6. Transformers, pp. 139–154.
- [14] “Grid Transformers,” visited on 17-08-2016. [Online]. Available: <https://www.sgb-smit.com/products/large-power-transformers/grid-transformers/>
- [15] J. J. Winders, Jr., *Power Transformers: Principles and Applications*. Marcel Dekker, Inc., 2002.
- [16] Y. Du, M. Zahn, B. C. Lesieutre, A. V. Mamishev, and S. R. Lindgren, “Moisture equilibrium in transformer paper-oil systems,” *IEEE Electrical Insulation Magazine*, vol. 15, no. 1, pp. 11–20, Jan 1999.
- [17] H. Jackson and K. Ripley, “7. Transformer Processing and Testing,” in *Modern Power Transformer Practice*, R. Feinberg, Ed. The Macmillan Press Ltd., 1979, pp. 153–186.
- [18] N. Irahhauten, “Optimization of the Impregnation Process of Cellulose Materials in High Voltage Power Transformers,” M. Sc. Thesis, Delft University of Technology, The Netherlands, September 2015.
- [19] H. Gasser, C. Krause, and T. Prevost, “Water Absorption of Cellulosic Insulating Materials used in Power Transformers,” in *2007 IEEE International Conference on Solid Dielectrics*, July 2007, pp. 289–293.
- [20] H. W. Kerr, “5. Windings,” in *Modern Power Transformer Practice*, R. Feinberg, Ed. The Macmillan Press Ltd., 1979, pp. 112–138.
- [21] M. Heathcote, *J & P Transformer Book*, 13th ed. Elsevier Science, 2011.
- [22] *Specification for cellulosic papers for electrical purposes*, IEC Std. 60 554.
- [23] *Specification for pressboard and presspaper for electrical purposes*, IEC Std. 60 641.
- [24] “Shielding Elements - Weidmann Electrical Technology,” visited on 25-08-2016. [Online]. Available: <http://www.weidmann-electrical.com/en/shielding-elements.html>
- [25] F. H. Kreuger, *Industrial High Voltage, Volume 1*. Delft University Press, 1991.
- [26] V. G. Arakelian and I. Fofana, “Water in Oil-Filled, High-Voltage Equipment, Part I: States, Solubility, and Equilibrium in Insulating Materials,” *IEEE Electrical Insulation Magazine*, vol. 23, no. 4, pp. 15–27, July 2007.

-
- [27] P. Gervais, M. Duval, M. Merabet, and T. K. Bose, "The state of water in oil-impregnated paper insulation," in *Conference Record of the 1990 IEEE International Symposium on Electrical Insulation*, Jun 1990, pp. 65–67.
- [28] S. Itahashi, H. Mitsui, T. Sato, and M. Sone, "Analysis of water in oil-impregnated kraft paper and its effect on conductivity," *IEEE Transactions on Dielectrics and Electrical Insulation*, vol. 2, no. 6, pp. 1111–1116, Dec 1995.
- [29] K. Mazeau, "The hygroscopic power of amorphous cellulose: A modeling study," *Carbohydrate Polymers*, vol. 117, pp. 585 – 591, 2015.
- [30] E. Princi, S. Vicini, E. Pedemonte, V. Arrighi, and I. McEwen, "Thermal characterisation of cellulose based materials," *Journal of Thermal Analysis and Calorimetry*, vol. 80, no. 2, pp. 369–373, 2005.
- [31] J. Harlow, *Electric Power Transformer Engineering*, ser. The Electric Power Engineering Hbk, Second Edition. CRC Press, 2004.
- [32] Weidmann, 2014, private communication.
- [33] C. Jialu, "Broadband Dielectric Properties of Impregnated Transformer Paper Insulation at Various Moisture Contents," M. Sc. Thesis, Kungliga Tekniska Högskolan, Stockholm, Sweden, 2011. [Online]. Available: <https://www.diva-portal.org/smash/get/diva2:511555/FULLTEXT01.pdf>
- [34] A. Akbari, S. DehPahlevan, and H. Borsi, "Analyzing dynamic of moisture equilibrium in oil-paper insulation in power transformers for efficient drying," in *2006 IEEE Conference on Electrical Insulation and Dielectric Phenomena*, Oct 2006, pp. 545–548.
- [35] F. H. Kreuger, *Industrial High Voltage, Volume 2*. Delft University Press, 1992.
- [36] *Power transformers - Part 3: Insulation levels, dielectric tests and external clearances in air*, IEC Std. 60 076-3:2013, Rev. 3.0.
- [37] *Power transformers - Part 1: General*, IEC Std. 60 076-1:2011, Rev. 3.0.
- [38] K. Karsai, D. Kerényi, and L. Kiss, *Large power transformers*, ser. Studies in electrical and electronic engineering. Elsevier, 1987.
- [39] J.-L. Bigourdan and J. M. Reilly, "Effects of fluctuating environments on paper materials - Stability and practical significance for preservation," visited on 08-08-2016. [Online]. Available: https://www.imagepermanenceinstitute.org/webfm_send/305
- [40] *High-voltage test techniques - Partial discharge measurements*, IEC Std. 60 270:2000, Rev. 3.0.
- [41] M. G. Niasar, H. Edin, X. Wang, and R. Clemence, "Partial discharge characteristics due to air and water vapor bubbles in oil," in *17th International Symposium on High Voltage Engineering*, Hannover, Germany, 22-26 August 2011.
- [42] R. J. V. Brunt, "Stochastic properties of partial-discharge phenomena," *IEEE Transactions on Electrical Insulation*, vol. 26, no. 5, pp. 902–948, Oct 1991.

- [43] *Assessing Water Content in Insulating Paper of Power Transformers*, ser. Electric Energy T & D Magazine, vol. 3, no. 11, 2007, visited on 11-08-2016. [Online]. Available: <http://www.electricenergyonline.com/page.php?page=magazine&ID=44>
- [44] A. Cavallini, G. C. Montanari, and F. Ciani, “Analysis of partial discharge phenomena in paper-oil insulation systems as a basis for risk assessment evaluation,” in *IEEE International Conference on Dielectric Liquids, 2005*, June 2005, pp. 241–244.
- [45] M. Rasi, “Permeability Properties of Paper Materials,” Ph.D. dissertation, University of Jyväskylä, Finland, December 2013. [Online]. Available: <http://www.jyu.fi/static/fysiikka/vaitoskirjat/2013/Rasi-Marko-2013.pdf>

List of Abbreviations

CTC	continuously transposed conductors
FAT	Factory Acceptance Tests
HV	High Voltage
IEC	International Electrotechnical Commission
IVPD	Induced voltage test with PD measurement
LV	Low Voltage
OIP	Oil Impregnated Paper
PD	Partial Discharge
PDEV	Partial Discharge Extinction Voltage
PDIF	Partial Discharge Inception Field
PDIV	Partial Discharge Inception Voltage
PRPD	Phase-Resolved Partial Discharge
RH	Relative Humidity
SF6	Sulphur hexafluoride

